PART A

LAHET^{TM}/MCNP^{TM}/CINDER'90 ACTIVATION CALCULATIONS FOR THE ATLAS INTEGRATED FORWARD CALORIMETER CONCEPT

Laurie Waters, William B. Wilson
Los Alamos National Laboratory
Los Alamos, New Mexico USA 87545
505-665-4127

ABSTRACT

A preliminary activation calculation has been performed for the Integrated Forward Calorimeter proposed for the ATLAS collaboration. We have computed the nuclear product inventory at 30 points in time over the period of 1 year of LHC operation. Along with the amount of each nuclide in number/barn-cm we have produced activity in curies/cc and decay heating from electrons and gammas in watts/cc. Multigroup gamma decay spectra are also available and have been used as a source term to calculate dose equivalent in mSv/hour at points around the setup. We also address in depth some statistical considerations for accuracy of these and similar results.

PART A

1 Introduction

We have undertaken preliminary calculations of the activation of the Integrated Forward Calorimeter proposed for the ATLAS collaboration at LHC. A model of the detector, materials and surrounding shielding has been constructed using standard MCNP^{TM} format. The spallation product inventory is calculated with the LAHET^{TM} Monte-Carlo code [Pra89], with DTUJET [Aur90] as the primary source. Neutrons generated with less than 20 MeV kinetic energy are transported with MCNP^{TM} [Bre81].[1] The spallation inventories and low energy neutron flux are input into the CINDER'90 [Wil93] activation code along with an assumed beam current profile. Output consists of nuclide inventory in number/barn-cm,[2] activity for each nuclide in curies, decay power heating in watts from recoverable energy from emitted particles, and gamma decay spectra. Results are reported at 30 different user-specified points in times. The gamma spectra are further used as sources in MCNP^{TM} to calculate dose equivalent around the detector. The dose results are given both as 2-dimensional histograms in HBOOK format and as rates with statistically analyzed errors at 20 different points around the setup.

This report summarizes the calculational procedures and output. Section 2 will review the geometrical setup, source term and normalization factors. Section 3 discusses the spallation product inventory and neutron flux calculated with the LAHET^{TM} and MCNP^{TM} codes. Section 4 summarizes the CINDER90 output, and Section 5 gives the result of the MCNP^{TM} dose equivalent calculation. Section 6 discusses calculational limitations and systematic errors.

We would like to emphasize that this calculation can be improved with more accurate description of the geometry and materials which at this time have not been finalized. Much of our purpose is to demonstrate the technique, emphasizing those areas of key importance to the calculation.

2 Problem Setup

The forward calorimeter alone was modeled for the activation calculations and consists of four elements: a borated polyethylene shield (BPOLY), a brass/liquid argon electromagnetic section (FCAL1), and two tungsten/liquid argon hadronic sections (FCAL2 and FCAL3). For the purposes of the gamma transport for the dose equivalent calculation an approximation for the accordion electromagnetic calorimeter (EM) and three proposed shielding elements (CU, UPLUG, DPLUG) were included. Figure 1a shows all these elements as defined for this study. Table 1 gives the positions and dimensions of the volumes, and Table 2 defines the materials used in each.

Activation calculations were done for the three FCAL modules and borated polyethylene shielding. In addition, the three FCAL modules were further divided into 13 segments each

---

[1]LAHET and MCNP are trademarks of the Regents of the University of California, Los Alamos National Laboratory.

[2]Number/barn-cm is exactly equivalent to Number/cubic Angstrom.

and a separate activation calculation done for these 39 regions. Each side of the modules was divided into segments of 1, 2 and 3 cm depth (Fig. 1b). This division was done to check the consistency of results between calculations which average over modules and those that emphasize possible residual nuclei and flux differences which should become evident with the finer structure.

The temporal beam current profile used in the CINDER'90 calculation is shown in Table 3. We assume four periods of beam on for 30 days each followed by 10 days downtime. After the 4 cycles have ended the downtime is extended to the end of the year. The thirty times at which the activation calculation data were obtained are given in the table.

The DTUJET event generator was used to provide the source particles from 7TeV + 7TeV p-p interactions for this calculation (DTU_7x7.EVE). Figure 2a shows the charged particle pseudorapidity plot from these events. The acceptance of the FCAL components is approximately $3 \prec \eta \prec 5$. Figure 2b is a plot of particle kinetic energy versus pseudorapidity which indicates the range of particle energies entering this acceptance.

1000 DTUJET events were prepared by Nikolai Mokhov at FERMILAB, who included multi-particle production events as well as single and double diffraction. No elastic events are included in the file. In the code, the total p-p cross section is 103 mb, and the inelastic cross section is 77.3 mb. On the basis of these figures we have used a normalization factor of 7.9×10^8 p-p events per second assuming luminosity of 10^{34}. Although we have only simulated the detector for positive Z, we can take advantage of particles emitted in the negative Z direction by reversing the sign of the Z component of momentum for those particles with $P_z \prec 0$. We therefore have available effectively 2000 p-p events into our geometry. Any correlations introduced by this procedure are negligible for this type of calculation.

3 Spallation Products and Neutron Flux

The Los Alamos High Energy Transport (LAHET^{TM}) Monte-Carlo code has been used to compute spallation product inventories for the 3 FCAL and the borated polyethylene modules. The code uses the HETC model to simulate hadronic interactions below 2.0 GeV, and the FLUKA code above 5.0 GeV. FLUKA is phased in linearly between 2 and 5 GeV. LAHET^{TM} includes a multi-stage pre-equilibrium exiton model, and the FERMI breakup model replaces the evaporation stage for light nuclei. The Rutherford-Appleton Fission model is also included. Details of the code may be found in [Pra94]. Figure 3 shows the distribution of spallation products as a function of A and as a plot of A versus Z for the 4 modules. Figure 3a show a breakdown of processes which are included in the total; fission of Tungsten, absorption and spallation products left after the cascading process. The plots of Figure 3a are shown after the residual nucleus has lost excitation energy by evaporation.

Hadrons, except neutrons are tracked down to 1.0 MeV, pions to .149 MeV, muons to .113 MeV. One additional concern that can be addressed in the activation calculation is the production of light nuclei gasses; hydrogen, helium, helium3, deuterium and tritium. The last plot in Figure 3a shows the amount of these four elements produced in the LAHET calculation for FCAL2; all except hydrogen are passed to CINDER. Only hadronic processes

3

are included in the calculation; photonuclear effects are excluded.

Figure 4 shows the density of inelastic hadronic collisions in the four modules as a function of radius and Z. The reader is cautioned not to use these figures for the purpose of making 'star density' estimates of activity. The tracking cuts used here are not consistent with plots usually generated for this technique. This information will however be extensively used in the analysis of dose equivalent as discussed in Section 5.

All neutrons with kinetic energies less than 20 MeV are passed to the coupled neutron/photon/electron Monte-Carlo $MCNP^{TM}$. The pattern of neutron flux is shown in number/cm^2/sec for each module in Figure 4a. The point cross section data libraries used in this calculation come primarily from ENDF/B-V. The neutron flux is an input to the CINDER'90 code and will be absorbed on all original and created nuclides. Figure 5 shows the neutron flux spectra for each of the four modules. A check of spectra for the smaller geometry divisions of Figure 1b shows remarkable consistency throughout the modules. Only the regions in FCAL1 close to the BPOLY unit show some evidence of downscattering. Figure 5a illustrates details of the neutron spectra for the 13 regions of FCAL1.

All evidence of a thermal peak in the BPOLY module has been eliminated by the 5% boron in the polyethylene. Therefore, even though the liquid argon temperature dependence and the polyethylene thermal scattering treatment have been included in the problem, these additions will have negligible effect on the results.

4   CINDER'90 Calculation

The CINDER code has been used for 3 decades to compute reactor fuel inventories and decay properties in similar applications. CINDER'90 is an adaption specifically designed to address accelerator problems, and is now used extensively in Accelerator Driven Transmutation programs. Specific benchmarking experiments are now underway, and other comparisons to existing data are available upon request. CINDER'90 [Wil93] produces and follows linear transmutation chains in the solution of the coupled differential equations describing the buildup and destruction of nuclide inventories, and relies on a large data set of evaluated libraries for cross sections, decay data and decay photon spectra. Although results are reported at specific points in time, the nuclide inventory is computed continuously, taking full account of isotope production, destruction and decay. The code inputs are the residual nuclei from the high energy LAHET reactions, and the material description adjusted to account for destruction caused by the high energy processes. The MCNP neutron flux acts both on these inputs and on all produced nuclides as they are created during the problem. CINDER'90 is typically run on a CRAY YMP, and once the initial problem setup is done total running time is about 20 seconds for a region. The output of the CINDER'90 code is very extensive, and full results are available upon request. For example, the calculation for FCAL2 produced 1349 nuclides, with inventory, curies and decay heat for each at all 30 time steps. This section focuses on the results obtained for inventory (given in number/barn-cm), activity density (given in curies), and decay heating (given in watts); the gamma decay spectra will be discussed in the next section.

Figure 5b shows nuclide inventory at time point 18 in Table 3 for FCAL2. The top plot shows the calculated CINDER'90 products as a function of A in number/barn-cm. This may be compared with the original material description which is shown in the second plot. The third plot subtracts the second from the first and thus shows the net number of nuclides produced in the calculation. At the sites of the original materials the situation is complex. For the Tungsten isotopes nothing higher in A is available to feed into these states, and some inventories will slightly decrease. In other cases the net increase in the nuclide is very small relative to the original amount, and the CINDER'90 printed output does not have the numerical accuracy to reflect the change. Both situations will result in a gap at those sites in the bottom plot.

The large amount of CINDER'90 output can be difficult to summarize in an effective manner. The four parts of Table 4 are one such presentation. For each FCAL module and the BPOLY shield the major contributors to activity and decay heat are shown at the times indicated in Table 3. The column under each time adds up to 100%, therefore each entry in the table gives the percent contribution of that nuclide to activity or decay heat at that point in time. Metastable excited states of nuclides are indicated with a *. The tables show at a glance the buildup and decay of the most important nuclides. Similar data is available for nuclide inventory and also for an analysis which rates nuclides by contributions to macroscopic absorption cross section.

Interest has been expressed in the buildup of Ar41. Figure 6 shows the profile of total curies of Ar41 for the year. The half life of Ar41 is 1.82 hours, therefore the buildup to equilibrium while beam is on, as well as decay after shutdown is very fast. While beam is on the Ar41 activity stays fairly constant at .09 curies total for the 4 modules. Figure 7 shows the time dependence of activity for all nuclides in each of the 4 modules, including Ar41. The activity profile is a delicate balance between short and long lived nuclides. In general we do not find that activity scales with luminosity. A calculation done for the SSC found that increasing luminosity from 10^{33} to 10^{34} increased activity by a factor of 10.05 overall, but with much higher increases at very early times.

Figure 8 shows the total decay heating power as a function of time for the four modules. Heating power is defined as the energy released by decay photons and electrons. The solid line is total heating power, given in watts/cc, while the dashed line shows the part due solely to photons. Figures such as these are most useful in analysis of potential heating damage to components. However the data presented in Figure 8 are averaged over each volume. To get a more reasonable estimate of the true distribution of heating power in each module, figure 9 takes the average value at time point number 25 in table 3 and uses the interaction density plots in figure 4 to distribute this value over the volume of each the module.

5 Equivalent Dose

Multigroup decay gamma spectra are available for the four modules at each time point. Figures 10 and 11 show these spectra at points 18 and 19 in Table 3 (just before shutdown and 1 day after shutdown). Emission rates and average energies of these decay spectra are

given in Table 5. Note that the spectra for BPOLY while the beam is on is dominated by high energy gammas from N16 and B12, and the average energy of the spectrum is 6.13 MeV. An interesting effect can be observed in dealing with photons of such energies. When incident upon lead shielding, the minimum of the total cross section is in this range, leading to a mean free path of about 2 cm. The range for a .4 MeV gamma is about .3 cm. This means that the BPOLY spectrum is very penetrating in lead while the beam is on. Fortunately the rate of gamma emission from the BPOLY module is about 3 orders of magnitude less than that from the FCAL modules.

The CINDER'90 decay gamma spectra are used as sources to MCNP^{TM}, and the gammas transported around the setup to determine dose equivalent. We have used fluence to dose equivalent conversion factors taken from ANSI/ANS 6.1.1-1977 [Ros71]. These factors are shown in Figure 12a. In order to give the average spectra a radial and Z dependence we have included the inelastic collision density in the source term for each module as shown in Figure 4. It is also possible to use the pattern of neutron flux for this purpose, but this has not been done in this study. A comparison of the two methods shows slight differences since the neutron flux is usually peaked farther out in radius than the collision density. The most accurate way to simulate the distribution of sources would be to divide each module up into many small pieces and do a separate CINDER'90 calculation for each. This was our intent in dividing up the FCAL into smaller units as shown in Figure 1b, however the analysis is not yet complete.

MCNP^{TM} uses the physics of ETRAN via the ITS code to simulate electromagnet interactions [Hal92]. ITS, the Integrated TIGER Series from Sandia is an active competitor of EGS4.

The results of the dose equivalent calculation are presented here in two forms. Two dimensional histograms in radius and Z for dose in mSv/hour are available in HBOOK format. In addition we use the technique of point detectors to obtain dose at 20 different points around the setup. These points are indicated in Figure 1a. Point and Ring detectors are variance reduction techniques in which every interaction in the problem is assumed to have a probability of contributing to the measurement at a certain point. More details may be found in [Bre81]. In shielding problems such as this is it extremely important to know if the answer has converged. In addition to quoting the relative error, MCNP^{TM} offers 10 statistical checks which must be passed in order to quote a valid confidence interval. All is not lost if all 10 of the tests are not passed, some are worse than others. Table 6 summarizes the tests and gives an indication of the importance of each. A few specific applications of this process are discussed in detail at the end of this section. A quick check of the histogram can also spot many trouble areas and supply a visual criteria of reasonableness.

Figure 12 contains profiles of the photon source distribution as a function of R and Z for the BPOLY and FCAL1 modules. The top figures show where the photons were initially generated in the MCNP^{TM} calculation. These data are integrated over each radial bin. therefore are not normalized per unit volume. The bottom two plots show the origins of all photons which cross a cylinder of radius 55 cm during the calculation. In the FCAL1 plot it is seen that only photons within a few centimeters of the surface regions make it to

6

this radius. However in the BPOLY plot photons throughout the volume of this module can escape, due to the very long radiation length of polyethylene. This effect is seen even in FCAL1 where photons from the surfaces at small R next to the polyethylene can pass through the BPOLY module and reach the R=55 cm cylinder. At the other end of FCAL1, the presence of a gap between it and FCAL2 also allows photons to reach the cylinder.

The first calculation was done for the three FCAL modules and the BPOLY unit alone, with no other volumes present. At time point 18, the 30 day beam on point in the third cycle, Table 7 shows the result of the point detector calculation, and Table 8 contains an error analysis for this points. The pattern of photon dose is shown in Figure 13, for each module separately. Figure 14 shows the dose pattern for all modules added together along with a cut through Z=494 cm, the midpoint of FCAL1. The cut demonstrates some expected behavior. In the beampipe area, less than radius=7.2 cm, the photon flux is constant. This is expected because there is no reason for photon flux to vary with radius in a cylindrical cavity contained within a homogenous mass of material. At the outer radius of the detector, R=53.3 cm, the dose suddenly drops by about a factor of 2. This surface effect is also expected. Within the detector the isotropic source term ensures that the gamma current is the same for photons going outward and inward in radius. Just after the edge of the detector the inward going current is eliminated, and the photon flux drops by a factor of 2.

For the unshielded case at point 19, one day after shutdown, Tables 9 and 10 contain the point detector doses and error analysis, and Figure 15 gives the total dose pattern and cut through Z=494 cm.

The second calculation was done for the FCAL and the BPOLY with the EM and CU units in place, again at time points 18 and 19. Results are shown in Tables 11 through 14, and in Figures 16 and 17.

The final calculation was done with all shielding in place. Results are given in Tables 15 through 18, and Figures 18 and 19.

5.1   Statistical Analysis of Shielded Point 19

The statistical analysis discussed here only concerns the calculation of the dose equivalent, assuming that the gamma decay spectra produced by CINDER'90 are correct. This of course ignores the component of error which comes from uncertainty in input neutron fluence and spallation product inventories. In this study these have been kept within reasonable bounds. The systematic uncertainties will be discussed in the next section. Future plans for update of the CINDER'90 code include provision to appropriately account for all sources of uncertainty.

The fully shielded point 19, taken one day after shutdown represents a reasonably realistic condition for detector access. and therefore we will go into a bit more detail on the statistical analysis of this calculation. Table 18, the error analysis figures for this point show a large variation in relative errors and other convergence criteria shown in table 6. One point which passes all tests is the contribution from BPOLY at R=300 cm, Z=300 cm. The estimated asymmetric confidence interval for this point can be quoted at:

1.3821E-13 to 1.4717E-13 (1 sigma)

1.3373E-13 to 1.5164E-13 (2 sigma)

1.2926E-13 to 1.5612E-13 (3 sigma)

The estimated symmetric confidence intervals are:

1.3807E-13 to 1.4702E-13 (1 sigma)

1.3360E-13 to 1.5149E-13 (2 sigma)

1.2913E-13 to 1.5596E-13 (3 sigma)

Figure 20 shows some of the details of the statistical analysis for this point. The basic probability density function, f(x), represents the probability that the score will fall between x and x+dx. f(x) is shown in the first plot in figure 20 after completion of a run of 200000 source photons. (The value for x=0.0 is not included in this plot.) The f(x) function integrated from minus to plus infinity is normalized to 1.0. The first moment of f(x) is the score value reported in Table 17, and the variance used in the calculation of relative error (R = sampled standard deviation/sampled mean) is the second moment of f(x). The bottom four plots of Figure 20 examine the behavior of these and other quantities derived from f(x) as a function of N, the number of source photons run. When considered within the context of convergence as defined by the Central Limit Theorem (CLT), these quantities should follow certain patterns which form much of the basis of the tests outlined in Table 6.

CLT requires the existence of the first and second moments of f(x). Test #1 checks for the stability of the mean of f(x), and tests #3 through #4 makes sure the second moment is inversely proportional to N. The maximum recommended value of R=.05 for point and ring detectors is the result of experience and is somewhat more strict than for other sam pling methods. The quantity known as Figure of Merit (FOM) is related to the variance, FOM=1/(R^{2}T), where T is the computer time used in the problem. R^2 is proportional to N^{-1} and T is roughly proportional to N, so FOM should stay constant throughout the problem (tests #8 and #9). The Variance of the Variance (VOV), is the estimated relative variance of the estimated R, and is a measure of how well the sampled variance estimates σ of the CLT. It involves the fourth moment of f(x), and can be shown to fall off as N^{-1} (tests #6 and #7).

In some difficult Monte Carlo situations f(x) is often similar to a truncated Cauchy distribution:

$$f(x)_{Cauchy} = 2/\pi(1 + x^2), 0 \le x \le x_{max} \tag{1}$$

Statistical studies of this function indicate that a value of VOV less than .1 will improve the chances of obtaining a reliable confidence interval, this forms the basis of the recommendation of test#5.

In forming confidence intervals it is critical that f(x) be sampled as well as possible, throughout the entire range of x. Large values of x are especially difficult. The last test in Table 6 tries to investigate the behavior of f(x) at the largest values of x. If the falloff in these values is less than x^{-3} it can be shown that the second moment of f(x) will not exist and the answer will never converge.

The example shown in Figure 21 illustrates one common problem which occurs in these types of analysis. The point is for FCAL3 at R=0.0, Z=700.0 cm, and the relative error of .0246 seems excellent. However tests #3 through #8 were not passed. An examination

8

of f(x) shows that points rarely sampled at highest values of x will have great effect on the calculation. All the distributions show a sudden discontinuity when one of these rare high x points is sampled. Application of variance reduction techniques which seek only to increase the sampling of f(x) throughout its entire range will not be the most efficient method to improve the accuracy of this calculation. Since the large x tail (corresponding to high energy photons which have large fluence-to-dose equivalent conversion factors) have the most effect on the answer, care should be taken to sample this range well. Energy biasing of the source will be more effective than simple adjustment of volume importances which may actually emphasize the wrong range in f(x).

This point carries over into radiation background calculations which are now being carried out throughout the LHC environment. For example, if one wishes to determine the background from neutron interactions in a detector, one must first know exactly what range in f(x) is most important to the answer. Biasing must be designed to ensure adequate sampling of that range. The exercise must seek to emphasize the most important contributions, not simply try to force the increase of the fluence of every particle distribution in the region of interest.

6 Comments

A discussion of the results of the calculations naturally divides itself into several topics. We must address the appropriateness of the geometry, the physics of the codes in use, and the techniques used to ensure convergence of the answers.

The geometry setup is the most serious controllable consideration for this calculation. None of the surrounding hall, and minimal simulation of the detector have been done. Material need to be carefully checked, for impurities can have a definite effect on activation, especially in tungsten. In addition we have not included any magnetic field effects in this calculation. Results must therefore be declared preliminary, although valid for the specifications used.

Simulation of hadronic interactions has come a long way in the past few years and most of the major Monte-Carlo codes show good agreement with data. MCNP^{TM} is considered the best available low energy neutron transport code around, and CINDER'90 is acknowledged as having the most complete set of libraries for activation calculations. Both are well tested and benchmarking efforts for accelerator applications are aggressively being undertaken. The LAHET^{TM} code has been used to design the LANSCE and WNR spallation sources at LAMPF, and has been well tested below a few GeV for many years. In contrast to codes such as FLUKA and GEANT, LAHET^{TM} is working its way up in energy, rather than down. It builds on the solid foundation of MCNP analysis techniques and is finding increasing applications in a variety of fields, and can now reach multi-TeV energies.

The weakest point in these calculations is the determination of spallation product inventory, especially for light nuclei. This is one of the topics needing research in the field, and we are actively investigating new models and benchmarking experiments that will improve the physics involved. In addition, LAHET^{TM} currently has no photonuclear capability, however

9

this contribution is of minimal importance in this application.

We have done little here to minimize statistical errors through use of various variance reduction techniques. Much improvement can be obtained with methods such as source biasing and splitting in the deep penetration parts of the problem, especially behind the shielding. We regard the present study as a first look at the situation, and can use the results here to design appropriate biasing as the ATLAS design matures.

7   Conclusions

We have made a preliminary calculation of various activation quantities for the proposed Integrated Forward Calorimeter for the Atlas Collaboration at LHC. Much more information than could be printed in this report has been generated. We will gladly make files available upon request.

This calculation represents state of the art techniques which have their origins in high intensity neutron beam accelerator applications, and also in many years of reactor experience. We believe this is a valid alternative to the traditional 'Star Density' approach, and is far more adaptable to problems involving shielding and deep penetration.

We hope to continue this work once the final geometry of the ATLAS detector is determined. We would like to express our sincerest thanks to John Rutherfoord and Mike Shupe at the University of Arizona at Tucson for their initiation and support of this work.

References

[Pra89]   R. E. Prael and H. Lichtenstein, "User Guide to LCS: The LAHET^{TM} Code System", LA-UR-89-3014, Los Alamos National Laboratory, Sept. 15, 1989.

[Bre81]   J. F. Briesmeister, ed., "MCNP^{TM} - A General Monte Carlo Code for Neutron and Photon Transport version 4A", LA-12625-M, Los Alamos National Laboratory, November 1993.

[Wil93]   W. B. Wilson, et. al., "Accelerator Transmutation Studies at Los Alamos with LAHET^{TM}, MCNP^{TM} and CINDER'90, LA-UR-93-3080, Los Alamos National Laboratory, January 11, 1993.

[Aur90]   P. Aurenche, F. Bopp, K. Hahn, M. Marie and J. Ranft, "DTUJET-90, Sampling Inelastic $p-p$ and $\bar{p}-p$ Collisions According to the Dual Topological Unitarization of Hard and Soft Hadronic Processes" unnumbered manual, L. P. T. H. E., Universitè de Paris XI, Orsay, France, 1990.

[Pra94]   R. E. Prael, "A Review of Physics Models in the LAHET^{TM} Code, LA-UR-94-1817, Los Alamos National Laboratory, May, 1994.

[Ros71]   H. H. Rossi, chairman, "Protection Against Neutron Radiation," NCRP-38, National Council on Radiation Protection and Measurements, January, 1971.

[Hal92]   J. A. Halbleib, et. al., "ITS Version 3.0: The Integrated TIGER Series of Coupled Electron/Photon Monte Carlo Transport Codes" SAND91-1634 Sandia National Laboratories, March 1992

[For94]   R. A. Forster, S. P. Pederson and T. E. Booth, 'Ten New Checks to Assess the Statistical Quality of Monte Carlo Soloutions in MCNP^{TM}', Proceedings of the 8th International Conference on Radiation Shielding, pp 414, Arlington, Texas, April 24-28, 1994.

SYSTEM	Name	R_{min}	R_{max}	Z_{min}	Z_{max}
FCAL					
	BPOLY	7.2	45.319	454.00	
		7.2	47.31544		474.00
	FCAL1	7.2	53.3083	474.00	514.00
	FCAL2	7.959494	58.29938	524.00	564.00
	FCAL3	8.567089	62.29225	564.00	604.00
EM Accordian					
	EM	35.2	200.00	352.00	421.00
Shielding					
	CU	75.00	179.00	612.00	632.00
	UPLUG	6.5	80.0	340.00	345.00
	DPLUG	6.5	80.0	654.00	659.00

Table 1: **Geometry Dimensions and Positions**
All volumes are cylindrically symmetric. Dimensions are in cm. The beam direction corresponds to the Z axis.

Name	MCNP	wt frac.	LAHET	Iso frac.	Temp °K	Density g/cc
BPOLY	H1	.115965	H1	.99985	300	.95
	H2	3.477e-5	H2	.00015		
	B10	.0092155	B10	.199		
	B11	.0407845	B11	.801		
	C12	.612	C12	.989		
			C13	.011		
	O16	.222	O16	.9976		
			O17	.0004		
			O18	.0020		
FCAL1	Ar_{nat}	.013877	Ar36	.00337	88	7.952
			Ar38	.00063		
			Ar40	.99600		
	Cu_{nat}	.690037	Cu63	.6917		
			Cu65	.3083		
	Zn_{nat}	.296086	Zn64	.486		
			Zn66	.279		
			Zn67	.041		
			Zn68	.188		
			Zn70	.006		
FCAL2&3	Ar_{nat}	.04210	Ar36	.00337	88	17.31
			Ar38	.00063		
			Ar40	.99600		
	Fe_{nat}	.02110	Fe54	.0582		
			Fe56	.9180		
			Fe57	.0210		
			Fe58	.0028		
	Ni_{nat}	.06719	Ni58	.6827		
			Ni60	.2610		
			Ni61	.0113		
			Ni62	.0359		
			Ni64	.0091		
	Cu_{nat}	.0286	Cu63	.6917		
			Cu65	.3083		
	W_{nat}	.84101	W180	.0012		
			W182	.2630		
			W183	.1428		
			W184	.3070		
			W186	.3070		

EM	Pb_{nat}	1.0	NA	300	4.0
CU	Cu_{nat}	1.0	NA	300	8.96
PLUGs	Pb_{nat}	1.0	NA	300	11.3
AIR	H1	5.5949e-4	NA	300	.001299
	N14	.752407	NA		
	N15	.002993	NA		
	O16	.2315	NA		
	Ar_{nat}	.0131	NA		

Table 2: **MCNP and LAHET Materials Definition**
The MCNP column lists neutron libraries used in the low energy neutron fluence calculation, along with the weight fractions specified. The LAHET column shows the specific isotopes used in the code, along with the isotopic percent abundance used for each element. No LAHET calculations were necessary for the shielding elements, therefore these columns are blank for EM, CU and the PLUGS. The MCNP weight fractions were also used in LAHET. Air contains .5% water by weight. A special $S(\alpha, \beta)$ thermal scattering treatment was used for polyethylene in the BPOLY component.

Number	Seconds	Cycle	Beam	Time in Cycle
1	600	one	on	10 minutes
2	3600	one	on	1 hour
3	86400	one	on	1 day
4	2592000	one	on	30 days
5	2678400	one	off	31 day
6	2851200	one	off	33 days
7	3456000	one	off	40 days
8	3456600	two	on	10 minutes
9	3459600	two	on	1 hour
10	3542400	two	on	1 day
11	6048000	two	on	30 days
12	6134400	two	off	31 day
13	6307200	two	off	33 days
14	6912000	two	off	40 days
15	6912600	three	on	10 minutes
16	6915600	three	on	1 hour
17	6998400	three	on	1 day
18	9504000	three	on	30 days
19	9590400	three	off	31 day
20	9763200	three	off	33 days
21	10368000	three	off	40 days
22	10368060	four	on	10 minutes
23	10371600	four	on	1 hour
24	10454400	four	on	1 day
25	12960000	four	on	30 days
26	13046400	four	off	31 day
27	13219200	four	off	33 days
28	13824000	four	off	40 days
29	18144000	four	off	90 days
30	31536000	four	off	end of year

Table 3: **Times at which CINDER'90 Data are calculated**
The CINDER'90 calculations are available at the above points in time. We assume 4 periods of beam on for 30 days, each followed by a 10 day shutdown. The beam remains off for the remainder of the year.

Major Contributions to Activity (> .1 %) in first fcal
Percent of Total

nucl	Cycle One				Down Time			Cycle Two			Down Time			Cycle 3		Down Time			Cycle 4		Post Shutdown				
	10mn	1hr	1day	30 d	1day	3day	10 d	1hr	1day	30 d	1day	3day	10 d	1day	30 d	1day	3day	10 d	1day	30 d	1day	3day	10 d	60 d	1 yr
Ar 41	0.1	0.2	0.2	0.1	0.0	0.0	0.0	0.2	0.1	0.1	0.0	0.0	0.0	0.1	0.1	0.0	0.0	0.0	0.1	0.1	0.0	0.0	0.0	0.0	0.0
Co 60	0.0	0.0	0.0	0.4	0.0	0.2	0.4	0.0	0.0	0.0	0.0	0.3	0.4	0.0	0.0	0.0	0.3	0.5	0.0	0.0	0.1	0.3	0.5	0.5	0.8
Co 60*	1.0	1.2	0.4	0.0	0.2	0.0	0.0	1.1	0.4	0.3	0.0	0.0	0.0	0.3	0.3	0.0	0.0	0.0	0.3	0.3	0.0	0.0	0.0	0.0	0.0
Co 62	0.5	0.3	0.1	0.1	0.0	0.0	0.0	0.3	0.1	0.1	0.0	0.0	0.0	0.2	0.1	0.0	0.0	0.0	0.1	0.1	0.0	0.0	0.0	0.0	0.0
Ni 63	0.0	0.0	0.0	0.1	0.0	0.1	0.2	0.0	0.2	0.1	0.0	0.1	0.2	0.2	0.1	0.0	0.1	0.2	0.2	0.1	0.0	0.0	0.2	0.3	0.4
Ni 65	0.0	0.1	0.2	0.0	0.0	0.0	0.0	0.1	0.2	0.1	0.0	0.0	0.0	0.2	0.1	0.0	0.0	0.0	0.2	0.1	0.0	0.0	0.0	0.0	0.0
Cu 62	14.5	15.9	4.9	3.8	0.0	0.0	0.0	15.2	4.8	3.8	0.0	0.0	0.0	4.7	3.7	0.0	0.0	0.0	4.7	3.7	0.0	0.0	0.0	0.0	0.0
Cu 64	5.2	17.4	72.0	76.7	93.0	54.5	0.0	16.5	70.9	75.9	88.7	39.1	0.0	70.0	75.1	85.1	31.3	0.0	69.1	74.5	82.2	26.5	0.0	0.0	0.0
Cu 66	75.2	57.3	17.3	13.5	0.0	0.0	0.0	54.6	17.0	13.3	0.0	0.0	0.0	16.8	13.2	0.0	0.0	0.0	16.6	13.1	0.0	0.0	0.0	0.0	0.0
Cu 67	0.0	0.0	0.0	0.0	0.1	0.6	0.0	0.0	0.0	0.0	0.1	0.4	0.0	0.0	0.0	0.1	0.4	0.0	0.0	0.0	0.1	0.3	0.1	0.0	0.0
Cu 68	0.2	0.1	0.0	0.0	0.0	0.0	0.0	0.1	0.0	0.0	0.0	0.0	0.0	0.0	0.0	0.0	0.0	0.0	0.0	0.0	0.0	0.0	0.0	0.0	0.0
Cu 68*	0.1	0.6	0.3	0.2	0.0	0.0	0.0	0.6	0.3	0.2	0.0	0.0	0.0	0.3	0.2	0.0	0.0	0.0	0.3	0.2	0.0	0.0	0.0	0.0	0.0
Zn 63	0.3	0.0	0.1	0.0	0.0	0.0	0.0	0.0	1.5	2.3	0.0	0.0	0.0	2.8	3.2	0.0	0.0	0.0	4.0	4.0	0.0	0.0	0.0	0.0	0.0
Zn 65	0.0	0.0	0.0	0.1	5.5	43.7	99.1	4.8	0.0	0.0	9.9	59.3	99.2	0.0	0.0	13.4	67.4	99.2	4.0	4.3	16.4	72.2	99.2	99.2	98.8
Zn 69	2.5	6.5	4.1	3.4	0.7	0.5	0.0	6.2	4.1	3.3	0.7	0.4	0.0	4.0	3.3	0.6	0.3	0.0	0.4	0.5	0.6	0.2	0.0	0.0	0.0
Zn 69*	0.0	0.1	0.4	0.5	0.7	0.5	0.0	0.1	0.4	0.5	0.6	0.3	0.0	0.4	0.5	0.6	0.3	0.0	0.0	0.0	0.6	0.6	0.0	0.0	0.0
Zn 71	0.2	0.1	0.0	0.0	0.0	0.0	0.0	0.1	0.0	0.0	0.0	0.0	0.0	0.0	0.0	0.0	0.0	0.0	0.0	0.0	0.0	0.0	0.0	0.0	0.0
all 408 others	0.1	0.1	0.1	0.1	0.0	0.0	0.0	0.1	0.1	0.1	0.0	0.0	0.0	0.1	0.1	0.0	0.0	0.0	0.1	0.0	0.0	0.0	0.0	0.0	0.0
Total	100	100	100	100	100	100	100	100	100	100	100	100	100	100	100	100	100	100	100	100	100	100	100	100	100

Major Contributions to Decay Power (> .1 %) In first fcal
Percent of Total

nucl	Cycle One				Down Time			Cycle Two			Down Time			Cycle 3		Down Time			Cycle 4		Post Shutdown				
	10mn	1hr	1day	30 d	1day	3day	10 d	1hr	1day	30 d	1day	3day	10 d	1day	30 d	1day	3day	10 d	1day	30 d	1day	3day	10 d	60 d	1 yr
Cl 40	0.4	0.2	0.1	0.1	0.0	0.0	0.0	0.2	0.1	0.1	0.0	0.0	0.0	0.1	0.1	0.0	0.0	0.0	0.1	0.1	0.0	0.0	0.0	0.0	0.0
Ar 41	0.1	0.2	0.4	0.4	0.0	0.0	0.0	0.2	0.5	0.4	0.0	0.0	0.0	0.4	0.4	0.0	0.0	0.0	0.4	0.4	0.0	0.0	0.0	0.0	0.0
Co 60	0.0	0.0	0.0	0.0	0.2	1.0	1.8	0.0	0.0	0.0	0.0	1.3	1.9	0.1	0.1	0.4	1.5	2.0	0.1	0.1	0.6	1.7	2.1	2.4	3.4
Co 62	1.5	1.0	0.6	0.0	0.0	0.0	0.0	0.9	0.6	0.2	0.0	0.0	0.0	0.6	0.2	0.0	0.0	0.0	0.6	0.2	0.0	0.0	0.0	0.0	0.0
Co 62*	0.3	0.4	0.2	0.3	0.0	0.0	0.0	0.4	0.2	0.3	0.0	0.0	0.0	0.2	0.3	0.0	0.0	0.0	0.2	0.3	0.0	0.0	0.0	0.0	0.0
Ni 65	0.0	0.1	0.3	0.0	0.0	0.0	0.0	0.1	0.4	0.3	0.0	0.0	0.0	0.3	0.3	0.0	0.0	0.0	0.3	0.4	0.0	0.0	0.0	0.0	0.0
Cu 62	25.8	31.5	19.4	16.6	0.0	0.0	0.0	30.7	19.1	16.4	0.0	0.0	0.0	18.8	16.2	0.0	0.0	0.0	18.6	16.1	0.0	0.0	0.0	0.0	0.0
Cu 64	1.3	4.7	39.2	46.0	86.4	36.0	0.0	4.6	38.6	45.5	79.5	24.1	0.0	38.1	45.0	74.2	18.6	0.0	37.6	44.5	70.0	15.4	0.0	0.0	0.0
Cu 66	67.5	57.3	34.8	29.8	0.0	0.0	0.0	55.8	34.2	29.4	0.0	0.0	0.0	33.7	29.1	0.0	0.0	0.0	33.3	28.8	0.0	0.0	0.0	0.0	0.0
Cu 67	0.0	0.0	0.1	0.4	2.4	7.9	2.2	0.0	0.0	0.4	2.2	5.3	1.2	0.1	0.4	2.0	4.1	0.8	0.1	0.4	1.9	3.4	0.6	0.0	0.0
Cu 68	1.2	0.8	0.3	0.2	0.0	0.0	0.0	0.8	0.5	0.2	0.0	0.0	0.0	0.5	0.2	0.0	0.0	0.0	0.5	0.2	0.0	0.0	0.0	0.0	0.0
Cu 68*	0.6	0.5	0.9	0.8	0.0	0.0	0.0	0.5	0.3	0.8	0.0	0.0	0.0	0.9	0.8	0.0	0.0	0.0	0.9	0.8	0.0	0.0	0.0	0.0	0.0
Zn 63	0.4	1.0	0.1	1.4	0.0	0.0	0.0	1.0	0.9	2.6	0.0	0.0	0.0	2.9	3.6	0.0	0.0	0.0	4.1	4.5	0.0	0.0	0.0	0.0	0.0
Zn 65	0.0	0.0	0.0	2.1	9.6	54.3	96.0	2.5	1.6	2.1	16.6	68.8	96.9	2.3	2.0	22.1	75.4	97.2	2.2	2.0	26.3	79.2	97.2	97.6	96.6
Zn 69	0.6	1.8	2.3	0.4	0.7	0.3	0.0	1.8	2.3	2.1	0.6	0.2	0.0	2.0	2.0	0.6	0.2	0.0	2.0	0.4	0.5	0.1	0.0	0.0	0.0
Zn 69*	0.0	0.0	0.3	0.1	0.8	0.4	0.0	0.0	0.3	0.4	0.8	0.3	0.0	0.3	0.4	0.7	0.2	0.0	0.3	0.1	0.7	0.2	0.0	0.0	0.0
Zn 71	0.2	0.1	0.1	0.1	0.0	0.0	0.0	0.1	0.1	0.1	0.0	0.0	0.0	0.1	0.1	0.0	0.0	0.0	0.1	0.1	0.0	0.0	0.0	0.0	0.0
all 408 others	0.2	0.2	0.2	0.2	0.0	0.0	0.0	0.2	0.2	0.2	0.0	0.0	0.0	0.2	0.2	0.0	0.0	0.0	0.2	0.2	0.0	0.0	0.0	0.0	0.0
Total	100	100	100	100	100	100	100	100	100	100	100	100	100	100	100	100	100	100	100	100	100	100	100	100	100

Major Contributions to Activity (> .1 %) in second fcal

nucl	Cycle One				Down Time			Cycle Two			Down Time			Cycle 3		Down Time			Cycle 4		Post Shutdown				
	10mn	1hr	1day	30 d	1day	3day	10 d	1hr	1day	30 d	1day	3day	10 d	1day	30 d	1day	3day	10 d	1day	30 d	1day	3day	10 d	60 d	1 yr
Ar 41	0.1	0.5	0.9	0.6	0.0	0.0	0.0	0.4	0.8	0.5	0.0	0.0	0.0	0.7	0.5	0.0	0.0	0.0	0.6	0.5	0.0	0.0	0.0	0.0	0.0
Mn 54	0.0	0.0	0.0	0.0	0.0	0.0	0.0	0.0	0.0	0.0	0.0	0.0	0.0	0.0	0.0	0.0	0.0	0.0	0.0	0.0	0.1	0.1	0.1	0.1	0.2
Mn 56	0.0	0.1	0.2	0.1	0.0	0.0	0.0	0.1	0.2	0.1	0.0	0.0	0.0	0.1	0.1	0.0	0.0	0.0	0.1	0.1	0.0	0.0	0.0	0.0	0.0
Fe 55	0.0	0.0	0.0	0.0	0.0	0.0	0.1	0.0	0.0	0.0	0.1	0.1	0.1	0.1	0.1	0.1	0.2	0.1	0.0	0.0	0.1	0.1	0.1	0.2	0.7
Co 57	0.0	0.0	0.0	0.0	0.1	0.2	0.4	0.0	0.1	0.1	0.2	0.3	0.4	0.1	0.1	0.2	0.3	0.4	0.1	0.0	0.3	0.4	0.5	0.6	1.7
Co 58	0.0	0.4	2.5	1.9	1.8	3.3	4.5	1.1	0.8	1.7	2.6	3.8	4.4	1.2	1.2	2.6	3.8	4.4	1.4	1.3	2.7	3.8	4.4	4.2	3.6
Co 58*	0.1	0.4	0.0	0.0	0.9	0.0	0.0	0.4	2.1	0.0	0.6	0.0	0.0	1.9	0.0	0.6	0.0	0.0	1.7	0.0	0.5	0.0	0.0	0.0	0.0
Co 60	0.0	0.0	0.0	0.1	0.0	0.0	0.0	0.0	0.0	0.0	0.0	0.0	0.0	0.0	0.0	0.0	0.0	0.0	0.0	0.0	0.0	0.0	0.0	0.0	0.1
Co 60*	0.1	0.2	0.1	0.1	0.0	0.0	0.0	0.2	0.1	0.1	0.0	0.0	0.0	0.2	0.1	0.0	0.0	0.0	0.2	0.2	0.0	0.0	0.0	0.0	0.0
Cu 62	0.3	0.5	0.3	0.2	0.0	0.0	0.0	0.4	0.1	0.0	0.0	0.0	0.0	0.1	0.2	0.0	0.0	0.0	0.2	0.2	0.0	0.0	0.0	0.0	0.0
Cu 64	0.1	0.5	4.4	3.8	2.9	0.4	0.0	0.4	3.6	3.5	2.0	0.3	0.0	3.2	3.3	2.0	0.2	0.0	3.0	3.1	1.8	0.2	0.0	0.0	0.0
Cu 66	1.7	2.2	1.4	0.9	0.0	0.0	0.0	1.7	1.1	0.8	0.0	0.0	0.0	1.0	0.8	0.0	0.0	0.0	0.9	0.7	0.0	0.0	0.0	0.0	0.0
W 181	0.0	0.0	0.0	0.8	2.2	4.0	5.5	1.4	1.0	1.3	3.5	4.7	5.8	1.0	1.6	3.5	5.2	6.1	1.9	1.9	3.9	5.5	6.4	7.6	12.2
W 183*	93.4	89.0	55.5	35.5	0.0	0.0	0.0	66.9	46.1	32.5	0.0	0.0	0.0	41.2	30.5	0.0	0.0	0.0	38.4	27.9	0.0	0.0	0.0	0.0	0.0
W 185	0.1	0.1	0.8	13.0	35.8	65.7	89.1	22.2	15.8	20.0	47.4	73.5	88.9	23.4	24.1	52.7	76.3	88.6	27.9	26.6	55.6	77.5	88.4	87.2	81.4
W 185*	3.5	3.4	2.1	1.4	0.0	0.0	0.0	2.6	1.8	1.3	0.0	0.0	0.0	1.6	1.2	0.0	0.0	0.0	1.5	1.1	0.0	0.0	0.0	0.0	0.0
W 187	0.5	2.9	31.5	40.5	56.1	26.1	0.3	2.2	26.2	36.7	43.9	17.2	0.2	23.4	34.5	38.1	13.9	0.1	21.8	33.1	34.9	12.3	0.1	0.0	0.0
all1332 others	0.2	0.3	0.3	0.2	0.1	0.2	0.2	0.2	0.3	0.2	0.1	0.1	0.1	0.2	0.2	0.1	0.1	0.1	0.2	0.2	0.1	0.1	0.1	0.1	0.1
Total	100	100	100	100	100	100	100	100	100	100	100	100	100	100	100	100	100	100	100	100	100	100	100	100	100

Major Contributions to Decay Power (> .1 %) in second fcal

nucl	Cycle One				Down Time			Cycle Two			Down Time			Cycle 3		Down Time			Cycle 4		Post Shutdown				
	10mn	1hr	1day	30 d	1day	3day	10 d	1hr	1day	30 d	1day	3day	10 d	1day	30 d	1day	3day	10 d	1day	30 d	1day	3day	10 d	60 d	1 yr
S 37	0.4	0.5	0.2	0.1	0.0	0.0	0.0	0.4	0.2	0.1	0.0	0.0	0.0	0.2	0.1	0.0	0.0	0.0	0.2	0.1	0.0	0.0	0.0	0.0	0.0
Cl 39	0.1	0.4	0.4	0.2	0.0	0.0	0.0	0.4	0.4	0.2	0.0	0.0	0.0	0.4	0.2	0.0	0.0	0.0	0.3	0.2	0.0	0.0	0.0	0.0	0.0
Cl 40	2.2	1.9	0.9	0.6	0.0	0.0	0.0	1.6	0.8	0.5	0.0	0.0	0.0	0.8	0.5	0.0	0.0	0.0	0.8	0.5	0.0	0.0	0.0	0.0	0.0
Ar 41	0.5	2.4	3.5	2.2	0.0	0.0	0.0	2.0	3.3	2.1	0.0	0.0	0.0	3.1	2.1	0.0	0.0	0.0	3.1	2.1	0.1	0.0	0.0	0.0	0.0
Mn 54	0.0	0.0	0.0	0.0	0.0	0.0	0.0	0.0	0.0	0.0	0.0	0.0	0.0	0.0	0.0	0.0	0.0	0.0	0.0	0.0	0.1	0.2	0.3	0.4	1.1
Mn 56	0.1	0.5	1.0	0.7	0.0	0.0	0.0	0.4	1.0	0.6	0.0	0.0	0.0	0.9	0.6	0.0	0.0	0.0	0.9	0.6	0.1	0.0	0.0	0.0	0.0
Co 57	0.0	0.0	0.0	0.0	0.1	0.1	0.2	0.0	0.1	0.1	0.1	0.2	0.3	0.1	0.0	0.1	0.2	0.3	0.0	0.0	0.1	0.2	0.4	0.5	1.4
Co 58	0.0	0.5	1.0	0.7	5.8	14.3	27.4	3.7	1.9	2.3	7.0	15.9	27.2	3.0	2.8	7.0	15.9	27.2	3.7	3.2	7.7	16.7	27.1	26.5	23.7
Co 58*	0.0	0.0	0.1	0.2	0.2	0.2	0.3	0.1	0.1	0.2	0.2	0.2	0.3	0.1	0.1	0.2	0.2	0.3	0.1	0.1	0.2	0.2	0.3	0.2	0.0
Co 60	0.0	0.0	0.0	0.0	0.0	0.0	0.0	0.0	0.0	0.0	0.0	0.0	0.0	0.0	0.0	0.0	0.0	0.0	0.0	0.0	0.0	0.0	0.0	0.5	2.0
Co 60*	0.0	0.0	0.1	0.0	0.0	0.0	0.0	0.1	0.0	0.0	0.0	0.0	0.0	0.1	0.0	0.0	0.0	0.0	0.1	0.0	0.0	0.0	0.0	0.0	0.0
Co 62	0.0	0.0	0.1	0.0	0.0	0.0	0.0	0.1	0.1	0.1	0.0	0.0	0.0	0.1	0.1	0.0	0.0	0.0	0.1	0.1	0.0	0.0	0.0	0.0	0.0
Co 62*	0.1	0.1	0.1	0.2	0.0	0.0	0.0	0.1	0.1	0.2	0.0	0.0	0.0	0.1	0.2	0.0	0.0	0.0	0.1	0.2	0.0	0.0	0.0	0.0	0.0
Ni 57	0.0	0.0	0.1	0.1	0.1	0.1	0.2	0.1	0.1	0.1	0.2	0.2	0.3	0.1	0.1	0.2	0.2	0.3	0.1	0.1	0.2	0.3	0.2	0.2	0.5
Ni 65	0.0	0.1	0.2	0.1	0.0	0.0	0.0	0.1	0.2	0.1	0.0	0.0	0.0	0.1	0.1	0.0	0.0	0.0	0.1	0.1	0.0	0.0	0.0	0.0	0.0
Cu 62	2.0	3.4	1.6	1.0	0.0	0.0	0.0	3.0	1.5	1.0	0.0	0.0	0.0	1.5	1.0	0.0	0.0	0.0	1.4	1.0	0.0	0.0	0.0	0.0	0.0
Cu 64	0.1	0.5	2.9	2.5	1.7	0.3	0.0	2.6	2.7	2.5	1.6	0.3	0.0	2.6	2.4	1.6	0.3	0.0	2.5	2.4	1.6	0.3	0.0	0.0	0.0
Cu 66	6.1	7.2	3.4	2.2	0.0	0.0	0.0	6.3	3.2	2.1	0.0	0.0	0.0	3.0	2.0	0.0	0.0	0.0	2.9	2.0	0.0	0.0	0.0	0.0	0.0
Ta182	0.0	0.0	0.0	0.0	0.0	0.0	0.0	0.0	0.0	0.0	0.0	0.0	0.0	0.0	0.0	0.0	0.0	0.0	0.0	0.0	0.1	0.1	0.2	0.3	0.5
Ta183	0.0	0.0	0.0	0.0	0.0	0.0	0.0	0.0	0.0	0.0	0.2	0.2	0.1	0.0	0.0	0.2	0.2	0.1	0.0	0.0	0.5	1.1	1.9	2.3	3.8
W 181	0.0	0.0	0.0	0.2	0.0	0.0	0.0	0.1	0.1	0.1	0.2	0.2	0.3	0.1	0.1	0.2	0.2	0.3	0.1	0.1	0.3	0.3	0.4	0.5	0.0
W 183*	84.9	74.8	35.2	22.4	0.0	0.0	0.0	64.7	32.9	21.6	0.0	0.0	0.0	31.4	21.1	0.0	0.0	0.0	30.5	20.8	0.0	0.0	0.0	0.0	0.0
W 185	0.0	0.0	0.2	4.8	9.4	26.8	68.5	7.7	4.8	5.7	14.6	35.8	68.9	7.2	7.2	17.7	40.1	69.1	8.1	9.5	19.6	42.5	69.1	69.4	67.5
W 185*	2.0	1.8	0.8	0.5	0.0	0.0	0.0	1.5	0.8	0.5	0.0	0.0	0.0	0.7	0.5	0.0	0.0	0.0	0.7	0.5	0.0	0.0	0.0	0.0	0.0
W 187	1.1	5.9	48.8	61.8	84.1	60.5	1.3	5.3	45.6	59.8	76.9	47.8	0.8	43.6	58.4	72.6	41.7	0.6	42.3	57.5	69.9	38.3	0.5	0.0	0.0
all1325 others	0.1	0.2	0.2	0.1	0.2	0.1	0.2	0.2	0.2	0.2	0.1	0.1	0.2	0.2	0.1	0.1	0.1	0.2	0.1	0.1	0.1	0.1	0.1	0.1	0.1
Total	100	100	100	100	100	100	100	100	100	100	100	100	100	100	100	100	100	100	100	100	100	100	100	100	100

Table 4c

Major Contributions to Activity (> .1 %) in third fcal
of the Forward Calorimeter of the ATLAS Detector for the Large Hadron Collider

	Cycle One				Down Time			Cycle Two			Down Time			Cycle 3		Down Time			Cycle 4		Post Shutdown				
nucl	10mn	1hr	1day	30 d	1day	3day	10 d	1hr	1day	30 d	1day	3day	10 d	1day	30 d	1day	3day	10 d	1day	30 d	1day	3day	10 d	60 d	1 yr
Ar 41	0.1	0.5	1.0	0.6	0.0	0.0	0.0	0.4	0.8	0.6	0.0	0.0	0.0	0.7	0.5	0.0	0.0	0.0	0.7	0.5	0.0	0.0	0.0	0.0	0.0
Mn 54	0.0	0.0	0.0	0.0	0.0	0.0	0.0	0.0	0.0	0.0	0.0	0.0	0.0	0.0	0.0	0.0	0.0	0.0	0.0	0.0	0.0	0.0	0.0	0.1	0.2
Mn 56	0.0	0.1	0.1	0.1	0.0	0.0	0.0	0.0	0.1	0.1	0.0	0.0	0.0	0.1	0.1	0.0	0.0	0.0	0.1	0.0	0.0	0.0	0.0	0.0	0.0
Fe 55	0.0	0.0	0.0	0.0	0.0	0.0	0.1	0.0	0.0	0.0	0.1	0.1	0.1	0.0	0.0	0.1	0.1	0.1	0.1	0.1	0.1	0.1	0.1	0.2	0.6
Co 57	0.0	0.0	0.0	0.0	0.1	0.2	0.3	0.1	0.0	0.0	0.2	0.2	0.3	0.0	0.1	0.2	0.2	0.3	0.1	0.1	0.2	0.3	0.3	0.5	1.3
Co 58	0.1	0.3	1.9	0.5	1.3	2.5	3.4	0.9	0.6	0.8	1.8	2.8	3.3	0.9	0.9	1.8	2.9	3.3	2.1	1.1	2.1	2.9	3.3	3.2	2.8
Co 58*	0.1	0.2	1.5	0.1	0.6	0.0	0.0	0.2	1.6	1.3	0.5	0.0	0.0	1.4	1.3	0.5	0.0	0.0	0.4	1.3	0.4	0.0	0.0	0.0	0.0
Co 60*	0.1	0.2	0.1	0.2	0.0	0.0	0.0	0.1	0.1	0.1	0.0	0.0	0.0	0.1	0.1	0.0	0.0	0.0	0.0	0.1	0.0	0.0	0.0	0.0	0.0
Cu 62	0.2	0.4	0.3	0.1	0.0	0.0	0.0	0.3	0.2	0.2	0.0	0.0	0.0	0.2	0.2	0.0	0.0	0.0	0.2	0.1	0.0	0.0	0.0	0.0	0.0
Cu 64	0.1	0.6	4.6	4.0	3.0	0.4	0.0	0.4	3.8	3.7	2.0	0.3	0.0	3.4	3.4	1.9	0.2	0.0	1.9	3.2	1.9	0.2	0.2	0.0	0.0
Cu 66	1.9	2.4	1.5	0.9	0.0	0.0	0.0	1.8	1.2	1.2	0.0	0.0	0.0	1.1	1.1	0.0	0.0	0.0	1.0	1.0	0.0	0.0	0.0	0.0	0.0
W 181	0.0	0.0	0.0	0.6	1.6	3.1	4.3	1.1	0.8	1.0	2.7	4.0	4.8	1.2	1.3	2.3	3.7	4.6	3.0	1.5	4.3	5.0	5.0	5.9	9.7
W 183*	93.9	89.4	54.4	34.6	0.0	0.0	0.0	66.4	45.0	31.4	0.0	0.0	0.0	40.2	29.5	0.0	0.0	0.0	37.4	28.3	0.0	0.0	0.0	0.0	0.0
W 185	0.0	0.1	0.8	13.4	36.1	66.8	91.5	23.5	16.4	20.6	47.9	75.1	91.4	24.4	24.8	53.5	78.0	91.2	29.0	27.5	56.5	79.4	91.0	90.1	85.4
W 185*	2.9	2.8	1.7	1.1	0.0	0.0	0.0	2.1	1.4	1.0	0.0	0.0	0.0	1.3	0.9	0.0	0.0	0.0	1.2	0.9	0.0	0.0	0.0	0.0	0.0
W 187	0.6	3.1	33.3	42.2	57.1	26.8	0.3	2.4	27.6	38.3	44.9	17.8	0.2	24.6	36.0	39.0	14.4	0.1	22.9	34.6	35.8	12.7	0.1	0.0	0.0
all1076 others	0.2	0.2	0.2	0.2	0.1	0.1	0.1	0.2	0.2	0.2	0.1	0.1	0.1	0.2	0.2	0.1	0.1	0.1	0.2	0.2	0.1	0.1	0.1	0.1	0.2
Total	100	100	100	100	100	100	100	100	100	100	100	100	100	100	100	100	100	100	100	100	100	100	100	100	100

Major Contributions to Decay Power (> .1 %) in third fcal
of the Forward Calorimeter of the ATLAS Detector for the Large Hadron Collider

	Cycle One				Down Time			Cycle Two			Down Time			Cycle 3		Down Time			Cycle 4		Post Shutdown				
nucl	10mn	1hr	1day	30 d	1day	3day	10 d	1hr	1day	30 d	1day	3day	10 d	1day	30 d	1day	3day	10 d	1day	30 d	1day	3day	10 d	60 d	1 yr
S 37	0.3	0.4	0.2	0.1	0.0	0.0	0.0	0.3	0.2	0.1	0.0	0.0	0.0	0.2	0.1	0.0	0.0	0.0	0.2	0.1	0.0	0.0	0.0	0.0	0.0
Cl 39	0.1	0.4	0.3	0.2	0.0	0.0	0.0	0.3	0.3	0.2	0.0	0.0	0.0	0.3	0.2	0.0	0.0	0.0	0.3	0.2	0.0	0.0	0.0	0.0	0.0
Cl 40	1.7	1.5	0.7	0.4	0.0	0.0	0.0	1.3	0.6	0.4	0.0	0.0	0.0	0.6	0.4	0.0	0.0	0.0	0.6	0.4	0.0	0.0	0.0	0.0	0.0
Ar 41	0.6	2.5	3.6	2.3	0.0	0.0	0.1	2.2	3.4	2.2	0.0	0.0	0.2	3.3	2.2	0.0	0.0	0.2	3.2	2.1	0.1	0.1	0.2	0.3	0.9
Mn 54	0.0	0.0	0.0	0.0	0.0	0.0	0.0	0.0	0.0	0.0	0.0	0.0	0.0	0.0	0.0	0.0	0.0	0.0	0.0	0.0	0.0	0.0	0.0	0.3	0.0
Mn 56	0.1	0.4	0.8	0.5	0.0	0.0	0.0	0.3	0.7	0.5	0.1	0.1	0.3	0.7	0.5	0.1	0.1	0.3	0.7	0.4	0.1	0.1	0.4	0.4	1.1
Co 57	0.0	0.4	0.0	0.0	0.1	0.1	0.2	0.0	0.0	0.0	0.1	0.1	0.3	0.0	0.0	0.1	0.1	0.3	0.1	0.0	0.1	0.2	0.3	0.4	1.1
Co 58	0.0	0.0	0.0	1.0	2.8	8.2	22.0	2.9	1.5	1.7	5.2	12.2	21.9	2.3	2.1	4.3	10.9	21.8	5.8	2.4	5.8	12.9	21.7	21.2	19.0
Co 60	0.0	0.0	0.0	0.0	0.1	0.1	0.2	0.0	0.1	0.0	0.1	0.1	0.2	0.0	0.0	0.1	0.1	0.2	0.0	0.0	0.1	0.3	0.3	0.4	1.6
Co 62	0.1	0.1	0.1	0.1	0.0	0.0	0.0	0.1	0.1	0.1	0.0	0.0	0.0	0.1	0.1	0.0	0.0	0.0	0.1	0.0	0.0	0.0	0.0	0.0	0.0
Ni 57	0.0	0.0	0.2	0.1	0.2	0.2	0.0	0.1	0.1	0.1	0.2	0.2	0.0	0.1	0.1	0.2	0.2	0.0	0.1	0.1	0.2	0.2	0.0	0.0	0.0
Ni 65	0.1	0.2	1.2	0.8	1.8	0.3	0.0	2.3	1.2	0.7	1.7	0.3	0.0	1.1	0.7	1.8	0.3	0.0	1.1	0.7	1.6	0.3	0.0	0.0	0.0
Cu 62	1.6	2.7	3.1	2.6	0.0	0.0	0.0	2.3	2.9	2.5	0.0	0.0	0.0	2.8	2.5	0.0	0.0	0.0	2.7	2.5	0.0	0.0	0.0	0.0	0.0
Cu 64	0.1	0.5	3.6	2.3	1.9	0.4	0.0	0.4	3.4	2.2	0.0	0.0	0.0	3.3	2.2	0.0	0.0	0.0	3.2	2.1	0.0	0.0	0.0	0.2	0.4
Cu 66	6.8	8.0	0.0	0.0	0.0	0.0	0.0	7.0	0.0	0.0	0.0	0.0	0.0	0.0	0.0	0.0	0.0	0.0	0.0	0.0	0.0	0.0	0.0	1.9	3.1
Ta182	0.0	0.0	0.0	0.1	0.2	0.5	1.3	0.2	0.1	0.1	0.3	0.7	1.4	0.1	0.1	0.3	0.7	1.5	0.4	0.2	0.4	0.9	1.6	0.0	0.0
W 181	0.0	0.0	0.0	0.0	0.0	0.0	0.0	0.2	0.0	0.0	0.0	0.0	0.0	0.0	0.0	0.0	0.0	0.0	0.0	0.0	0.0	0.0	0.0	0.0	0.0
W 183*	85.6	75.2	34.1	21.4	0.0	0.0	0.0	65.2	31.9	20.7	0.0	0.0	0.0	30.5	20.3	0.0	0.0	0.0	29.7	20.0	0.0	0.0	0.0	0.0	0.0
W 185	0.0	0.0	0.2	3.6	9.5	27.5	74.4	9.9	5.0	5.8	17.9	41.9	75.0	8.0	7.3	14.7	37.2	74.9	9.9	8.3	19.9	44.5	75.1	75.5	73.8
W 185*	1.6	1.5	0.7	0.4	0.0	0.0	0.0	1.3	0.6	0.4	0.0	0.0	0.0	0.6	0.4	0.0	0.0	0.0	0.6	0.4	0.0	0.0	0.0	0.0	0.0
W 187	1.2	6.4	50.9	63.8	85.3	62.8	1.4	5.7	47.7	61.8	78.5	50.2	0.8	45.7	60.5	78.5	44.0	0.6	44.4	59.6	71.8	40.6	0.6	0.0	0.0
all1071 others	0.2	0.3	0.3	0.2	0.1	0.1	0.2	0.3	0.3	0.2	0.1	0.1	0.2	0.3	0.2	0.1	0.1	0.2	0.3	0.2	0.1	0.1	0.2	0.1	0.1
Total	100	100	100	100	100	100	100	100	100	100	100	100	100	100	100	100	100	100	100	100	100	100	100	100	100

Table 4d

Major Contributions to Activity (> .1 %) in borated polyethylene
of the Forward Calorimeter of the ATLAS Detector for the Large Hadron Collider
Calculated for 7.9E+8 Minimum-Bias Events per Second with CINDER'90 using May'93
Libraries and Spallation Product Yields and Neutron Fluxes from SUPERHET/HMCNP

Percent of Total

nucl	Cycle One 10mn	1hr	1day	30 d	Down Time 1day	3day	10 d	Cycle Two 1hr	1day	30 d	Down Time 1day	3day	10 d	Cycle 3 1day	30 d	Down Time 1day	3day	10 d	Cycle 4 1day	30 d	Post Shutdown 1day	3day	10 d	60 d	1 yr
H 3	0.0	0.0	0.0	0.0	98.2	98.3	98.4	0.0	0.0	0.1	98.6	98.6	98.7	0.1	0.1	98.8	98.9	99.0	0.1	0.1	99.0	99.0	99.1	99.5	99.9
He 5	0.2	0.2	0.2	0.2	0.0	0.0	0.0	0.2	0.2	0.2	0.0	0.0	0.0	0.2	0.2	0.0	0.0	0.0	0.2	0.2	0.0	0.0	0.0	0.0	0.0
Li 8	6.9	6.9	6.9	6.9	0.0	0.0	0.0	6.9	6.9	6.9	0.0	0.0	0.0	6.9	6.9	0.0	0.0	0.0	6.9	6.9	0.0	0.0	0.0	0.0	0.0
Be 7	0.0	0.0	0.0	0.0	1.7	1.7	1.5	0.0	0.0	0.0	1.4	1.4	1.2	0.0	0.0	1.1	1.1	1.0	0.0	0.0	1.0	0.9	0.8	0.4	0.1
Be 8	39.8	39.7	39.7	39.7	0.0	0.0	0.0	39.7	39.7	39.7	0.0	0.0	0.0	39.7	39.7	0.0	0.0	0.0	39.7	39.7	0.0	0.0	0.0	0.0	0.0
Be 11	0.7	0.7	0.7	0.7	0.0	0.0	0.0	0.7	0.7	0.7	0.0	0.0	0.0	0.7	0.7	0.0	0.0	0.0	0.7	0.7	0.0	0.0	0.0	0.0	0.0
B 9	0.7	0.7	0.7	0.7	0.0	0.0	0.0	0.7	0.7	0.7	0.0	0.0	0.0	0.7	0.7	0.0	0.0	0.0	0.7	0.7	0.0	0.0	0.0	0.0	0.0
B 12	16.2	16.2	16.2	16.2	0.0	0.0	0.0	16.2	16.2	16.2	0.0	0.0	0.0	16.2	16.2	0.0	0.0	0.0	16.2	16.1	0.0	0.0	0.0	0.0	0.0
C 15	0.1	0.1	0.1	0.1	0.0	0.0	0.0	0.1	0.1	0.1	0.0	0.0	0.0	0.1	0.1	0.0	0.0	0.0	0.1	0.1	0.0	0.0	0.0	0.0	0.0
N 16	35.0	35.0	35.0	35.0	0.0	0.0	0.0	35.0	35.0	35.0	0.0	0.0	0.0	35.0	35.0	0.0	0.0	0.0	35.0	34.9	0.0	0.0	0.0	0.0	0.0
O 15	0.3	0.3	0.3	0.3	0.0	0.0	0.0	0.3	0.3	0.3	0.0	0.0	0.0	0.3	0.3	0.0	0.0	0.0	0.3	0.3	0.0	0.0	0.0	0.0	0.0
all 44 others	0.1	0.1	0.1	0.1	0.0	0.0	0.0	0.1	0.1	0.1	0.0	0.0	0.0	0.1	0.1	0.0	0.0	0.0	0.1	0.1	0.0	0.0	0.0	0.0	0.0
Total	100	100	100	100	100	100	100	100	100	100	100	100	100	100	100	100	100	100	100	100	100	100	100	100	100

Major Contributions to Decay Power (> .1 %) in borated polyethylene
of the Forward Calorimeter of the ATLAS Detector for the Large Hadron Collider
Calculated for 7.9E+8 Minimum-Bias Events per Second with CINDER'90 using May'93
Libraries and Spallation Product Yields and Neutron Fluxes from SUPERHET/HMCNP

Percent of Total

nucl	Cycle One 10mn	1hr	1day	30 d	Down Time 1day	3day	10 d	Cycle Two 1hr	1day	30 d	Down Time 1day	3day	10 d	Cycle 3 1day	30 d	Down Time 1day	3day	10 d	Cycle 4 1day	30 d	Post Shutdown 1day	3day	10 d	60 d	1 yr
H 3	0.0	0.0	0.0	0.0	86.4	86.7	87.7	0.0	0.0	0.0	88.8	89.0	89.9	0.0	0.0	90.6	90.8	91.5	0.0	0.0	92.0	92.0	92.2	96.0	99.2
Li 8	16.2	16.2	16.2	16.2	0.0	0.0	0.0	16.2	16.2	16.2	0.0	0.0	0.0	16.2	16.2	0.0	0.0	0.0	16.2	16.2	0.0	0.0	0.0	0.0	0.0
Be 7	0.0	0.0	0.0	0.0	13.3	13.0	12.1	0.0	0.0	0.0	11.0	10.7	9.9	0.0	0.0	9.1	8.9	8.2	0.0	0.0	7.7	7.5	6.9	3.8	0.5
Be 8	0.8	0.8	0.8	0.8	0.0	0.0	0.0	0.8	0.8	0.8	0.0	0.0	0.0	0.8	0.8	0.0	0.0	0.0	0.8	0.8	0.0	0.0	0.0	0.0	0.0
Be 11	1.0	1.0	1.0	1.0	0.0	0.0	0.0	1.0	1.0	1.0	0.0	0.0	0.0	1.0	1.0	0.0	0.0	0.0	1.0	1.0	0.0	0.0	0.0	0.0	0.0
B 12	23.7	23.7	23.7	23.7	0.0	0.0	0.0	23.7	23.7	23.7	0.0	0.0	0.0	23.7	23.7	0.0	0.0	0.0	23.7	23.7	0.2	0.2	0.0	0.0	0.2
C 14	0.0	0.0	0.0	0.0	0.2	0.2	0.2	0.0	0.0	0.0	0.2	0.2	0.2	0.0	0.0	0.2	0.2	0.2	0.0	0.0	0.2	0.2	0.2	0.2	0.0
C 15	0.2	0.2	0.2	0.2	0.0	0.0	0.0	0.2	0.2	0.2	0.0	0.0	0.0	0.2	0.2	0.0	0.0	0.0	0.2	0.2	0.0	0.0	0.0	0.0	0.0
N 16	57.9	57.9	57.9	57.9	0.0	0.0	0.0	57.9	57.9	57.9	0.0	0.0	0.0	57.9	57.9	0.0	0.0	0.0	57.9	57.9	0.0	0.0	0.0	0.0	0.0
O 15	0.1	0.1	0.1	0.1	0.0	0.0	0.0	0.1	0.1	0.1	0.0	0.0	0.0	0.1	0.1	0.0	0.0	0.0	0.1	0.1	0.0	0.0	0.0	0.0	0.0
all 45 others	0.1	0.1	0.1	0.1	0.0	0.0	0.0	0.1	0.1	0.1	0.0	0.0	0.0	0.1	0.1	0.0	0.0	0.0	0.1	0.1	0.1	0.1	0.1	0.1	0.1
Total	100	100	100	100	100	100	100	100	100	100	100	100	100	100	100	100	100	100	100	100	100	100	100	100	100

Name	Time Point	Average Energy (MeV)	Rate (no/cc/sec)
BPOLY	18	6.1321	2.086e2
	19	.39384	8.168e4
FCAL1	18	.41826	5.413e5
	19	.40841	1.357e5
FCAL2	18	.17521	1.317e6
	19	.38125	2.398e5
FCAL3	28	.17903	2.497e5
	19	.38074	4.657e4

Table 5: **Decay Gammas and Average Energy**
At each of the indicated time points the average decay gamma energy and emission rate is given.

Number	Name	Creiteria	Seriousness
1	MEAN	Non-monotonic behavior (no up or down trend) as a function of N for the last half of the problem	2
2	ERROR	acceptable value of relative error $\prec.05$ for point and ring detectors $\prec.1$ for all others	1
3		monotonically decreasing R as a function of N for the last half of the problem	2
4		$N^{-.5}$ decrease in R as a function of N for the last half of the problem	3
5	VOV	magnitude less than .1	1
6		monotonically decreasing VOV as a function of N for the last half of the problem	3
7		1/N decrease in VOV as a function of N for the last half of the problem	3
8	FOM	statistically constant value of FOM as a function of N for the last half of the problem	1
9		non-monotonic behavior of FOM as a function of N for the last half of the problem	2
10	f(x)	the slope of the 25 to 201 largest positive history scores x should be greater than 3.0	1

Table 6: **10 Statistical Tests for Convergence**
Description of the 10 statistical tests available in $MCNP^{TM}$ to aid in the assessment of confidence interval reliability. An indication of the seriousness of not passing a test is indicated in the last column, with 1 being the most and 3 being the least critical.

Z	R	FCAL1	FCAL2	FCAL3	BPOLY	TOTAL
300	0	1.25059E-01	2.18293E-03	3.88468E-04	4.59732E-03	1.32228E-01
300	40	1.35255E-01	3.07800E-03	3.79256E-05	4.34150E-03	1.42712E-01
300	80	1.05496E-01	1.63933E-03	1.28128E-04	3.71338E-03	1.10977E-01
300	120	7.35676E-02	2.31790E-03	3.11309E-04	2.97698E-03	7.91738E-02
300	200	3.58480E-02	2.96506E-03	1.75237E-04	1.76389E-03	4.07522E-02
300	300	1.66503E-02	2.48620E-03	1.58923E-04	9.29998E-04	2.02254E-02
200	0	4.96922E-02	5.74498E-04	1.09286E-04	1.80557E-03	5.21816E-02
200	40	5.51879E-02	2.11554E-03	1.38595E-04	1.77072E-03	5.92128E-02
200	80	5.32621E-02	1.22825E-03	1.63261E-04	1.65083E-03	5.63044E-02
200	120	4.52152E-02	1.07329E-03	7.39659E-05	1.49318E-03	4.78556E-02
200	200	2.87233E-02	1.34908E-03	9.63211E-05	1.12046E-03	3.12892E-02
200	300	1.56600E-02	1.39416E-03	9.54705E-05	7.42258E-04	1.78919E-02
700	0	2.97647E-02	1.32800E-02	3.29852E-02	3.75759E-05	7.60675E-02
700	40	4.49634E-04	3.60078E-03	3.25957E-02	8.73008E-07	3.66470E-02
700	80	4.29991E-04	1.90116E-04	1.91788E-02	1.14907E-06	1.98001E-02
700	120	2.99960E-03	9.08052E-04	1.43985E-02	2.89097E-06	1.83090E-02
700	200	6.88765E-03	1.57457E-03	3.59313E-03	1.90692E-05	1.20744E-02
700	300	6.90955E-04	1.00245E-02	3.36463E-02	1.70619E-06	4.43635E-02
450	25	1.76762E+00	1.44684E-03	1.35591E-06	1.36433E-01	1.90550E+00
494	55	1.15629E+00	2.61097E-02	8.53340E-05	1.22850E-04	1.18261E+00

Table 7: **Dose at Time Point 18, No Shielding**
Dose in mSv/hour for the 20 point detectors from FCAL1, FCAL2, FCAL3 and BPOLY
with no other elements in the setup. Time is 30 days into beam on in the third cycle.

Z	R	FCAL1	FCAL2	FCAL3	BPOLY
300	0	.0084 10	.0741 8	.2613 5	.0022 8
300	40	.0110 4	.0820 8	.3388 7	.0026 9
300	80	.0084 9	.0646 7	.2674 6	.0021 9
300	120	.0093 9	.0500 10	.6066 2	.0025 9
300	200	.0259 3	.0474 5	.0686 9	.0022 9
300	300	.0100 9	.0368 9	.0639 8	.0024 10
200	0	.0088 10	.1087 9	.3404 5	.0019 8
200	40	.0156 8	.0609 9	.0834 9	.0024 9
200	80	.0084 8	.0644 9	.5574 4	.0022 10
200	120	.0084 10	.0611 9	.1099 3	.0023 10
200	200	.0103 10	.0414 10	.0641 9	.0021 10
200	300	.0094 9	.0361 10	.0664 9	.0024 8
700	0	.0352 3	.0535 8	.0228 10	.0559 4
700	40	.1727 7	.2468 3	.0270 4	.1163 6
700	80	.0960 2	.3184 5	.0295 7	.0453 9
700	120	.0296 10	.0929 9	.2934 4	.0417 8
700	200	.0170 10	.0595 9	.0520 7	.0344 7
700	300	.1559 6	.0579 9	.0217 10	.2331 7
450	25	.0161 8	.6207 2	.4645 7	.0029 10
494	55	.0240 10	.0711 9	.7536 5	.0451 10

Table 8: **Error Analysis for Table 7**
Relative errors for the values given in Table 7. along with the number of statistical confidence interval tests passed (out of 10).

Z	R	FCAL1	FCAL2	FCAL3	BPOLY	TOTAL
300	0	3.18097E-02	1.01623E-03	1.47326E-04	2.68057E-09	3.29733E-02
300	40	3.43954E-02	1.47309E-03	1.38203E-05	2.50952E-09	3.58823E-02
300	80	2.69505E-02	8.86920E-04	4.59292E-05	2.09511E-09	2.78834E-02
300	120	1.88157E-02	1.13471E-03	6.57600E-05	1.59021E-09	2.00162E-02
300	200	9.19697E-03	1.37408E-03	7.59541E-05	8.28056E-10	1.06470E-02
300	300	4.23026E-03	1.15087E-03	7.11346E-05	3.80096E-10	5.45227E-03
200	0	1.26631E-02	2.95025E-04	3.51056E-05	1.04268E-09	1.29932E-02
200	40	1.40097E-02	1.00552E-03	6.33816E-05	1.02371E-09	1.50786E-02
200	80	1.35520E-02	5.48555E-04	2.33169E-05	9.45606E-10	1.41239E-02
200	120	1.16363E-02	5.25227E-04	3.28860E-05	8.34923E-10	1.21944E-02
200	200	7.36326E-03	6.83931E-04	4.34422E-05	5.92126E-10	8.09063E-03
200	300	4.00690E-03	6.86941E-04	5.09893E-05	3.55790E-10	4.74483E-03
700	0	7.21440E-03	7.52797E-03	1.55015E-02	1.80412E-11	3.02439E-02
700	40	1.00736E-04	1.38958E-03	1.58531E-02	3.23468E-12	1.73434E-02
700	80	1.05012E-04	6.80784E-05	8.89581E-03	4.35342E-12	9.06890E-03
700	120	7.68983E-04	4.75506E-04	4.73017E-03	5.11925E-12	5.97466E-03
700	200	1.70444E-03	7.14272E-04	1.59038E-03	9.71340E-12	4.00909E-03
700	300	1.47529E-04	4.65699E-03	1.80106E-02	2.95301E-12	2.28151E-02
450	25	4.53762E-01	1.21168E-03	1.58419E-06	6.65387E-08	4.54975E-01
494	55	2.86706E-01	1.32012E-02	2.12634E-06	1.68794E-11	2.99909E-01

Table 9: **Dose at Time Point 19, No Shielding**
Dose in mSv/hour for the 20 point detectors from FCAL1, FCAL2, FCAL3 and BPOLY with no other elements in the setup. Time is one day after beam off in the third cycle.

20

Z	R	FCAL1	FCAL2	FCAL3	BPOLY
300	0	.0083 10	.0520 8	.0823 6	.0028 8
300	40	.0111 4	.0576 7	.2950 7	.0025 9
300	80	.0086 9	.1077 2	.0811 3	.0030 9
300	120	.0097 9	.0335 10	.0688 3	.0024 9
300	200	.0252 3	.0249 8	.0412 10	.0034 3
300	300	.0099 9	.0214 10	.0406 6	.0040 7
200	0	.0086 9	.1531 7	.0692 8	.0026 8
200	40	.0153 9	.0444 10	.0583 7	.0031 8
200	80	.0085 8	.0526 6	.0594 9	.0025 7
200	120	.0086 10	.0366 10	.0548 9	.0026 7
200	200	.0106 9	.0270 10	.0438 8	.0025 10
200	300	.0090 10	.0246 10	.1314 5	.0033 9
700	0	.0261 3	.1921 2	.0186 3	.0348 7
700	40	.1664 7	.0786 9	.0536 3	.0598 2
700	80	.0993 4	.2298 7	.0187 9	.0256 5
700	120	.0335 9	.0517 9	.0196 9	.0215 7
700	200	.0175 10	.0357 9	.0195 9	.0154 9
700	300	.1570 6	.0409 10	.1189 5	.0392 6
450	25	.0164 8	.3445 7	.4427 6	.0044 3
494	55	.0242 10	.0693 7	.2006 7	.0494 9

Table 10: **Error Analysis for Table 9**
Relative errors for the values given in Table 9, along with the number of statistical confidence interval tests passed (out of 10).

Z	R	FCAL1	FCAL2	FCAL3	BPOLY	TOTAL
300	0	1.64495E-01	2.58187E-03	3.16579E-04	4.79837E-03	1.72192E-01
300	40	1.22742E-01	2.89920E-03	9.14360E-06	3.91289E-03	1.29563E-01
300	80	1.05264E-03	4.96339E-06	1.65338E-07	7.44462E-05	1.13221E-03
300	120	3.49456E-04	4.99949E-06	3.74421E-07	9.89396E-06	3.64724E-04
300	200	1.37959E-04	1.16679E-05	1.31116E-06	1.84978E-06	1.52788E-04
300	300	1.96065E-04	3.72988E-05	1.58866E-05	2.39826E-06	2.51649E-04
200	0	4.93856E-02	6.57873E-04	7.14417E-05	1.79018E-03	5.19051E-02
200	40	4.89422E-02	1.86349E-03	1.12819E-04	1.63825E-03	5.25568E-02
200	80	2.62158E-02	1.02156E-04	1.34350E-06	8.43524E-04	2.71628E-02
200	120	1.96070E-03	9.13352E-06	6.16026E-07	1.58428E-04	2.12888E-03
200	200	2.59799E-04	8.88944E-06	9.74324E-07	6.11267E-06	2.75775E-04
200	300	1.44120E-04	1.66317E-05	2.93852E-06	1.88471E-06	1.65575E-04
700	0	2.93697E-02	1.35868E-02	3.37566E-02	3.81553E-05	7.67513E-02
700	40	3.45993E-04	2.99226E-03	3.31865E-02	3.96944E-06	3.65287E-02
700	80	3.21651E-04	8.44611E-05	1.90117E-02	5.49116E-06	1.94233E-02
700	120	8.98351E-05	9.06051E-06	1.41514E-02	3.46440E-07	1.42506E-02
700	200	1.60124E-04	1.86747E-05	2.97953E-03	2.34402E-06	3.16067E-03
700	300	9.41353E-04	1.09113E-02	3.41742E-02	3.41821E-06	4.60303E-02
450	25	1.80149E+00	2.94268E-03	2.12567E-05	1.36951E-01	1.94141E+00
494	55	1.14508E+00	2.43214E-02	3.99365E-05	2.50871E-04	1.16969E+00

Table 11: **Dose at Time Point 18, Partial Shielding**
Dose in mSv/hour for the 20 point detectors from FCAL1, FCAL2, FCAL3 and BPOLY with Partial Shielding (no UPLUG or DPLUG). Time is 30 days into beam on in the third cycle.

Z	R	FCAL1	FCAL2	FCAL3	BPOLY
300	0	.1990 4	.1803 7	.1065 2	.0028 4
300	40	.0110 5	.0780 9	.6527 4	.0030 9
300	80	.0961 9	.2897 7	.6141 6	.0325 9
300	120	.1281 8	.2903 6	.5546 7	.0453 4
300	200	.0876 7	.3157 7	.4430 5	.0590 7
300	300	.0867 7	.1090 8	.1441 5	.2784 3
200	0	.0533 3	.2072 7	.0992 9	.0054 3
200	40	.0102 8	.0685 9	.0857 9	.0043 7
200	80	.0119 10	.4368 7	.4176 7	.0049 10
200	120	.0598 8	.2311 8	.3897 7	.0127 10
200	200	.0812 8	.2752 6	.4415 6	.0316 10
200	300	.0710 8	.1890 8	.3580 4	.0303 10
700	0	.0167 9	.0444 10	.0278 4	.0311 7
700	40	.2547 6	.1166 9	.0248 5	.0441 6
700	80	.1226 4	.2748 7	.0234 10	.0213 4
700	120	.1598 7	.3153 6	.2985 4	.0680 4
700	200	.0803 8	.2729 6	.0415 7	.0288 6
700	300	.1899 5	.0597 9	.0213 10	.0688 7
450	25	.0145 9	.4974 7	.7896 6	.0029 9
494	55	.0223 10	.0698 9	.3548 2	.0587 7

Table 12: **Error Analysis for Table 11**
Relative errors for the values given in Table 11, along with the number of statistical confidence interval tests passed (out of 10).

Z	R	FCAL1	FCAL2	FCAL3	BPOLY	TOTAL
300	0	4.14536E-02	1.01363E-03	1.40265E-04	2.77362E-09	4.26075E-02
300	40	3.10202E-02	1.32544E-03	5.88057E-06	2.18783E-09	3.23515E-02
300	80	2.76156E-04	4.76470E-06	2.43123E-07	2.46546E-11	2.81164E-04
300	120	9.97530E-05	2.97280E-06	3.33384E-07	7.28548E-12	1.03059E-04
300	200	3.47328E-05	7.37644E-06	1.23731E-06	2.64991E-12	4.33466E-05
300	300	4.23248E-05	2.80419E-05	9.34921E-06	2.05788E-12	7.97159E-05
200	0	1.25631E-02	2.37014E-04	3.12261E-05	9.90522E-10	1.28313E-02
200	40	1.22499E-02	8.78137E-04	5.90392E-05	9.06371E-10	1.31871E-02
200	80	6.68273E-03	6.39782E-05	2.66009E-06	4.38478E-10	6.74937E-03
200	120	4.57050E-04	4.78662E-06	9.28471E-07	7.32019E-11	4.62765E-04
200	200	6.10356E-05	5.57230E-06	7.87559E-07	4.57404E-12	6.73955E-05
200	300	3.37419E-05	1.36631E-05	2.07508E-06	2.15892E-12	4.94801E-05
700	0	7.15075E-03	6.15081E-03	1.56187E-02	1.78391E-11	2.89203E-02
700	40	6.97770E-05	2.18360E-03	1.68023E-02	2.52779E-12	1.90557E-02
700	80	7.18927E-05	6.19211E-05	8.69335E-03	4.01010E-12	8.82716E-03
700	120	1.90019E-05	1.95213E-05	4.47367E-03	8.71696E-13	4.51219E-03
700	200	3.10624E-05	1.17119E-05	1.34574E-03	2.06307E-12	1.38851E-03
700	300	2.55757E-04	4.55072E-03	1.59027E-02	2.50103E-12	2.07092E-02
450	25	4.56992E-01	1.07684E-03	5.69195E-06	6.72769E-08	4.58075E-01
494	55	2.90236E-01	1.12841E-02	1.58251E-05	7.07828E-11	3.01536E-01

Table 13: **Dose at Time Point 19, Partial Shielding**
Dose in mSv/hour for the 20 point detectors from FCAL1, FCAL2, FCAL3 and BPOLY with partial shielding (no UPLUG or DPLUG). Time is one day after beam off in the third cycle.

Z	R	FCAL1	FCAL2	FCAL3	BPOLY
300	0	.1936 5	.0549 8	.0823 7	.0025 8
300	40	.0111 7	.0504 9	.4328 7	.0030 9
300	80	.1036 9	.4779 6	.3189 7	.0380 10
300	120	.1427 9	.2108 7	.2827 7	.0442 9
300	200	.1021 7	.2399 6	.3232 7	.0481 4
300	300	.0571 9	.2306 7	.1161 5	.0337 9
200	0	.0519 4	.0795 9	.0601 8	.0026 9
200	40	.0097 8	.0406 10	.0565 8	.0029 9
200	80	.0152 4	.2510 7	.5849 2	.0042 7
200	120	.0460 8	.1576 8	.4130 2	.0813 3
200	200	.0869 8	.1946 6	.2382 7	.0347 10
200	300	.0662 9	.2487 7	.1855 7	.0436 4
700	0	.0149 10	.0281 8	.0186 4	.0321 7
700	40	.1785 7	.3335 5	.0629 6	.0659 2
700	80	.1106 4	.2309 6	.0146 9	.0200 10
700	120	.1366 7	.4016 7	.0172 10	.0541 5
700	200	.0634 9	.1738 7	.0209 9	.0260 10
700	300	.1757 7	.0392 10	.0165 4	.1448 6
450	25	.0145 9	.3591 7	.6400 5	.0036 10
494	55	.0224 10	.0434 10	.1237 8	.0206 10

Table 14: **Error Analysis for Table 13**
Relative errors for the values given in Table 13, along with the number of statistical confidence interval tests passed (out of 10).

Z	R	FCAL1	FCAL2	FCAL3	BPOLY	TOTAL
300	0	8.33319E-02	2.10928E-03	2.85529E-04	2.88009E-03	8.86068E-02
300	40	1.20439E-03	2.53365E-05	3.17317E-07	4.85265E-04	1.71531E-03
300	80	1.21819E-04	4.92270E-06	2.16580E-07	1.81799E-05	1.45138E-04
300	120	3.73043E-05	4.35056E-06	2.87821E-07	2.38176E-06	4.43244E-05
300	200	6.25716E-05	1.20996E-05	7.44306E-07	6.25042E-07	7.60405E-05
300	300	1.76863E-04	4.03645E-05	1.58945E-05	1.29177E-06	2.34414E-04
200	0	1.34378E-02	4.76655E-04	6.32305E-05	4.61799E-04	1.44395E-02
200	40	1.66278E-03	1.67990E-05	1.11190E-06	2.62129E-04	1.94282E-03
200	80	2.38177E-04	6.33766E-06	4.35183E-07	9.65529E-05	3.41503E-04
200	120	8.13972E-05	6.99717E-06	5.09866E-07	2.40098E-05	1.12914E-04
200	200	5.87002E-05	9.68940E-06	6.49516E-07	2.37436E-06	7.14135E-05
200	300	9.22405E-05	1.54518E-05	1.84480E-06	9.43715E-07	1.10481E-04
700	0	2.92432E-02	1.39998E-02	2.18550E-02	3.56367E-05	6.51336E-02
700	40	5.02676E-05	2.27305E-05	2.41243E-04	2.05210E-07	3.14446E-04
700	80	5.89382E-05	1.04269E-05	1.49788E-04	2.22045E-07	2.19375E-04
700	120	6.03832E-05	1.80895E-05	3.50914E-04	5.37224E-07	4.29924E-04
700	200	1.67207E-04	3.16332E-05	2.88526E-03	2.37566E-06	3.08648E-03
700	300	2.30979E-04	1.16849E-04	6.85370E-04	1.99946E-07	1.03340E-03
450	25	1.80657E+00	7.04828E-03	6.03504E-06	1.38087E-01	1.95171E+00
494	55	1.18038E+00	2.43808E-02	2.64178E-05	2.44338E-04	1.20503E+00

Table 15: **Dose at Time Point 18, With Full Shielding**
Dose in mSv/hour for the 20 point detectors from FCAL1, FCAL2, FCAL3 and BPOLY with full shielding. Time is 30 days into beam on in the third cycle.

Z	R	FCAL1	FCAL2	FCAL3	BPOLY
300	0	.0191 6	.0831 8	.0696 9	.0105 5
300	40	.2941 5	.1920 6	.6044 4	.0568 5
300	80	.7162 3	.3396 7	.5277 7	.1252 6
300	120	.2974 6	.3322 7	.5519 6	.0728 9
300	200	.0756 9	.2921 7	.3051 7	.0588 7
300	300	.0672 9	.3502 7	.1166 9	.0441 8
200	0	.0137 10	.1178 6	.0923 8	.0125 9
200	40	.0587 6	.1687 7	.2338 4	.0164 9
200	80	.1202 7	.2418 7	.3996 7	.0269 3
200	120	.3003 5	.2689 7	.3474 7	.0471 7
200	200	.1033 5	.2528 7	.3084 7	.0484 8
200	300	.0558 9	.1900 8	.2113 8	.0668 3
700	0	.0156 8	.0634 7	.0389 4	.0297 7
700	40	.1581 2	.2306 7	.1304 7	.0563 9
700	80	.1770 2	.3514 6	.5327 2	.0479 6
700	120	.0963 4	.4425 6	.1068 5	.4276 2
700	200	.0894 4	.4542 6	.0333 10	.0218 9
700	300	.8178 2	.4243 2	.2019 7	.0601 7
450	25	.0166 9	.5218 5	.5381 7	.0035 8
494	55	.0263 9	.0747 9	.1665 8	.0561 6

Table 16: **Error Analysis for Table 15**
Relative errors for the values given in Table 15, along with the number of statistical confidence interval tests passed (out of 10).

Z	R	FCAL1	FCAL2	FCAL3	BPOLY	TOTAL
300	0	2.15735E-02	1.09068E-03	1.34560E-04	1.29543E-09	2.27987E-02
300	40	2.65383E-04	7.68451E-06	3.63249E-07	2.23904E-12	2.73431E-04
300	80	1.29306E-05	2.98305E-06	4.35220E-07	5.77879E-13	1.63489E-05
300	120	8.15292E-06	3.49659E-06	4.15313E-07	5.11926E-13	1.20648E-05
300	200	1.70937E-05	6.75797E-06	1.19513E-06	9.88209E-13	2.50468E-05
300	300	4.32035E-05	2.76519E-05	1.04691E-05	1.42543E-12	8.13245E-05
200	0	3.51596E-03	2.63468E-04	3.21841E-05	1.27362E-10	3.81161E-03
200	40	4.49702E-04	6.12804E-06	6.72638E-07	4.37014E-11	4.56503E-04
200	80	9.14304E-05	4.14384E-06	5.14422E-07	1.36931E-12	9.60887E-05
200	120	3.38515E-05	4.54876E-06	5.81031E-07	7.87396E-13	3.89813E-05
200	200	1.79889E-05	5.38604E-06	9.77418E-07	7.77255E-13	2.43524E-05
200	300	2.39277E-05	1.24220E-05	1.86699E-06	8.84082E-13	3.82167E-05
700	0	7.32468E-03	5.93040E-03	9.72922E-03	1.63495E-11	2.29843E-02
700	40	1.29534E-05	5.88191E-06	1.05542E-04	5.62579E-13	1.24377E-04
700	80	1.49819E-05	2.40300E-06	3.71155E-05	6.53266E-13	5.45004E-05
700	120	1.64370E-05	3.71925E-06	1.82532E-04	7.63615E-13	2.02688E-04
700	200	3.88443E-05	1.19859E-05	1.38466E-03	2.22320E-12	1.43549E-03
700	300	1.82049E-05	4.38336E-05	2.42283E-04	5.49582E-13	3.04322E-04
450	25	4.54954E-01	9.40397E-04	2.09443E-06	6.69519E-08	4.55897E-01
494	55	2.94776E-01	1.18807E-02	2.82864E-05	7.21842E-11	3.06685E-01

Table 17: **Dose at Time Point 19, Full Shielding**
Dose in mSv/hour for the 20 point detectors from FCAL1, FCAL2, FCAL3 and BPOLY with full shielding. Time is one day after beam off in the third cycle.

Z	R	FCAL1	FCAL2	FCAL3	BPOLY
300	0	.0186 7	.0789 6	.0699 7	.0036 9
300	40	.1164 5	.1253 4	.2598 7	.1515 4
300	80	.3710 6	.1915 8	.2975 7	.1521 7
300	120	.3065 1	.1999 7	.3026 7	.1170 5
300	200	.0924 5	.2504 7	.2672 7	.0473 6
300	300	.0602 9	.2353 7	.1244 7	.0314 10
200	0	.0182 8	.1316 6	.0615 9	.0071 9
200	40	.1017 6	.1123 5	.2014 6	.0143 8
200	80	.2560 2	.1738 8	.2382 7	.0930 4
200	120	.5320 2	.1785 7	.2531 7	.0612 8
200	200	.2201 2	.1932 7	.2804 7	.0361 10
200	300	.0663 6	.2633 6	.1968 7	.0289 10
700	0	.0168 10	.0274 9	.0246 4	.0313 7
700	40	.1327 4	.1360 6	.1434 6	.0433 10
700	80	.1712 2	.1756 8	.2543 7	.0508 6
700	120	.0971 5	.1624 8	.0748 9	.0397 10
700	200	.0713 8	.2019 7	.0220 10	.0510 5
700	300	.3274 2	.4690 5	.1178 7	.0443 10
450	25	.0169 10	.3322 7	.3690 5	.0035 9
494	55	.0266 10	.0479 10	.4670 6	.0210 10

Table 18: **Error Analysis for Table 17**
Relative errors for the values given in Table 17, along with the number of statistical confidence interval tests passed (out of 10).

Figure Captions

1. Geometry Setup: Figure 1A shows the FCAL geometry and surrounding shielding and detector components. Also shown are the locations of the 20 point detectors used in the equivalent dose calculation. Figure 1B shows a detail of the fine structure implemented for the FCAL in this calculation.

2. DTUJET events: Figure 2A shows the charged particle pseudorapidity distribution for the 7x7_dtu.eve file used in this calculation. Figure 2B is a plot of kinetic energy versus η around the acceptance of the FCAL.

3. Spallation Product Distribution from LAHET: The distribution of spallation products which will be input into the CINDER'90 code are shown for each module as a function of A, and as a plot of A versus Z. All values are in number/cc/p-p event, and the distributions are averaged over the volume of each module.
Figure 3A is a breakdown of the processes for FCAL2; fission, spallation and absorption. In addition we show the production of light particles in the last plot of Figure 3A. The values on the horizontal axis here are $LAHET^{TM}$ particle identification number.

4. Inelastic Collision Density: The density of inelastic collisions in each of the four modules is shown in units of number/cc/p-p event. All such interactions in the LAHET calculation are included. The X and Y axes on each plot are distance along the beam axis and radius, respectively (in cm.).

5. Neutron Fluence: The energy spectrum of neutrons for each of the four modules is shown as a 'lethergy' plot, i.e., in units of dn/dlog(E). Energies are in MeV. The Y axes are in units of $Number/cm^2/p-p$ event.
Figure 5A compares the shapes of the neutron spectra for the outer layers of FCAL 1 as shown in Figure 1. Little variation in shape is seen except for the regions close to the BPOLY unit. The spectra in Figure 5A are normalized relative to one another, the absolute value is arbitrary.

6. Ar41 Activity: The number of curies built up in each FCAL module is shown as a function of time. Due to the short half life of Ar41 equilibrium is quickly reached and the decay at shutdown is prompt.

7. Total Activity: For each module the total number of curies is shown as a function of time.

8. Total Heating Power: For each module the average heating power from decay electrons and gammas is shown as a function of time. Values are in watts/cc. The solid line is total heating power, and the dashed line is the component due to photons.

9. Distributed Heating Power: The average heating power for each module has been weighted according to the R/Z distribution shown in Figure 4. Values are in Watts/cc.

10. Average Decay Gamma Spectra for Time Point 18: The shape of the decay gamma spectra for the 4 modules is shown as lethergy plots. Spectra are not normalized. This time point is 30 days into beam on in the third cycle.

11. Average Decay Gamma Spectra for Time Point 19: The shape of the decay gamma spectra for the 4 modules is shown as lethergy plots. This time point is 1 day after beam off in the third cycle. Spectra are not normalized.

12. Sources of Decay Photons for Time Point 18: The top two plots show as a function of R and Z the source of photons used in the equivalent dose calculation for the BPOLY and FCAL1 modules. The bottom two plots show the source of photons which pass a cylinder of radius 55 cm.
Figure 12A shows the ICRP-21 photon fluence to dose conversion factors used in this calculation. Units are $(mSv/hour)(photons/cm^2 \cdot sec)$

13. Equivalent Dose profiles in mSv/hour for each of the four modules. Data are for time point 18: 30 days of beam on in the third cycle. No shielding present.

14. Equivalent Dose profile in mSv/hour for time point 18: 30 days of beam on in the third cycle. No shielding present. See Table 6 and 7. The bottom figure is a cut through Z=494 cm.

15. Equivalent Dose profile in mSv/hour for time point 19: 1 day after beam shutdown in the third cycle. No shielding present. See Table 8. The bottom figure is a cut through Z=494 cm.

16. Equivalent Dose profile in mSv/hour for time point 18: 30 days of beam on in the third cycle. Partial shielding present, EM and CU only. See Table 9. The bottom figure is a cut through Z=494 cm.

17. Equivalent Dose profile in mSv/hour for time point 19: 1 day after beam shutdown in the third cycle. Partial shielding present, EM and CU only. See Table 10. The bottom figure is a cut through Z=494 cm.

18. Equivalent Dose profile in mSv/hour for time point 18: 30 days of beam on in the third cycle. Full shielding present. See Table 11. The bottom figure is a cut through Z=494 cm.

19. Equivalent Dose profile in mSv/hour for time point 19: 1 day after beam shutdown in the third cycle. Full shielding present. See Table 12. The bottom figure is a cut through Z=494 cm.

20. Statistical quantities for BPOLY R=300 cm, Z=300 cm. This point passes all the tests of Table 6.

21. Statistical quantities for FCAL2 R=0 cm, Z=700 cm. This point passes 4 of the tests in Table 6.

Figure 1

Figure 2

2A

number per unit eta

pseudorapidity

2B

kinetic energy (GeV)

pseudorapidity
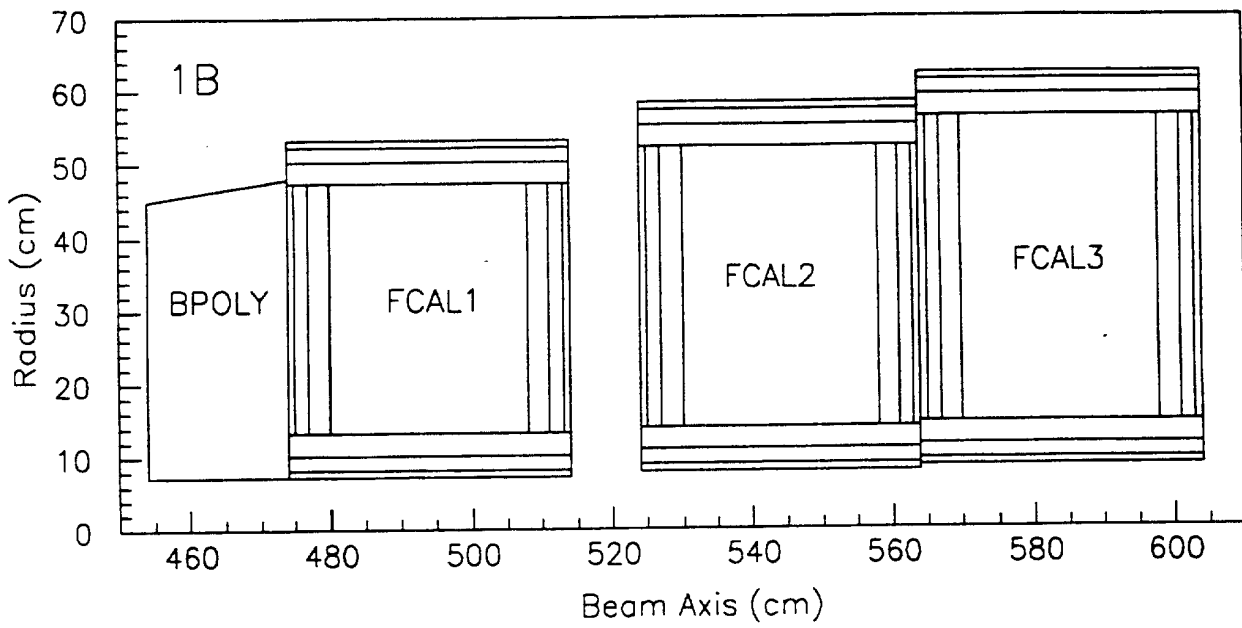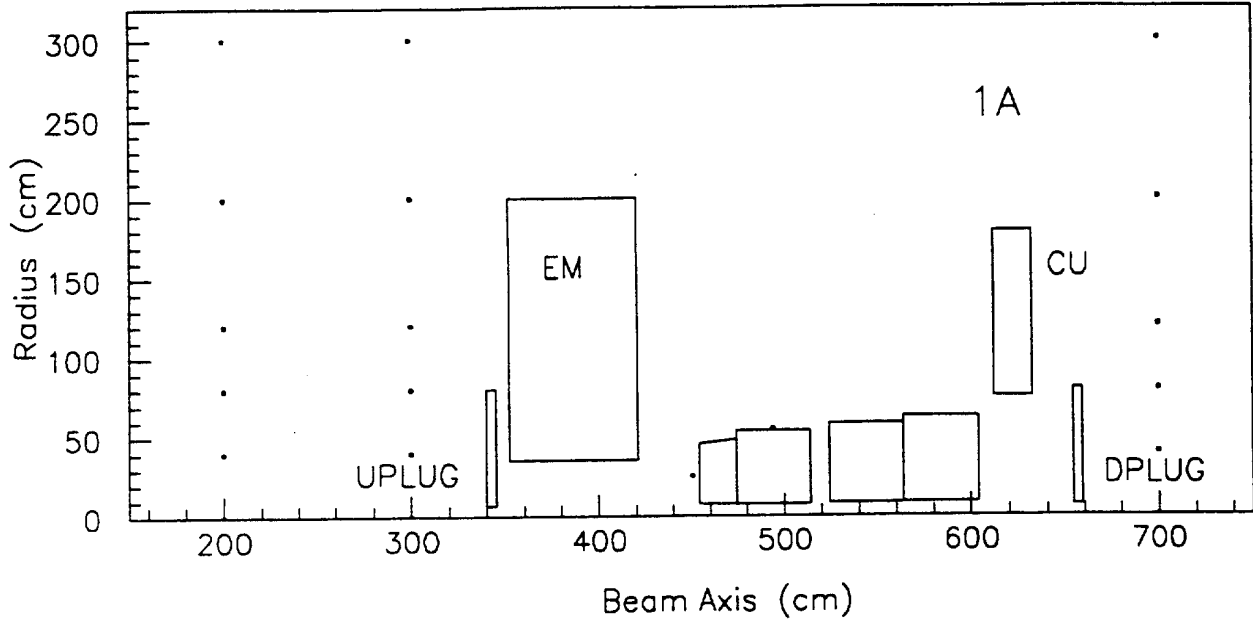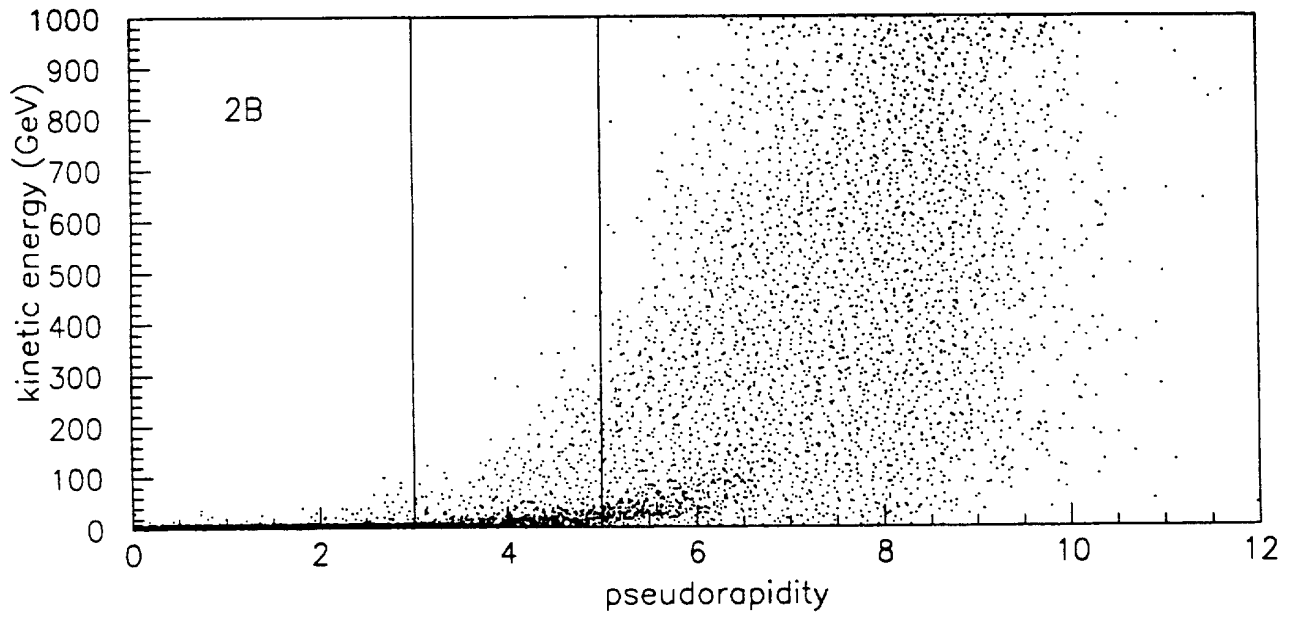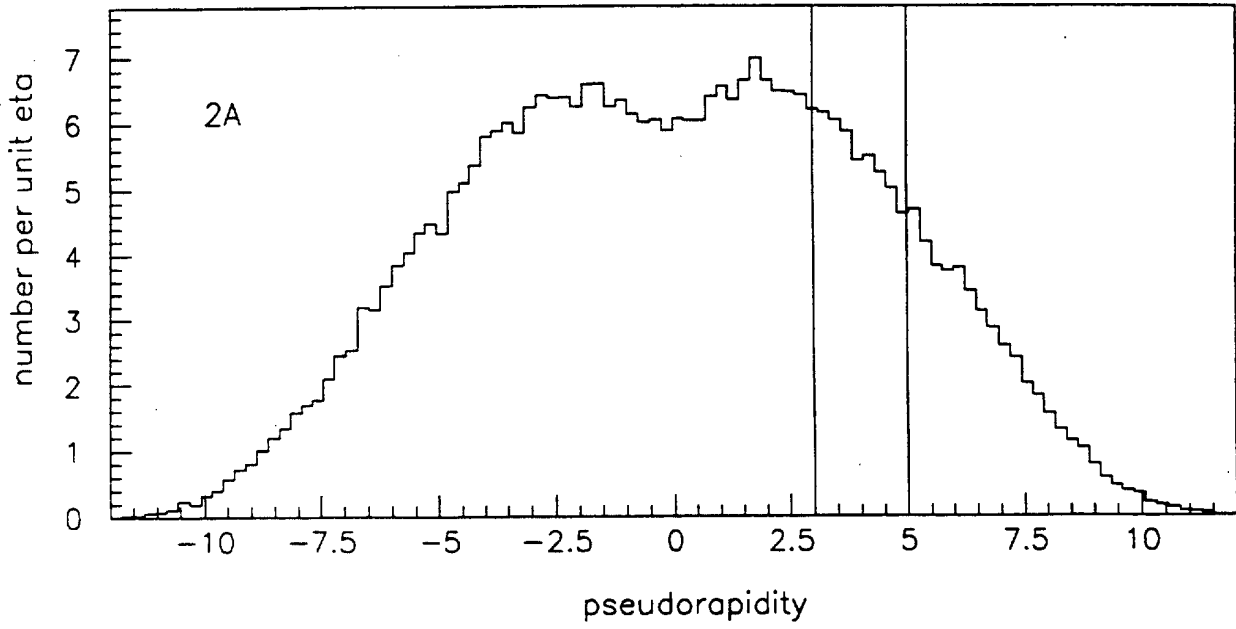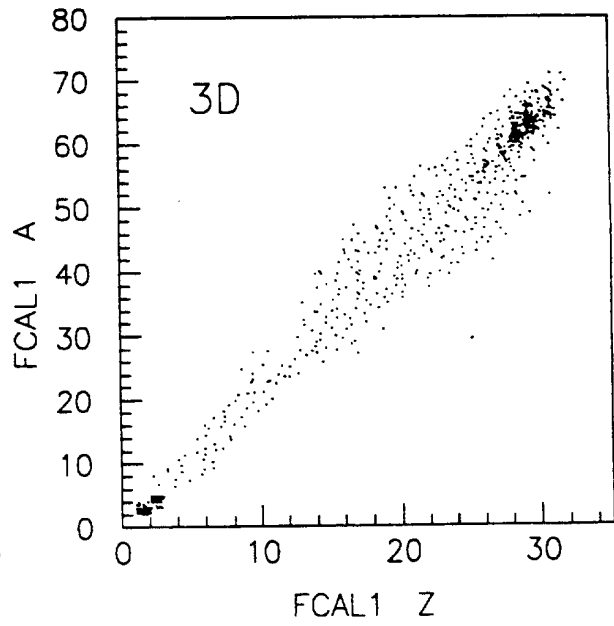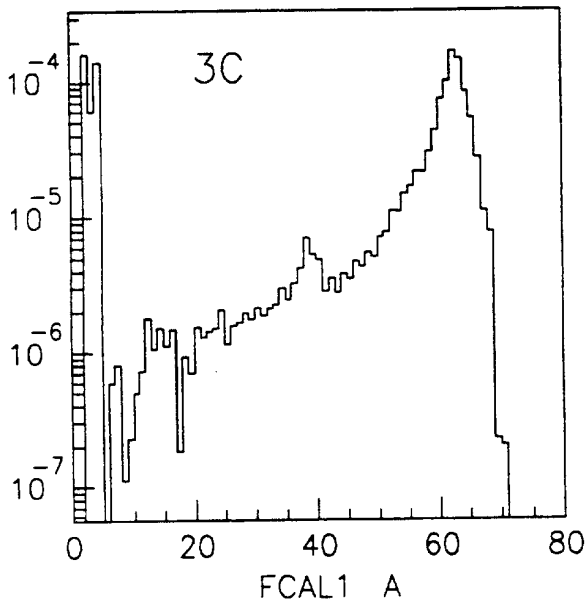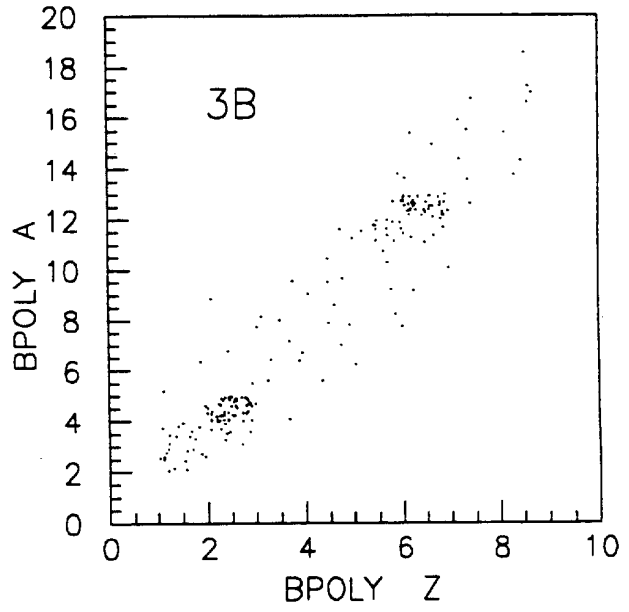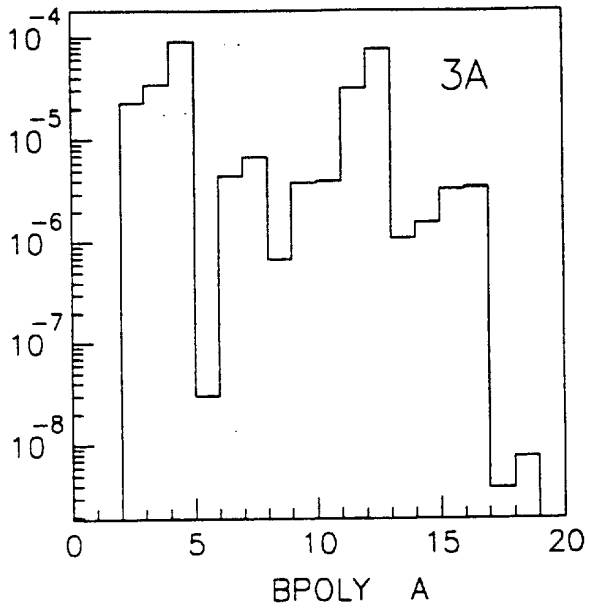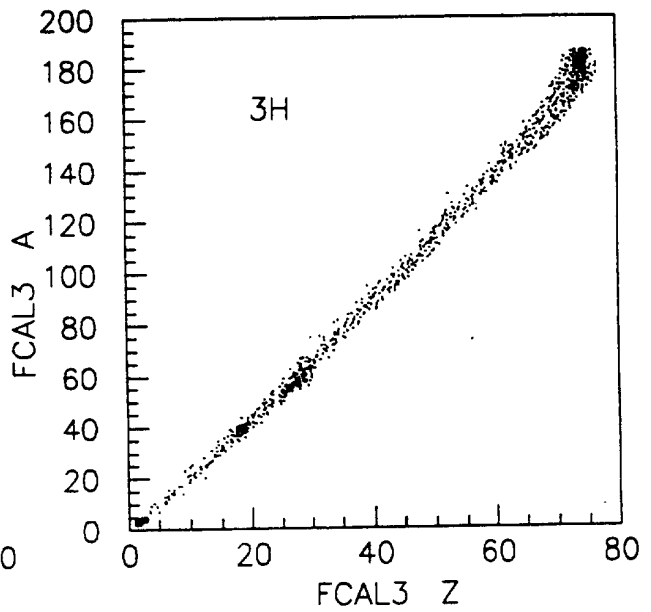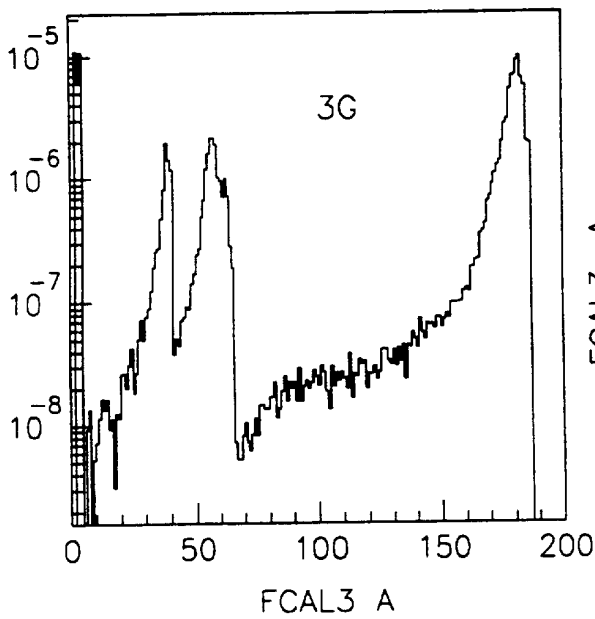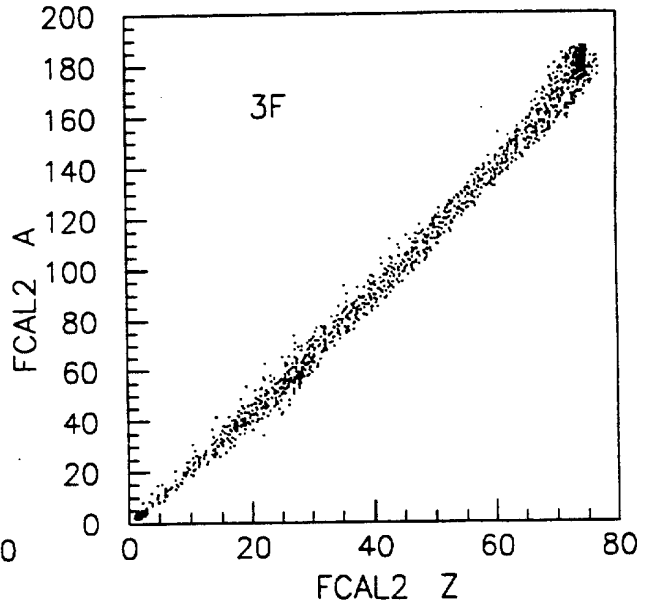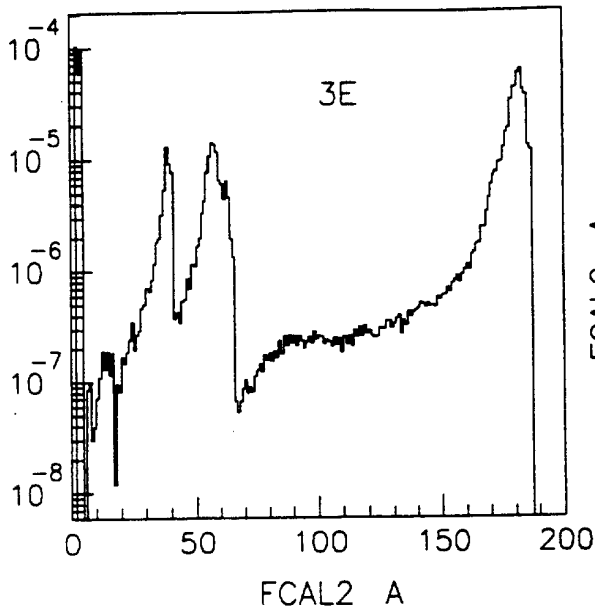
Figure 3

Figure 3

Figure 3A   FCAL2 Breakdown
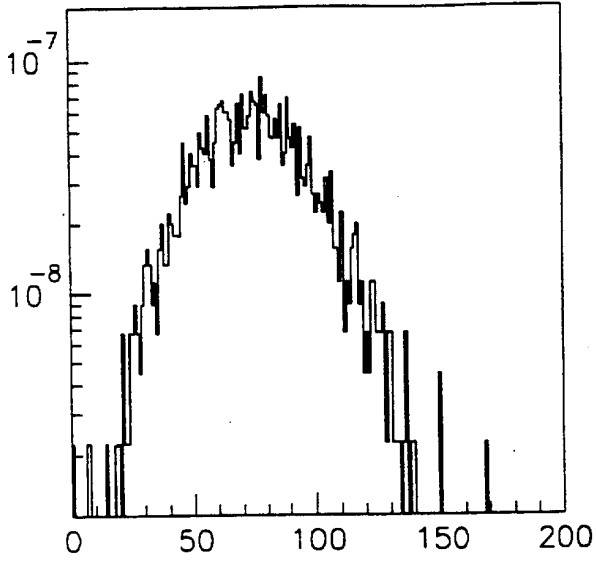
FCAL2 fission
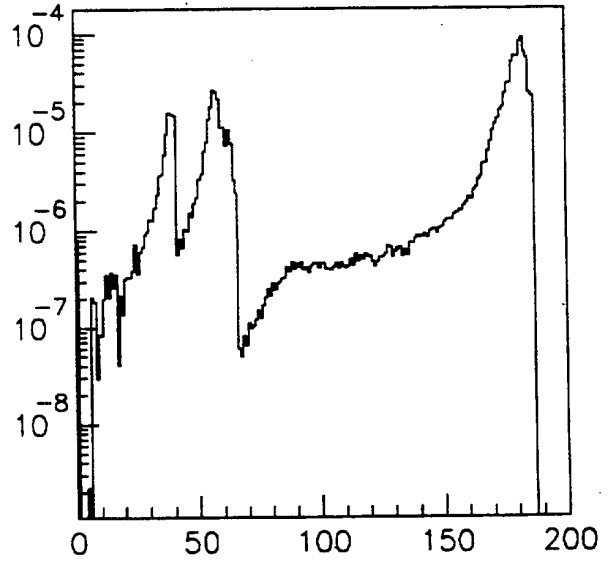
FCAL2 spallation
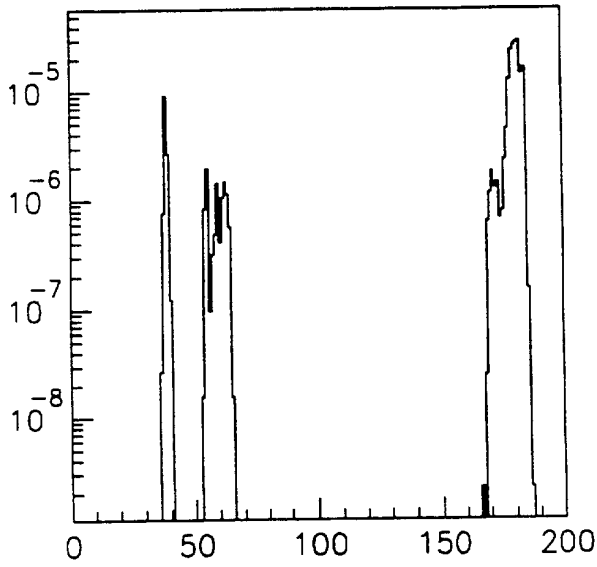
FCAL2 absorption
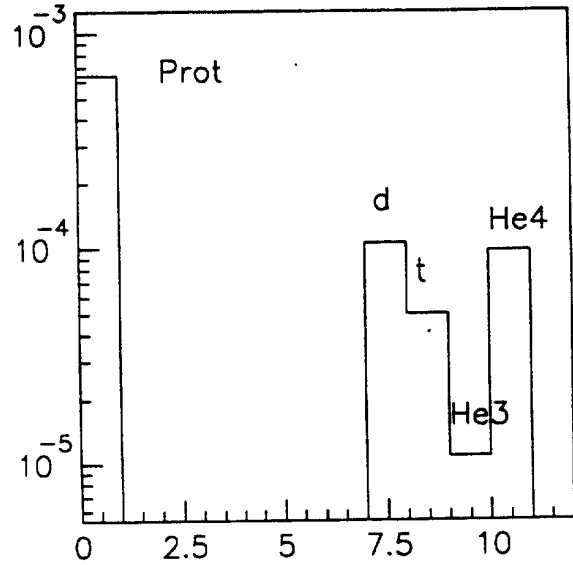
gas production

Figure 4
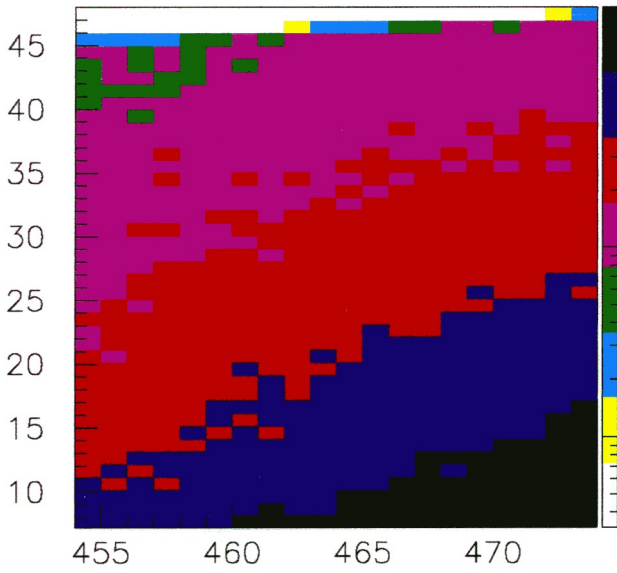
borated poly
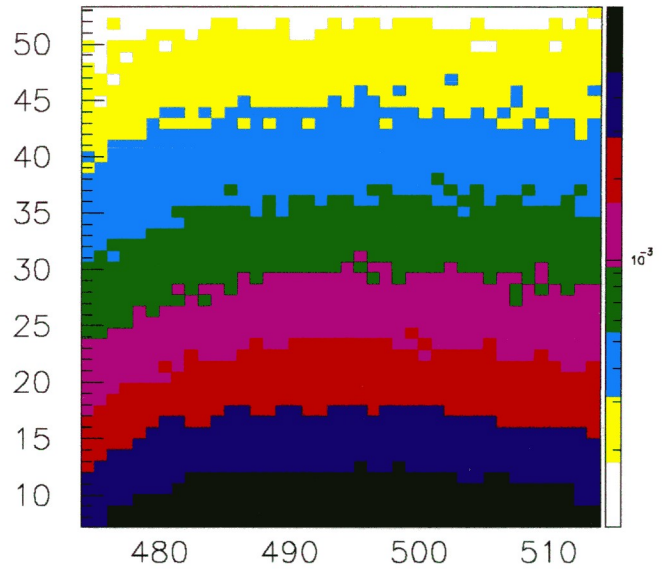
fcal1
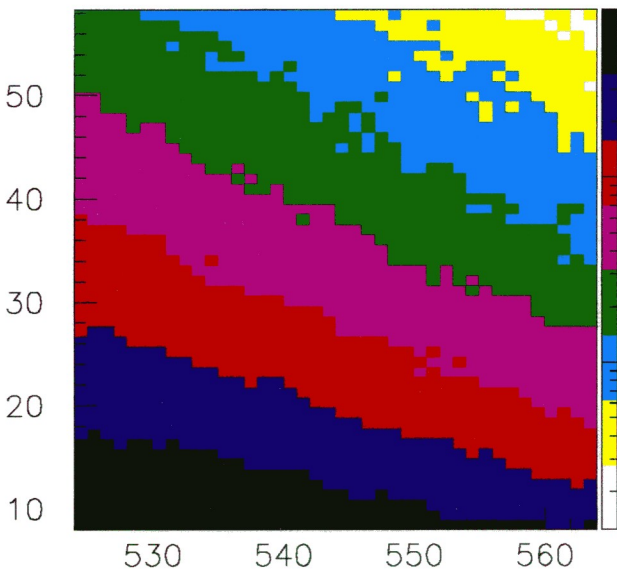
fcal2
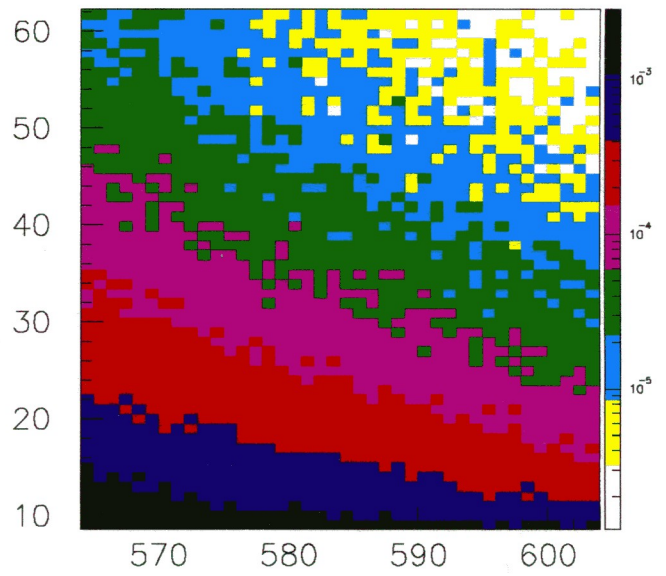
fcal3

Figure 4A   Neutron Flux
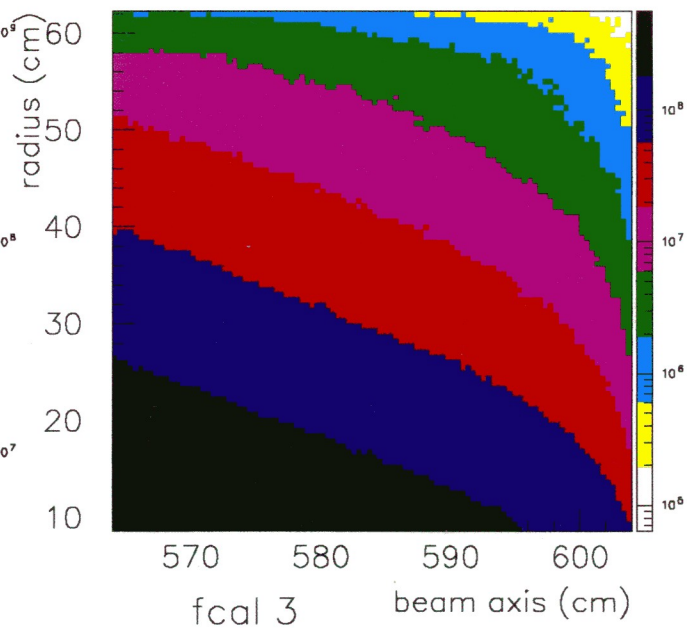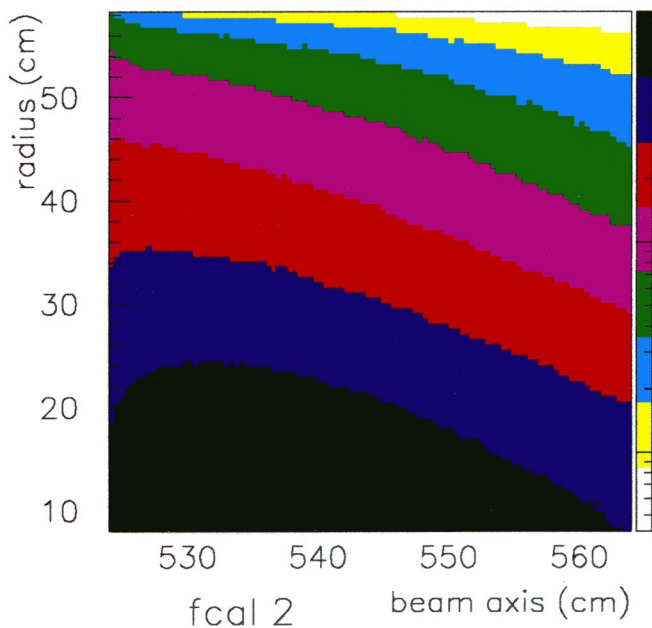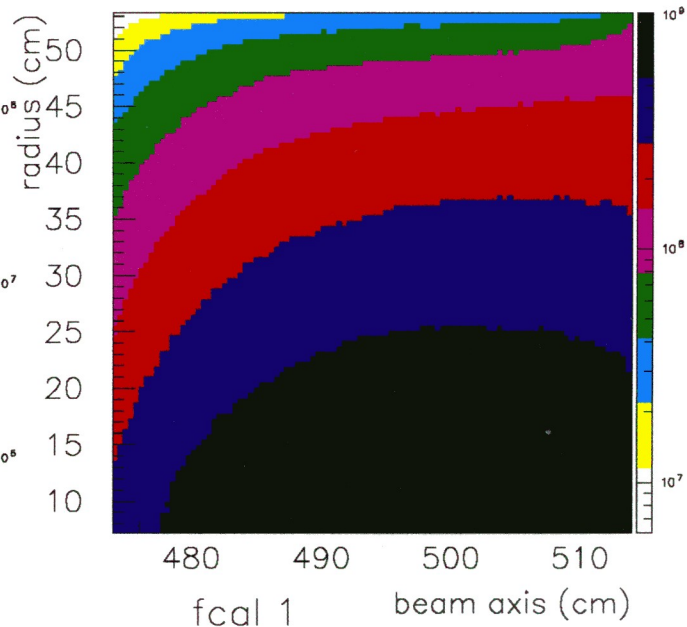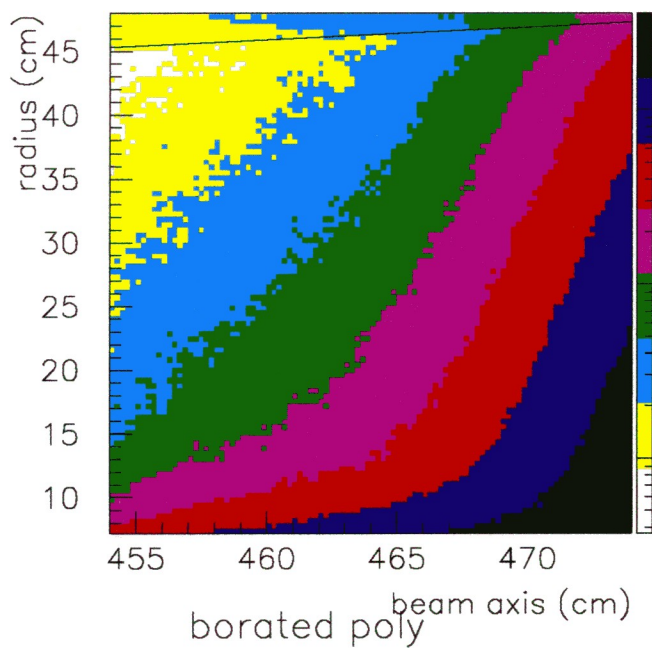
Figure 5: Neutron Fluence Spectra
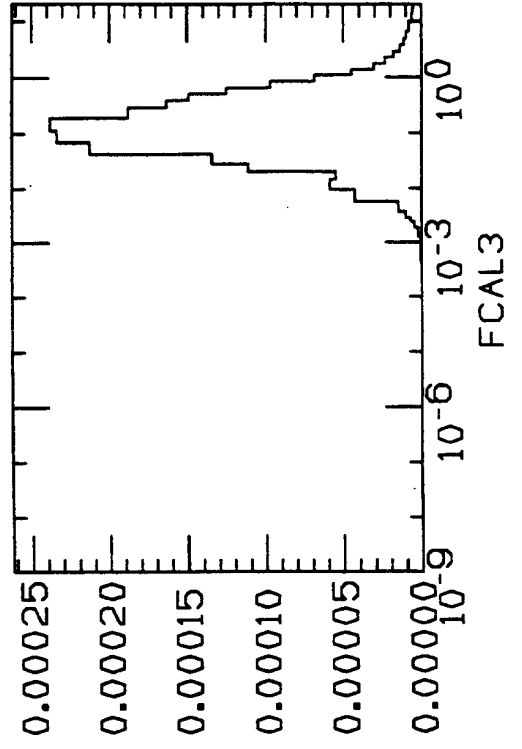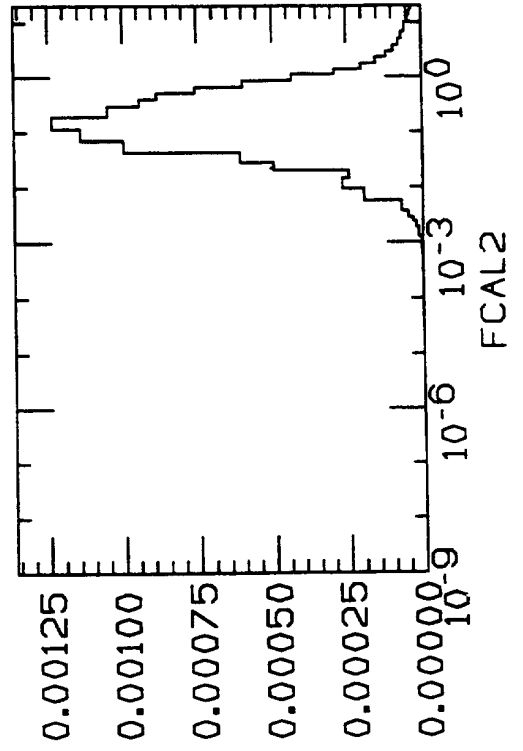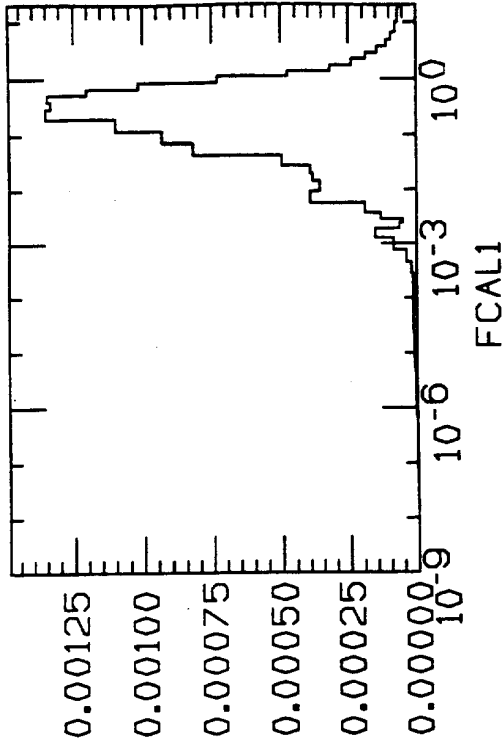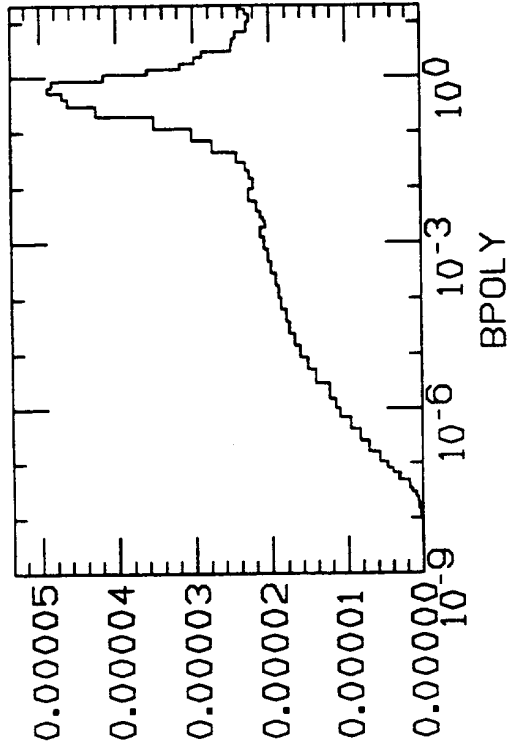
Figure 5a: FCAL1 Neutron Fluence
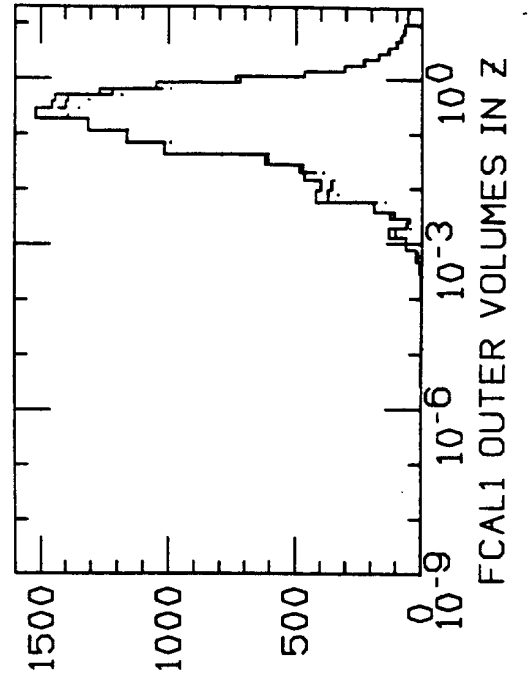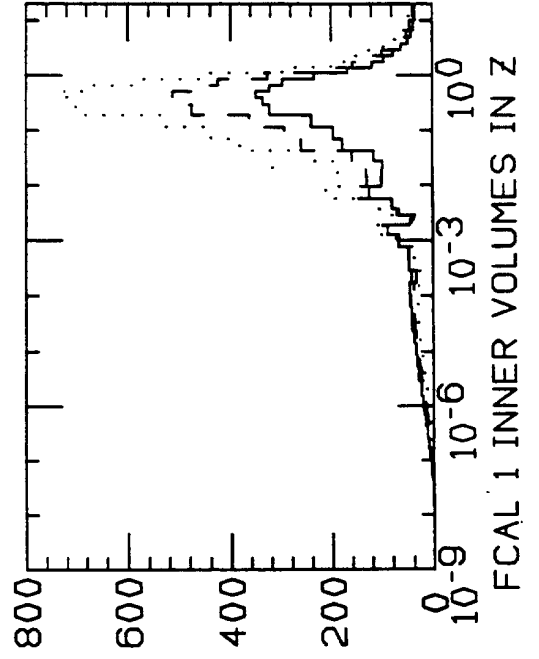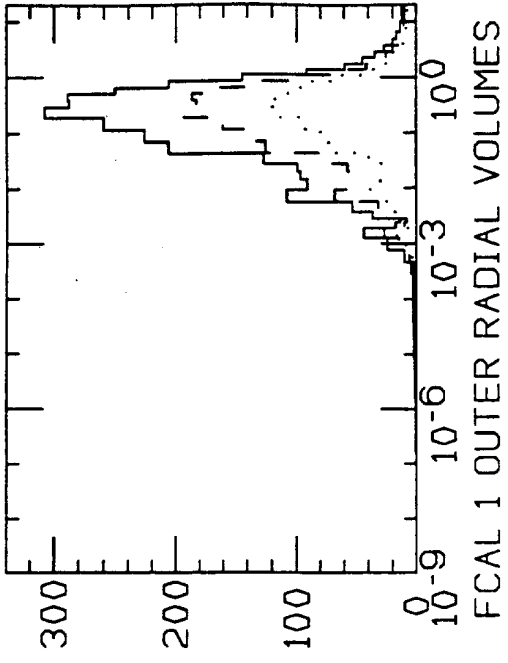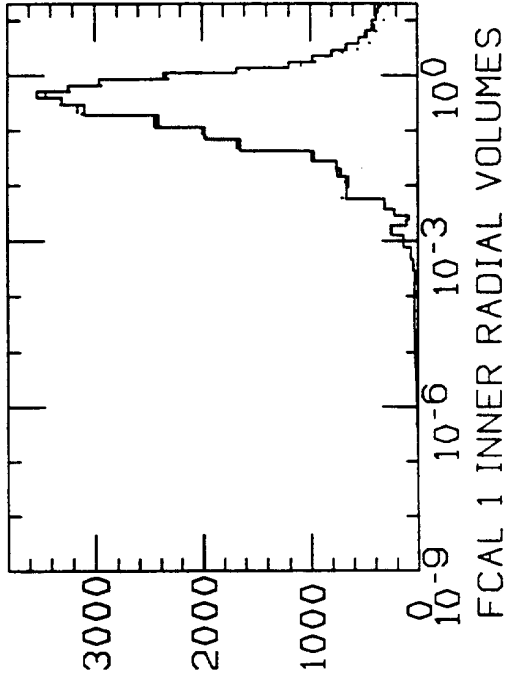
Figure 5b FCAL2 CINDER Calculation

FIGURE 6: Ar41

FCAL 1

FCAL 2

FCAL 3

FIGURE 7: All Nuclides
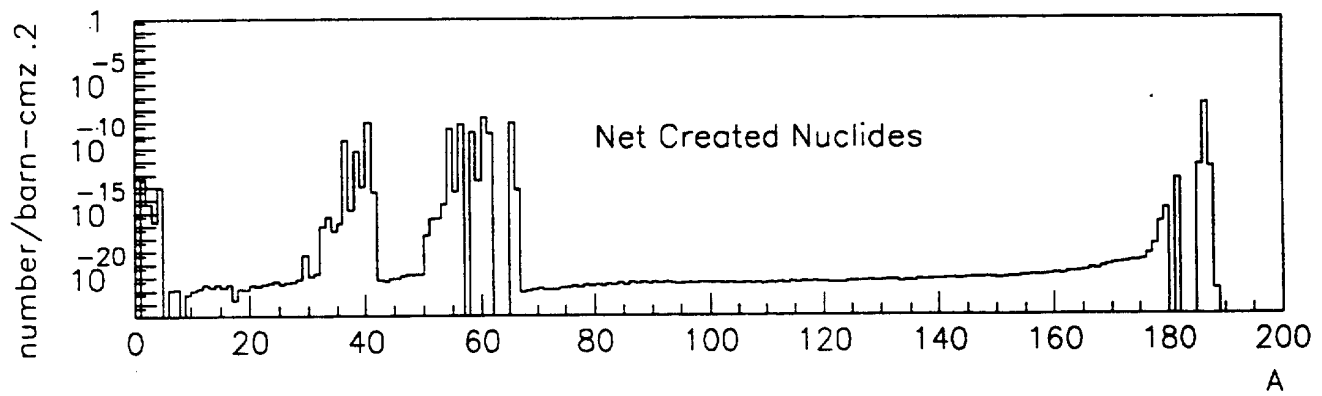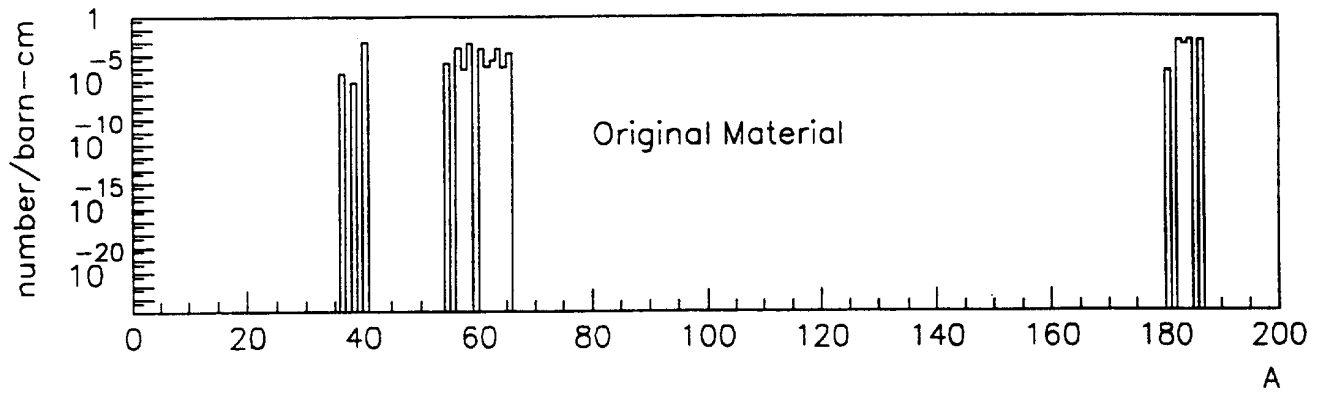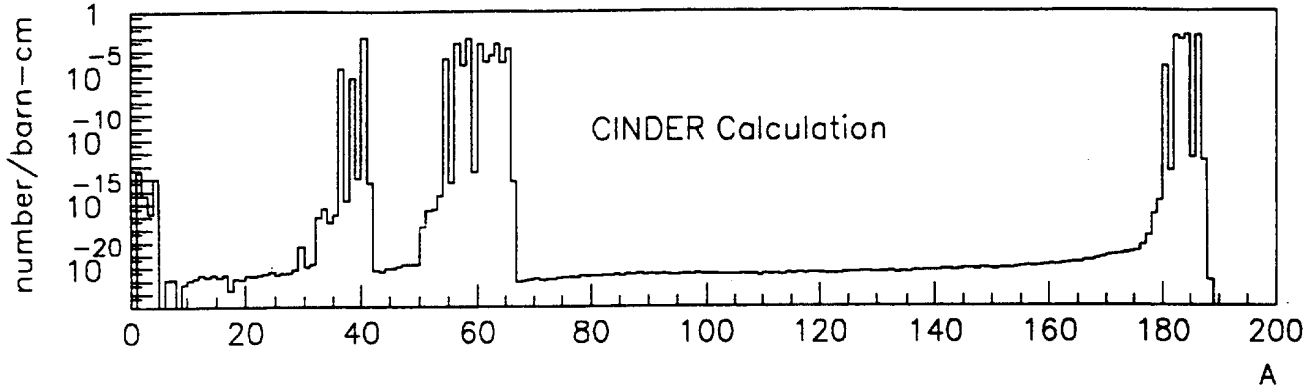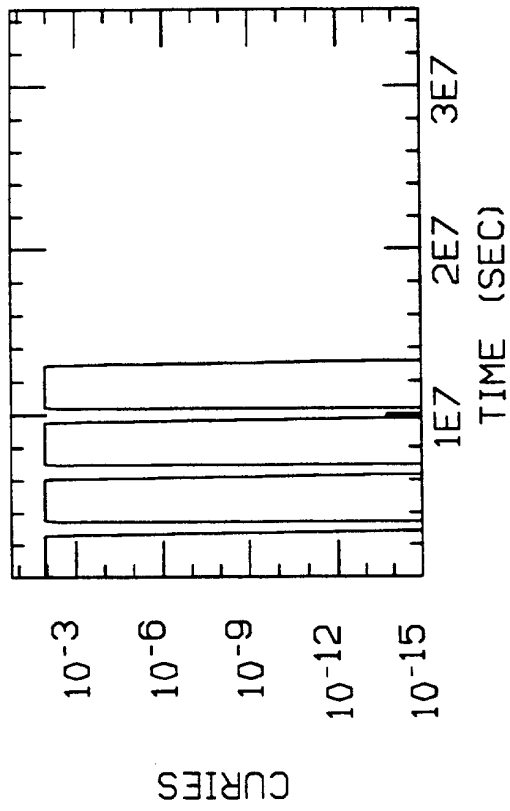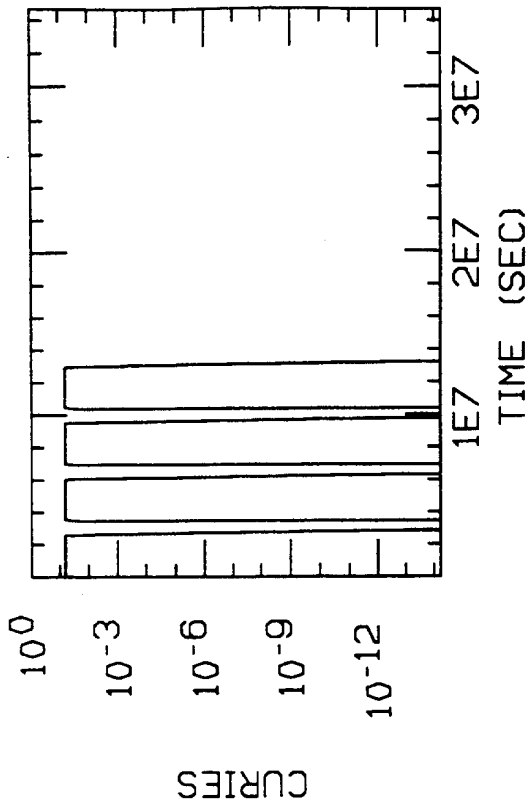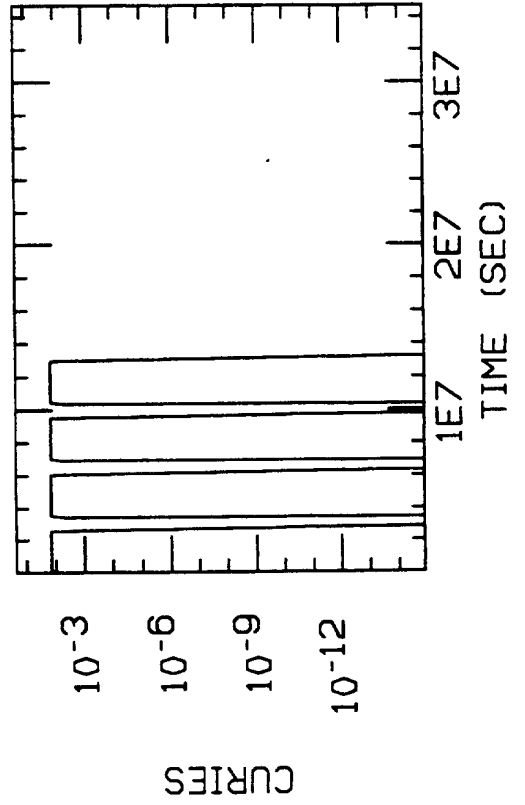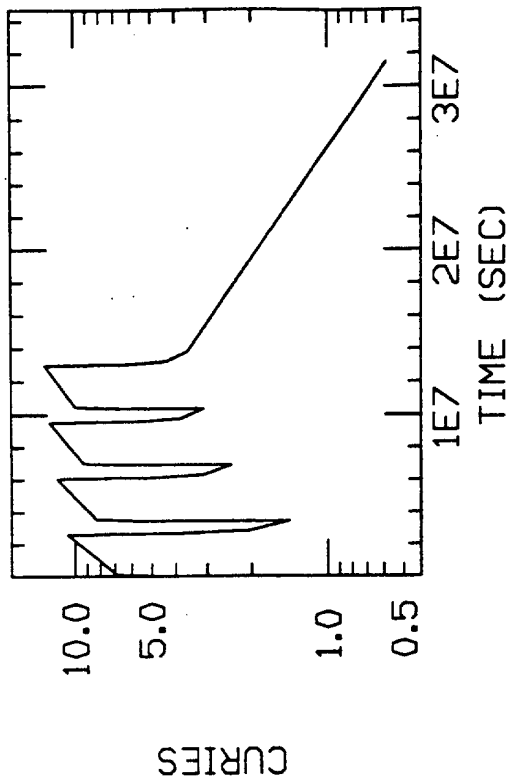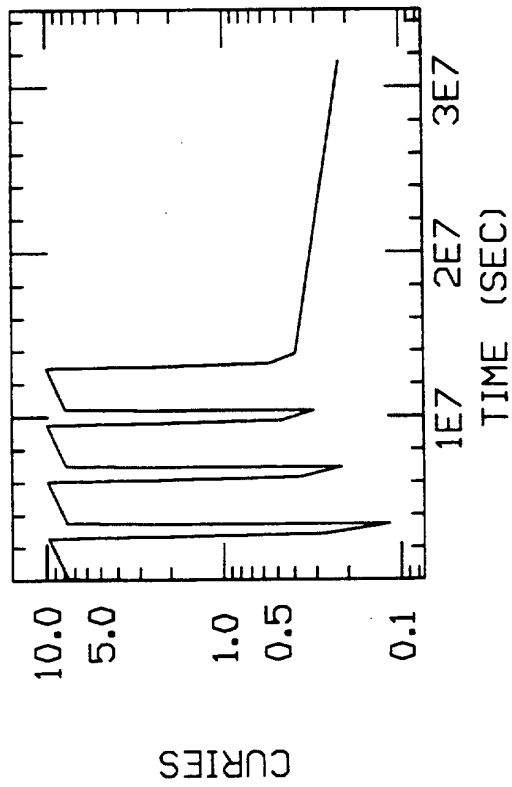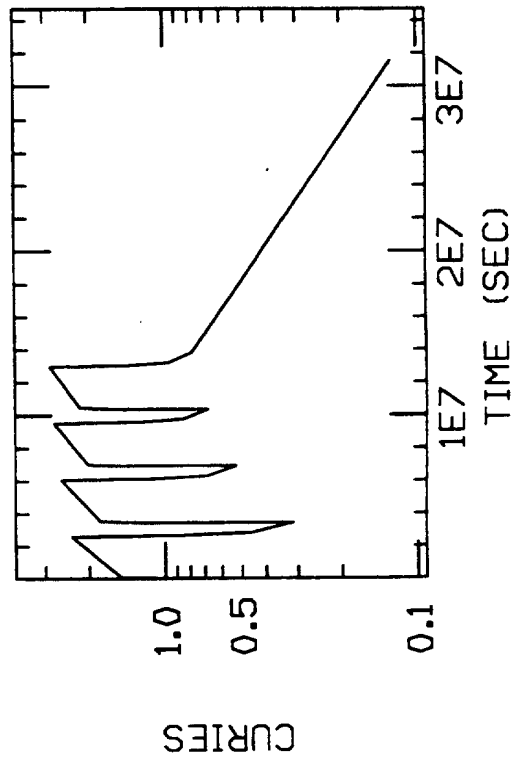
FCAL 1
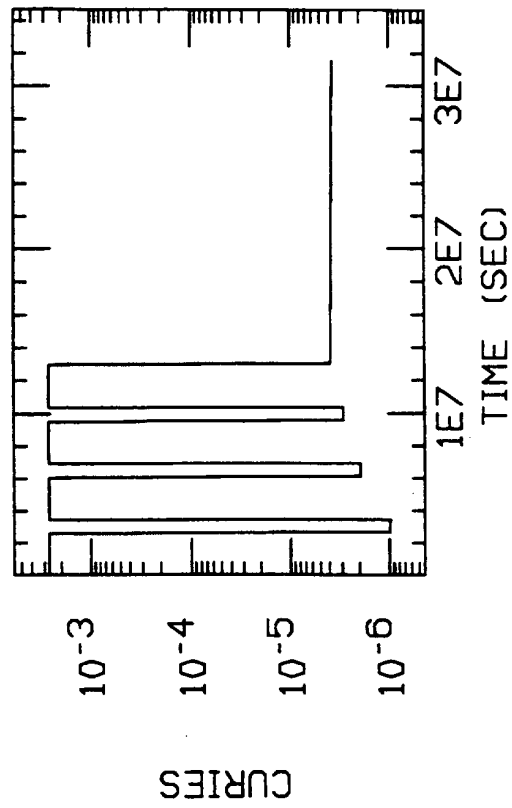
FCAL 2

FCAL 3

BORATED POLY

FIGURE 8: Heating Power

FCAL 1
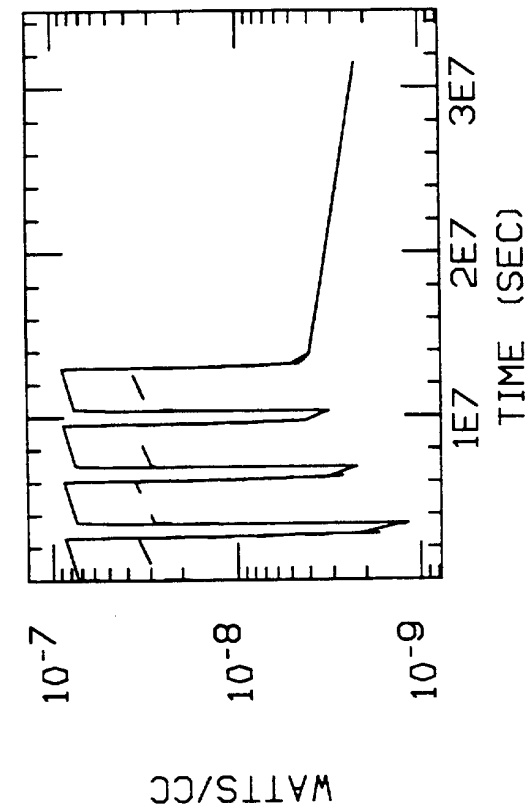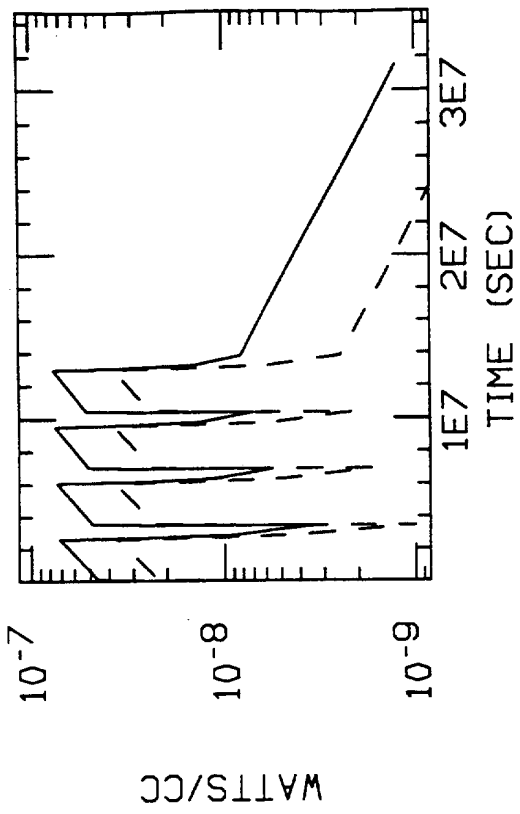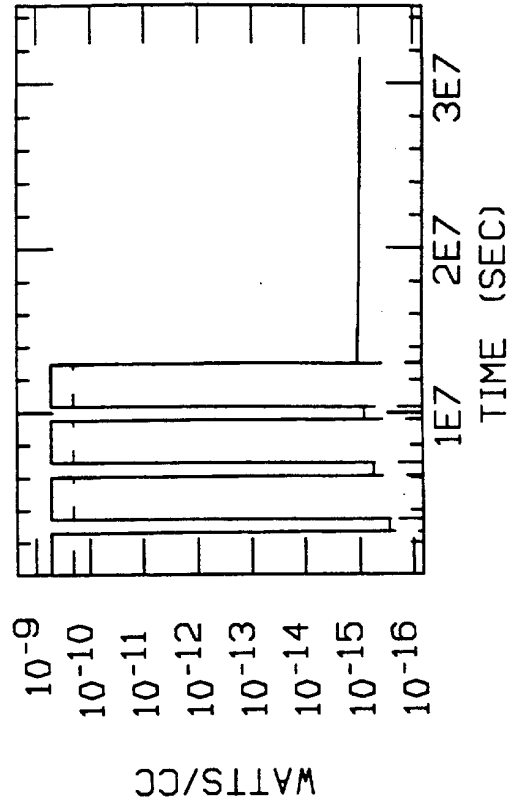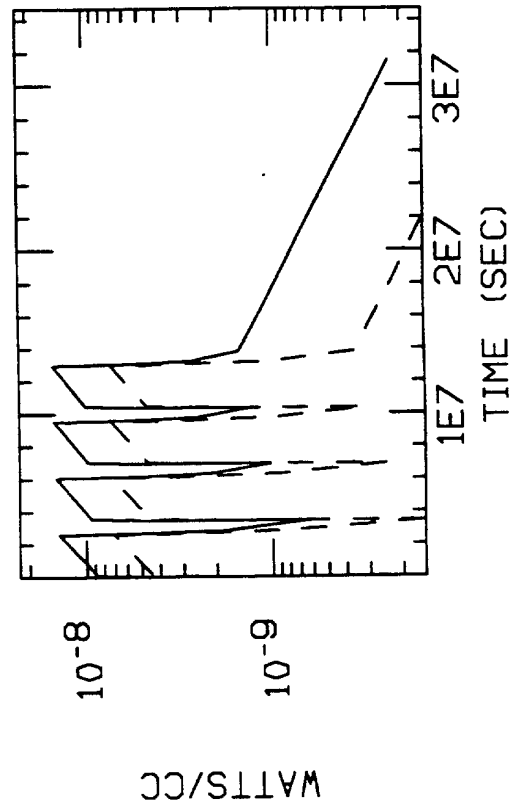
FCAL 2

FCAL 3

BORATED POLY

Figure 9 Watts per cc
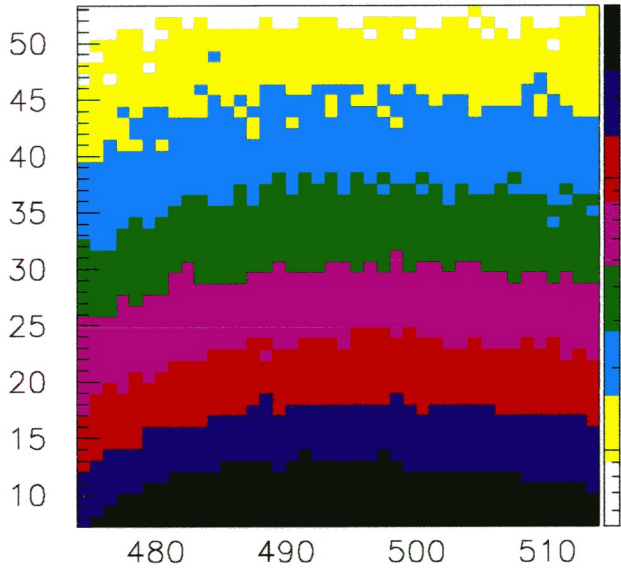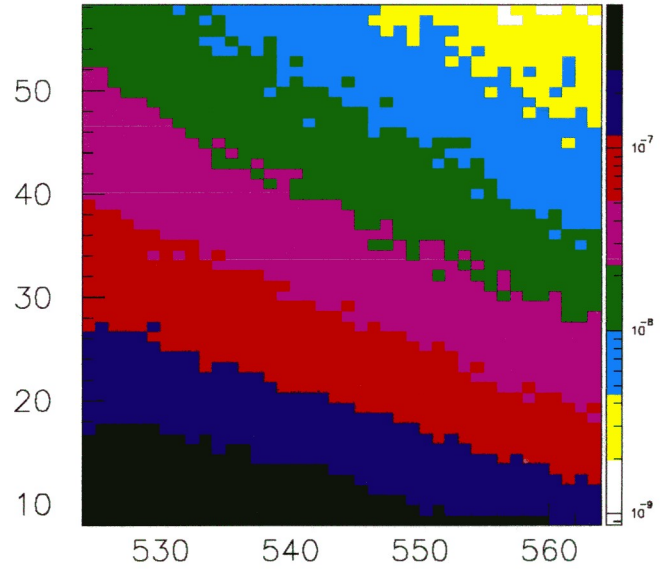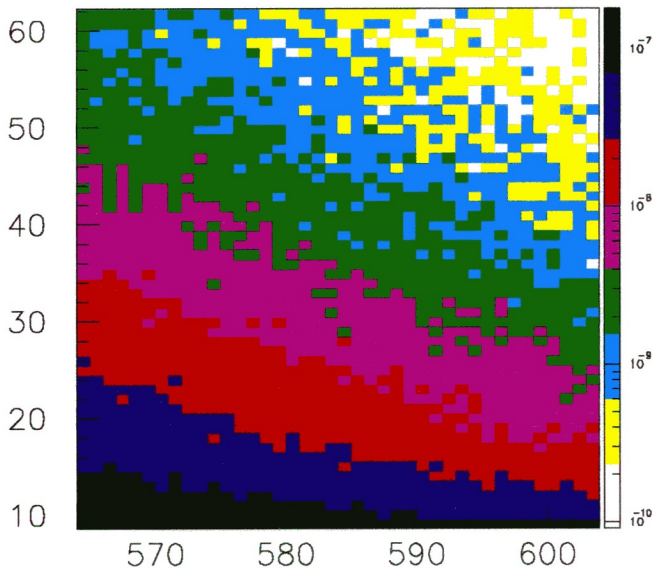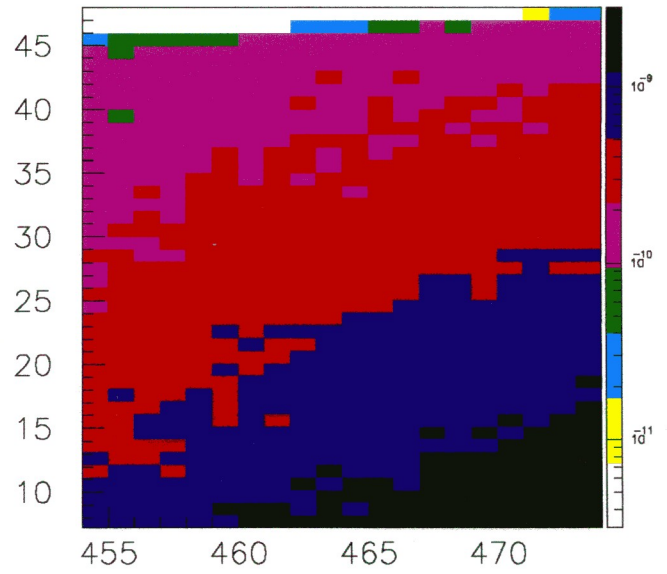
Figure 10   30 day Gamma Decay Spectra
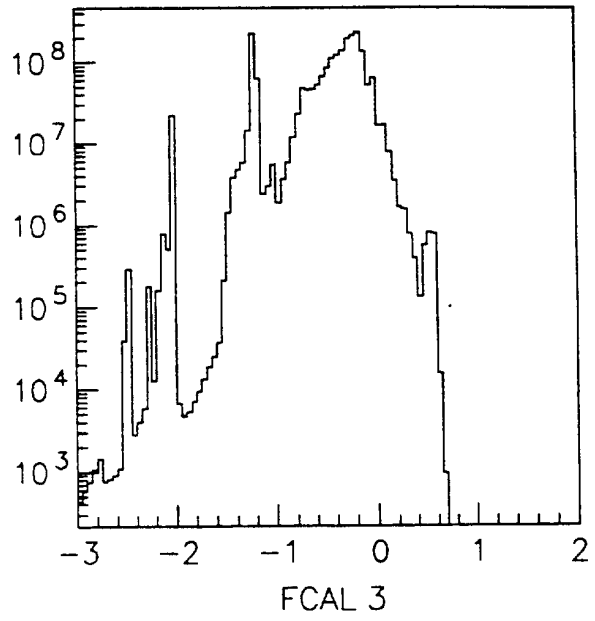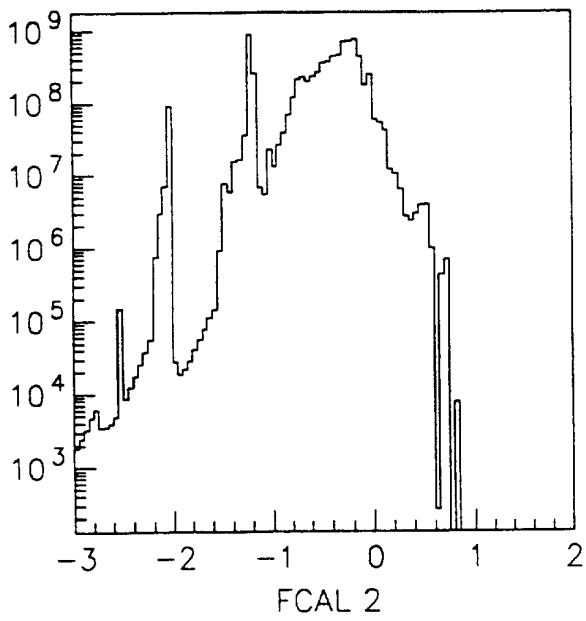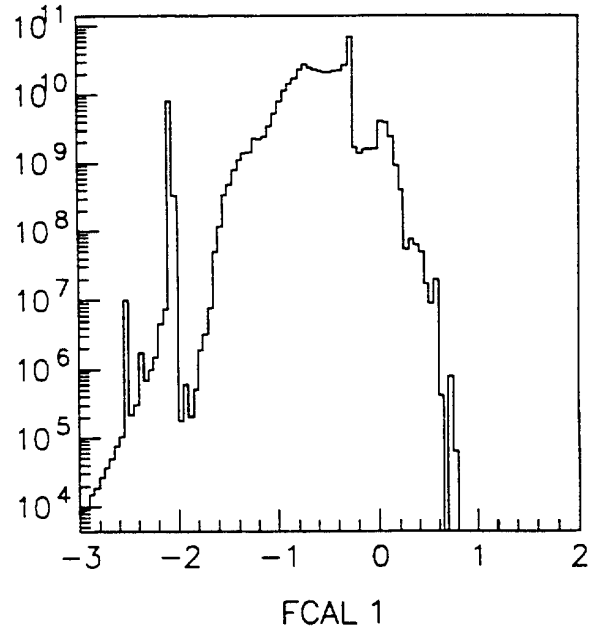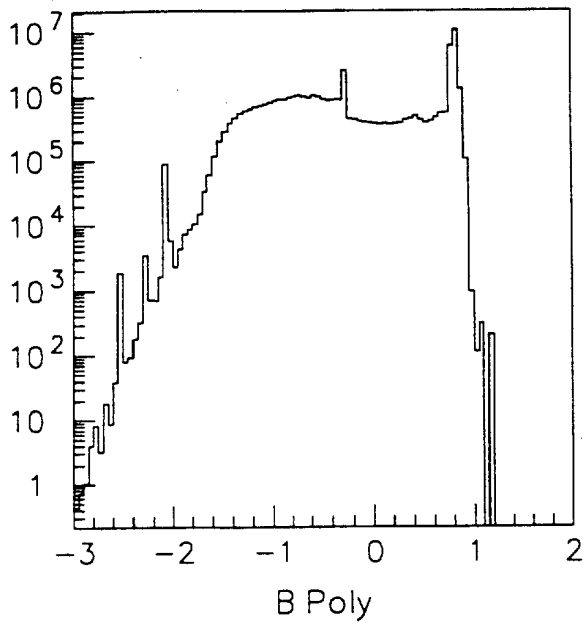
Figure 11   1 day down Gamma Decay Spectra
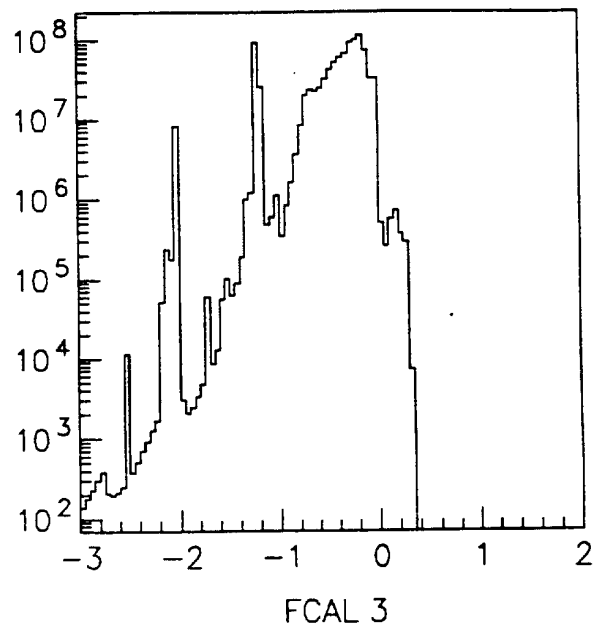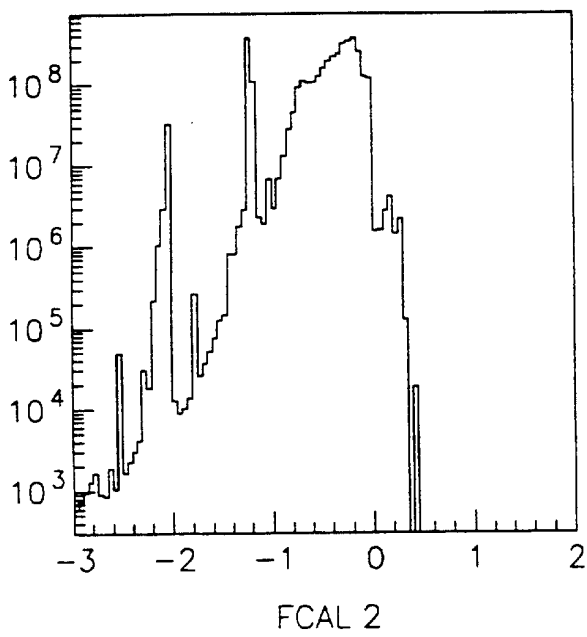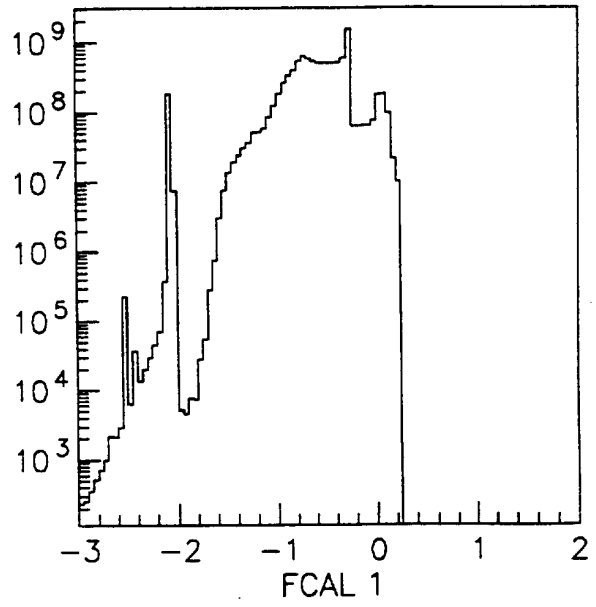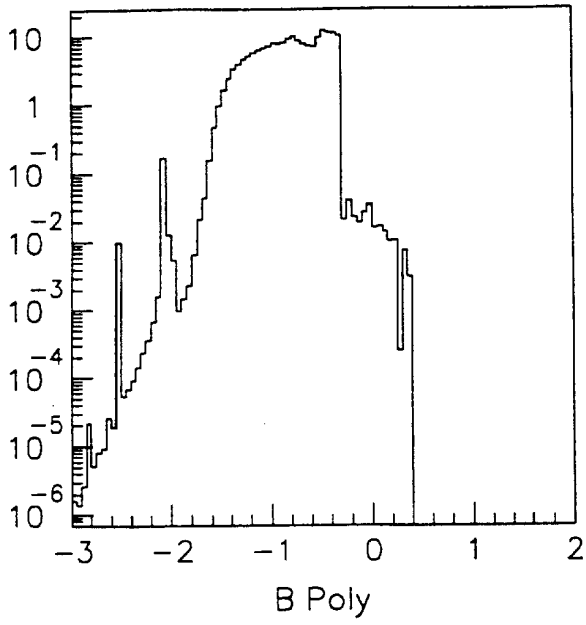
Figure 12   Source of Photons
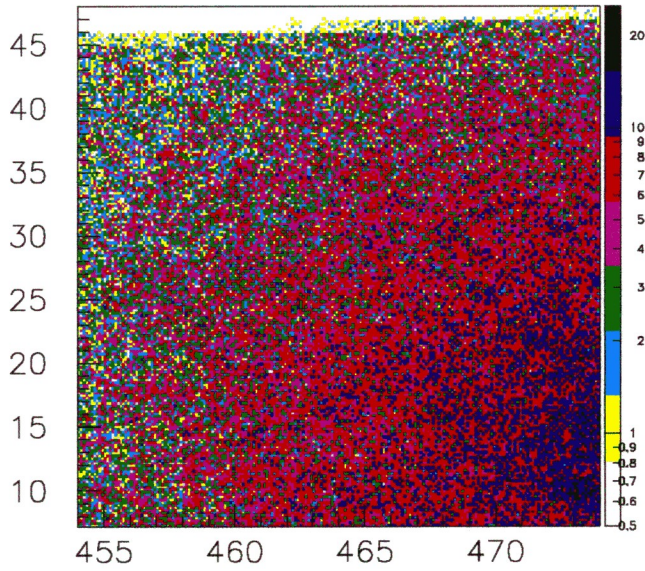
BPOLY Source
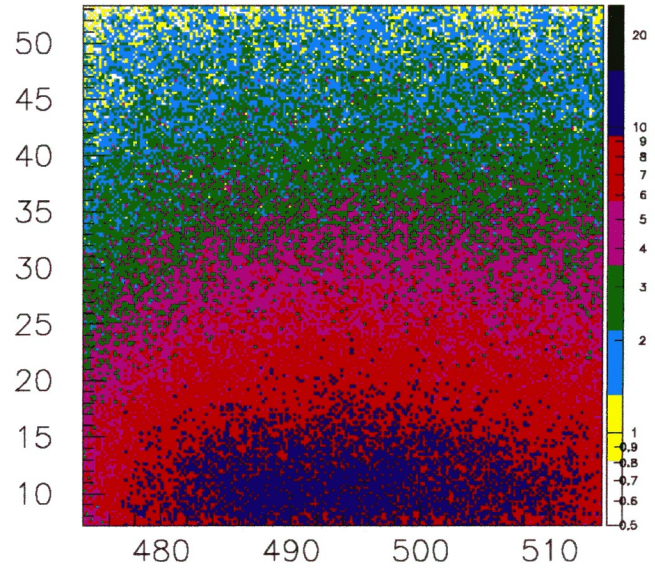
FCAL1 Source
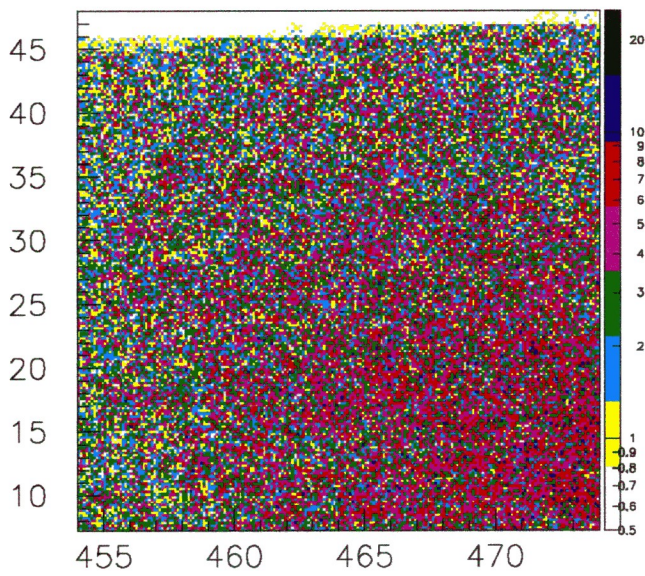
BPOLY Origins
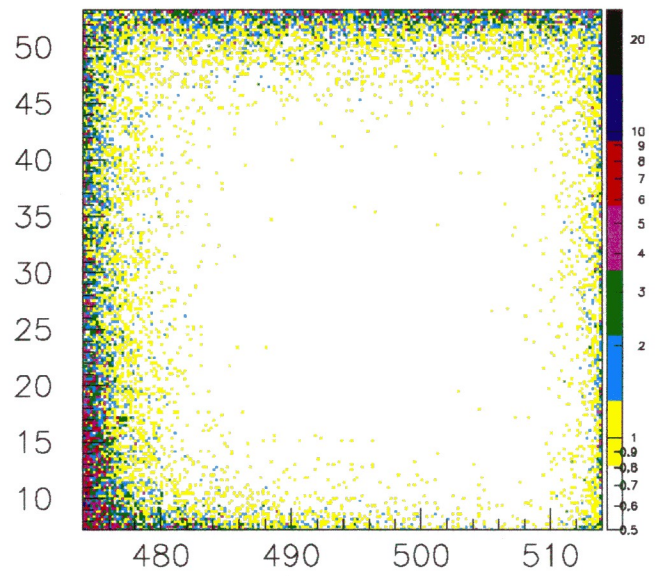
FCAL1 Origins

Figure 12a   Photon Fluence to Dose Conversion Factors
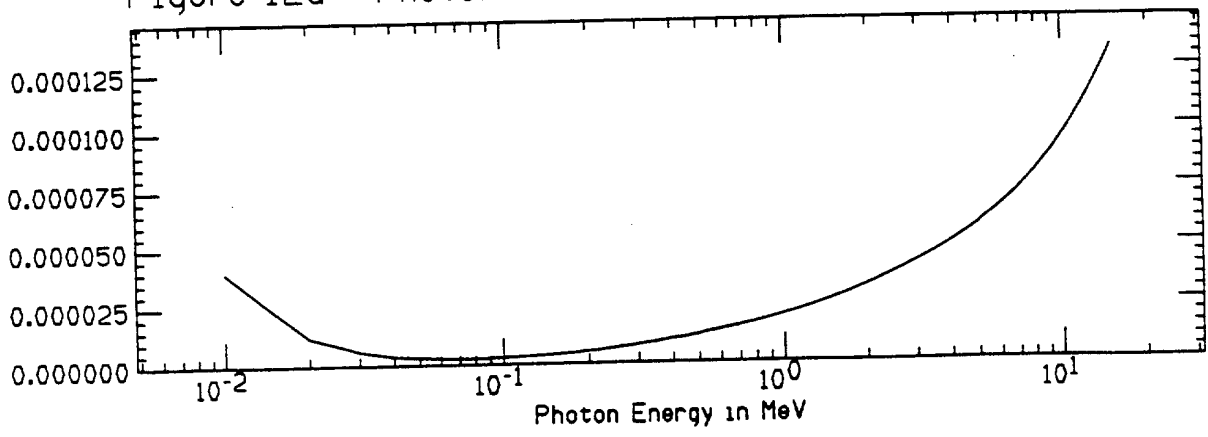
Figure 13
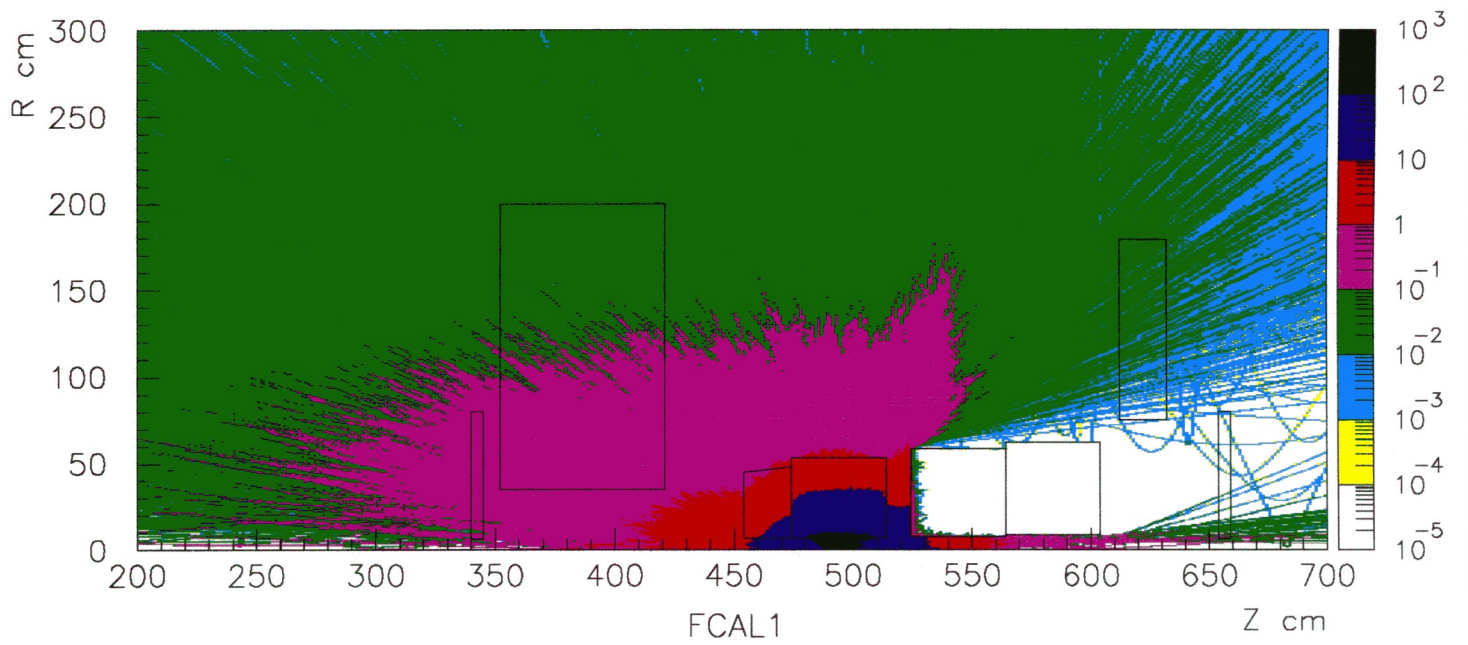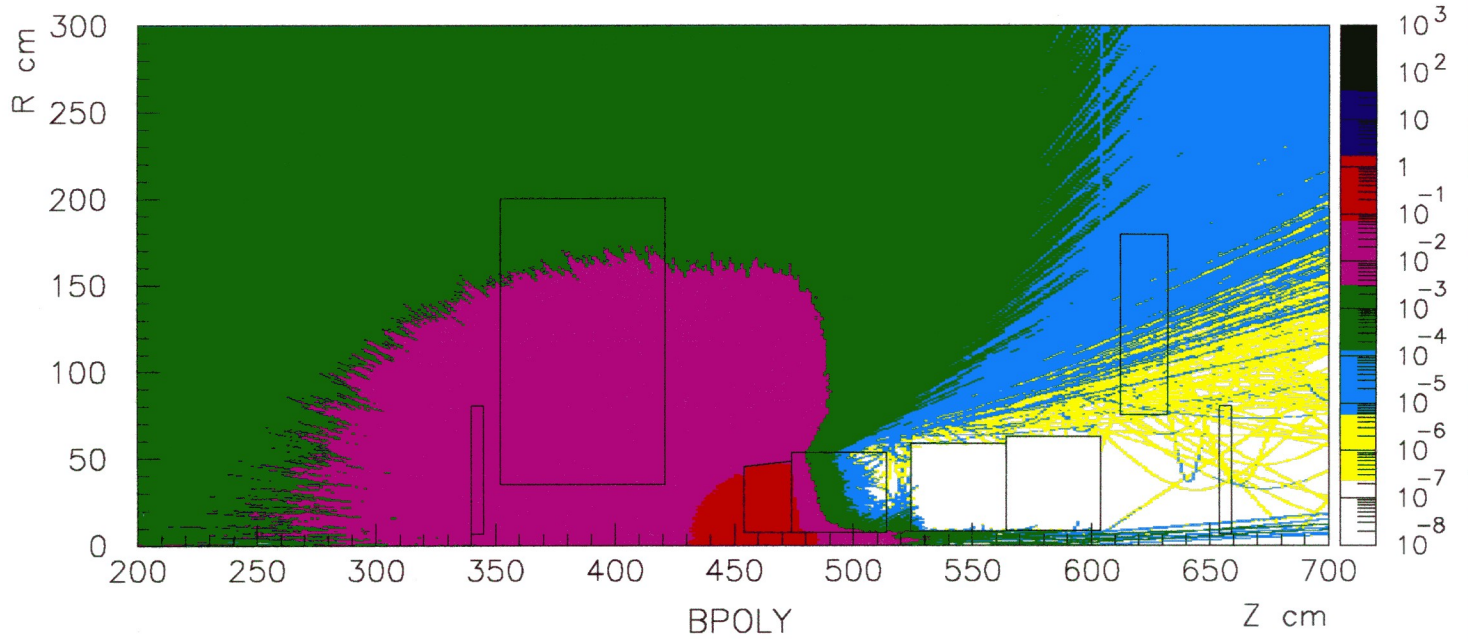
Figure 13
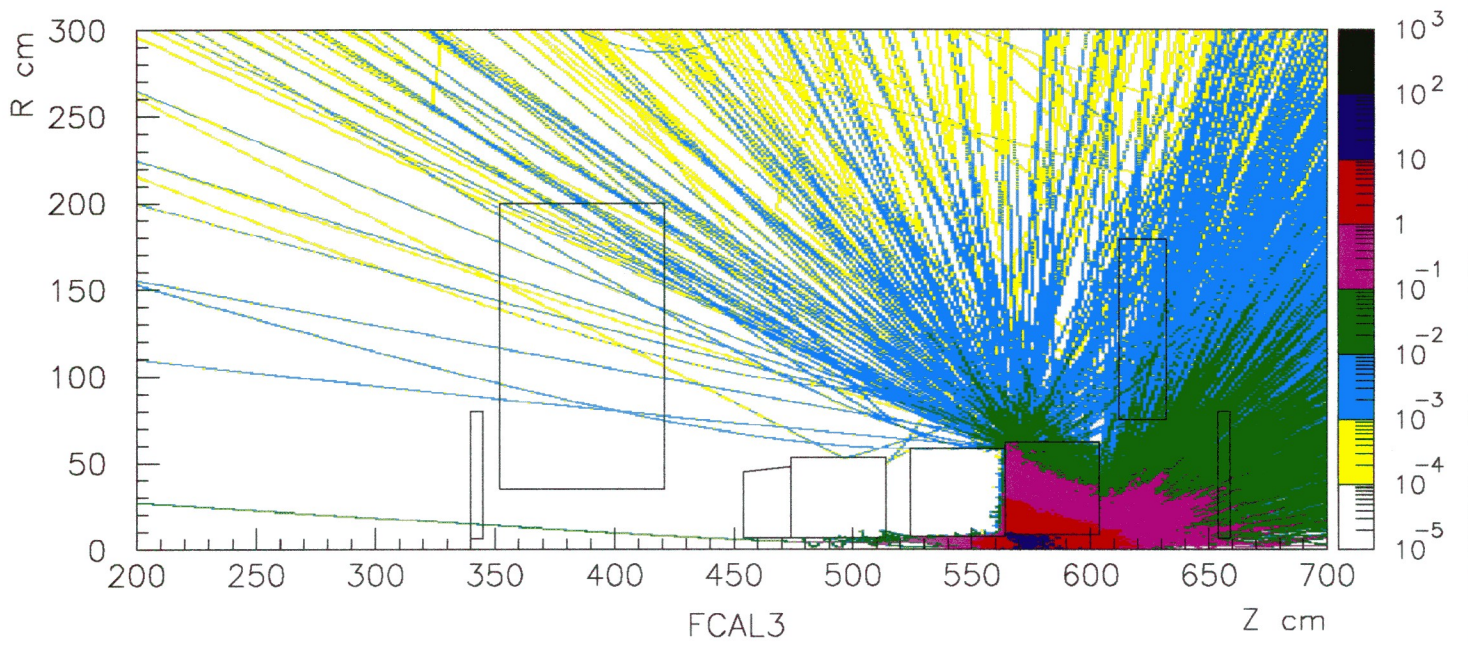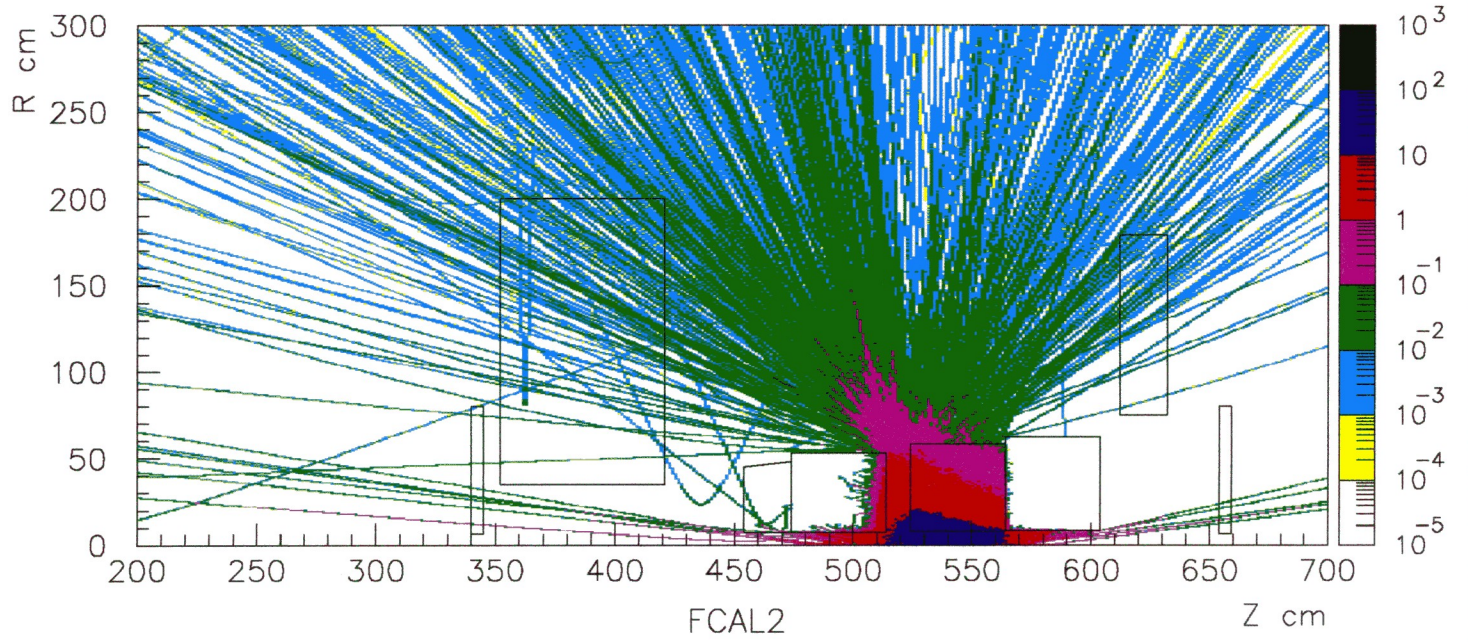
Figure 14 Dose point 18, No Shielding   mSv/hr
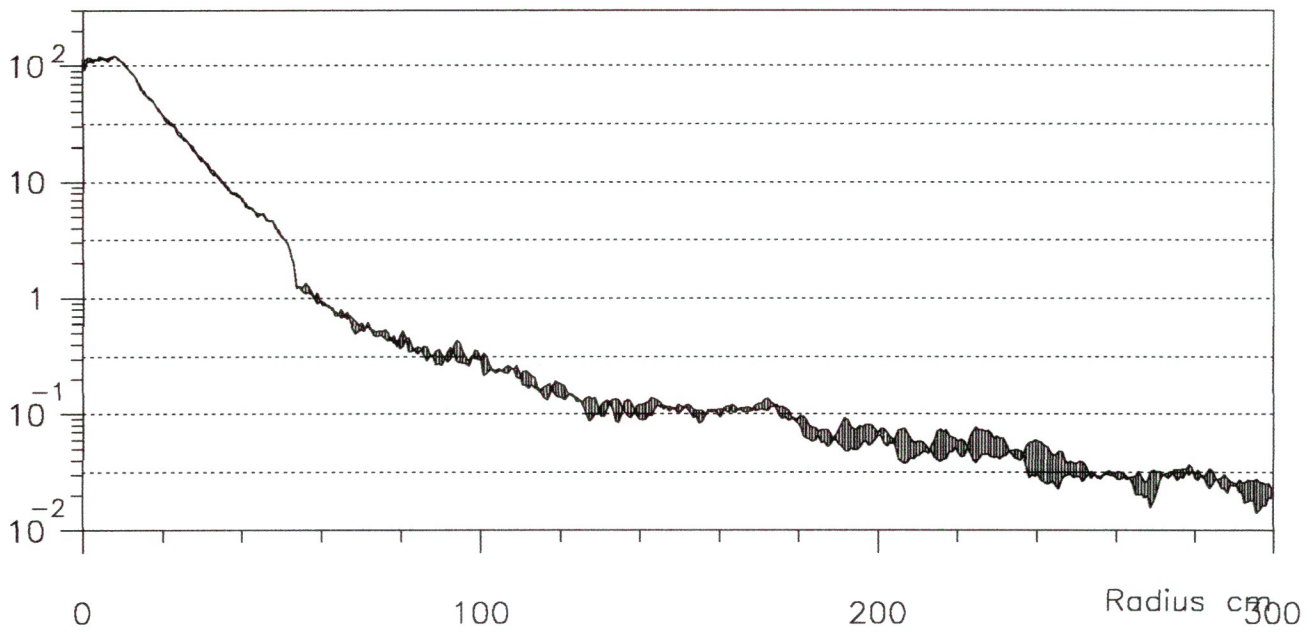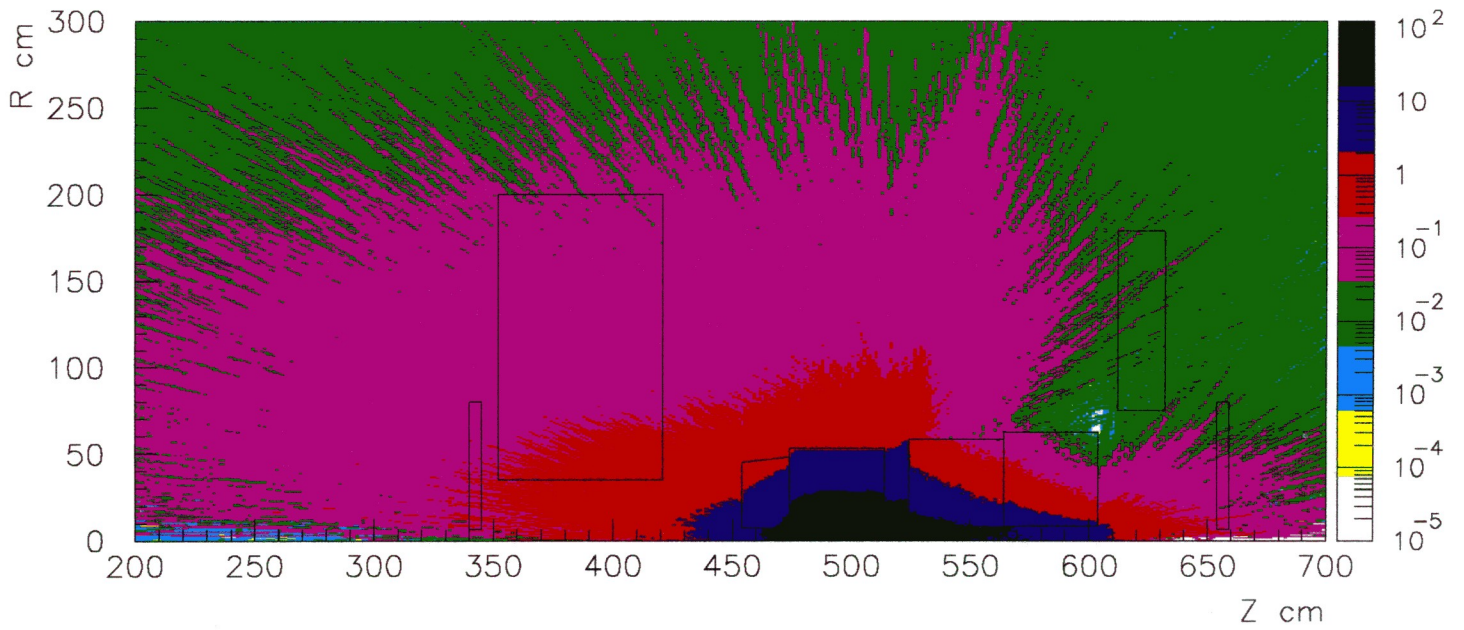
Figure 15 Dose point 19, No Shielding   mSv/hr
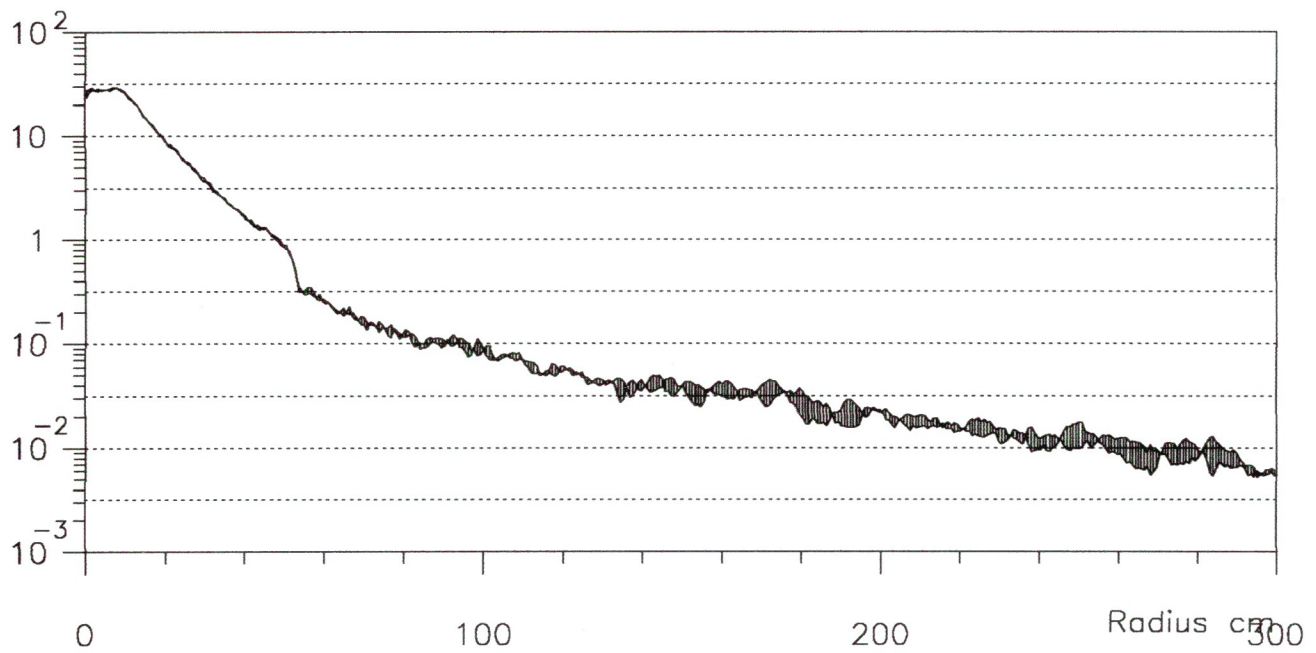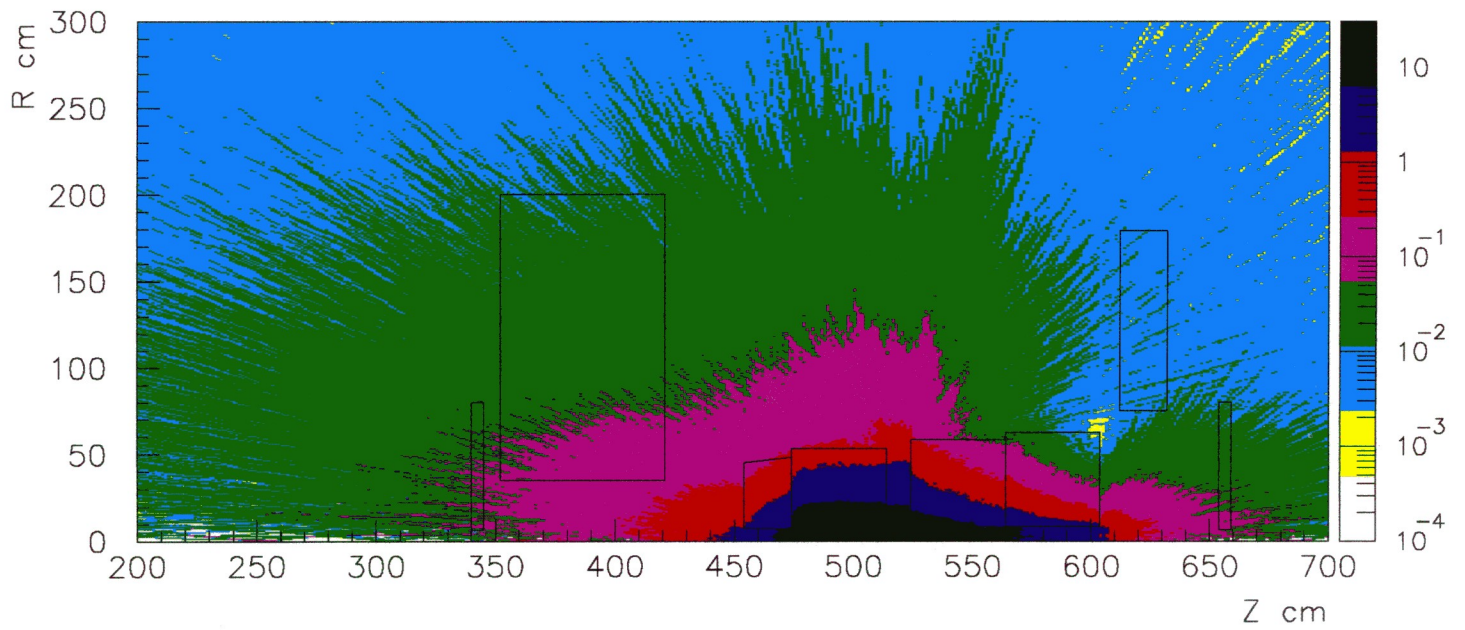
Figure 16 Dose point 18, Partial Shielding mSv/hr
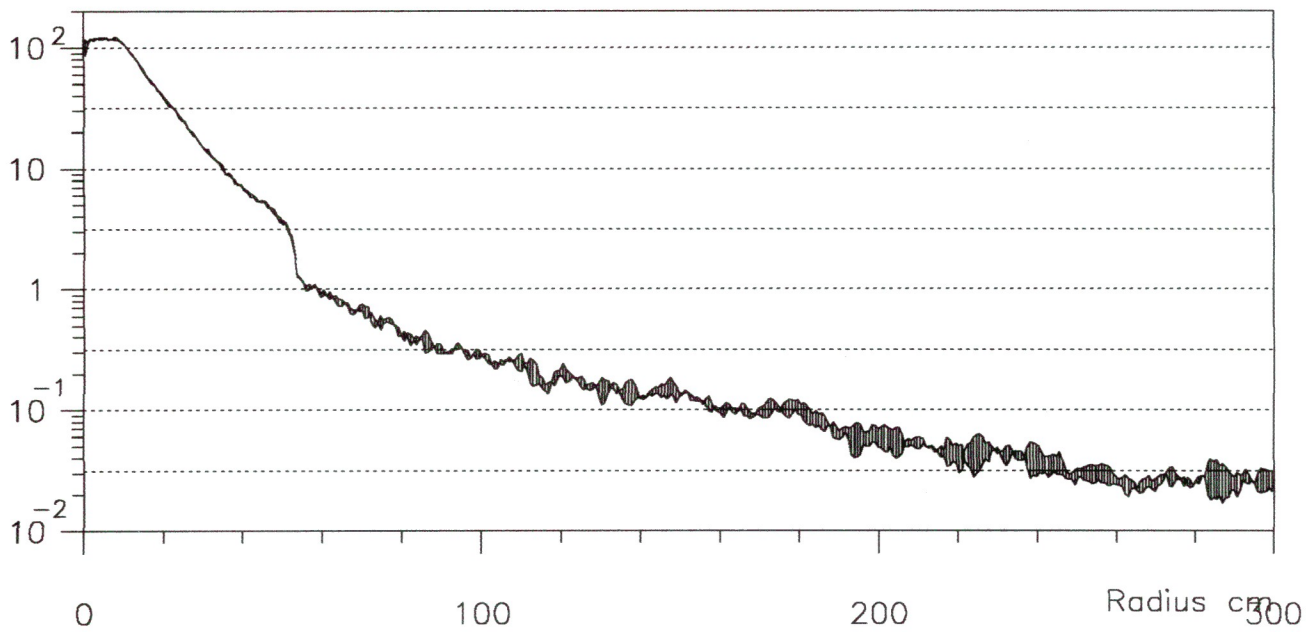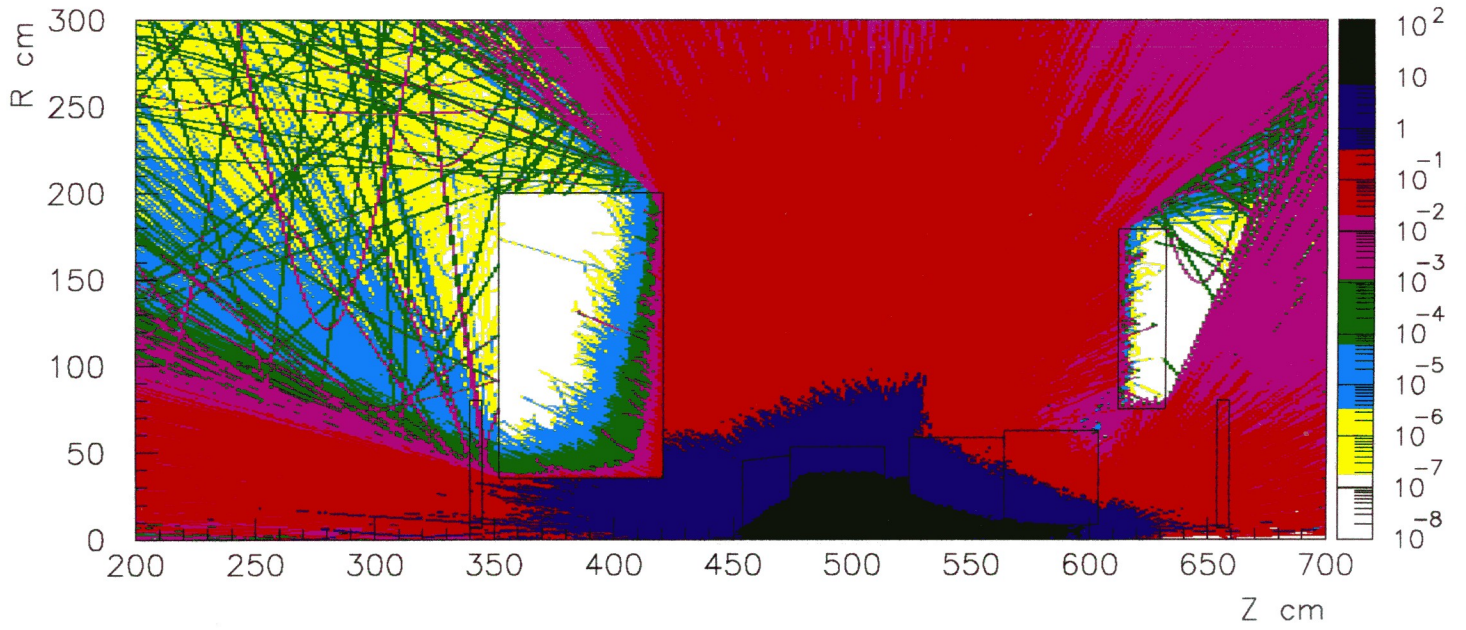
Figure 17 Dose point 19, Partial Shielding   mSv/hr
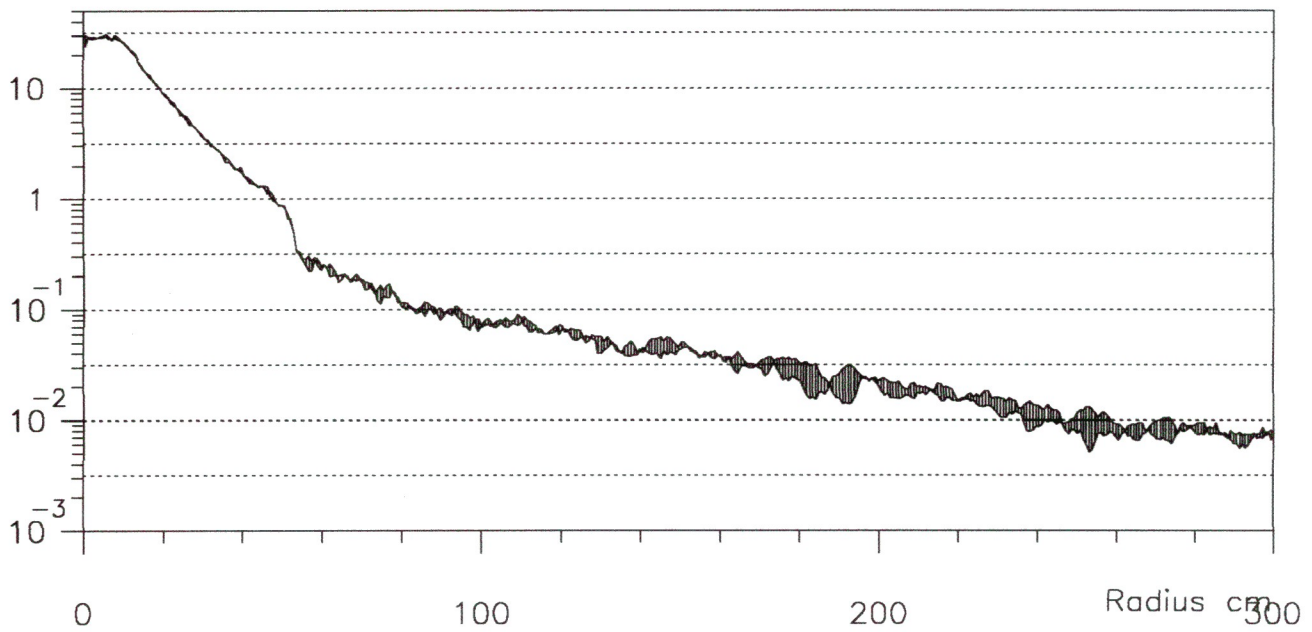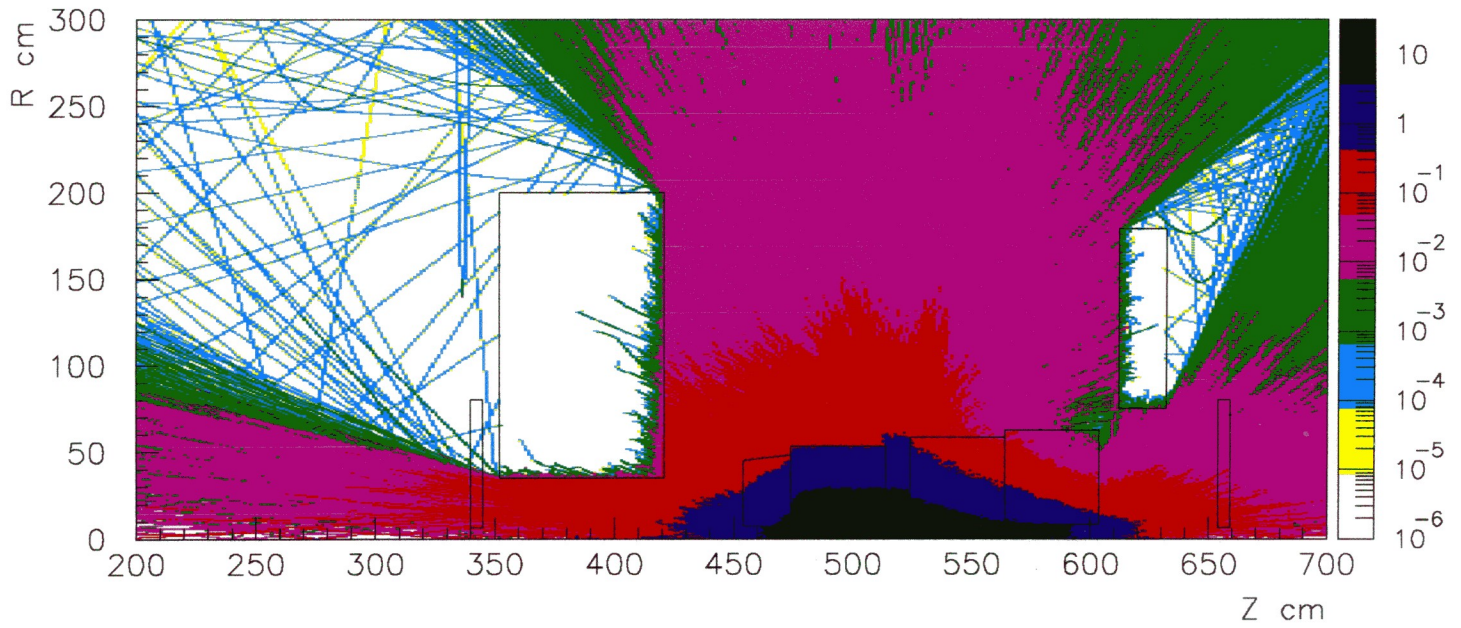
Figure 18 Dose point 18, Full Shielding mSv/hr
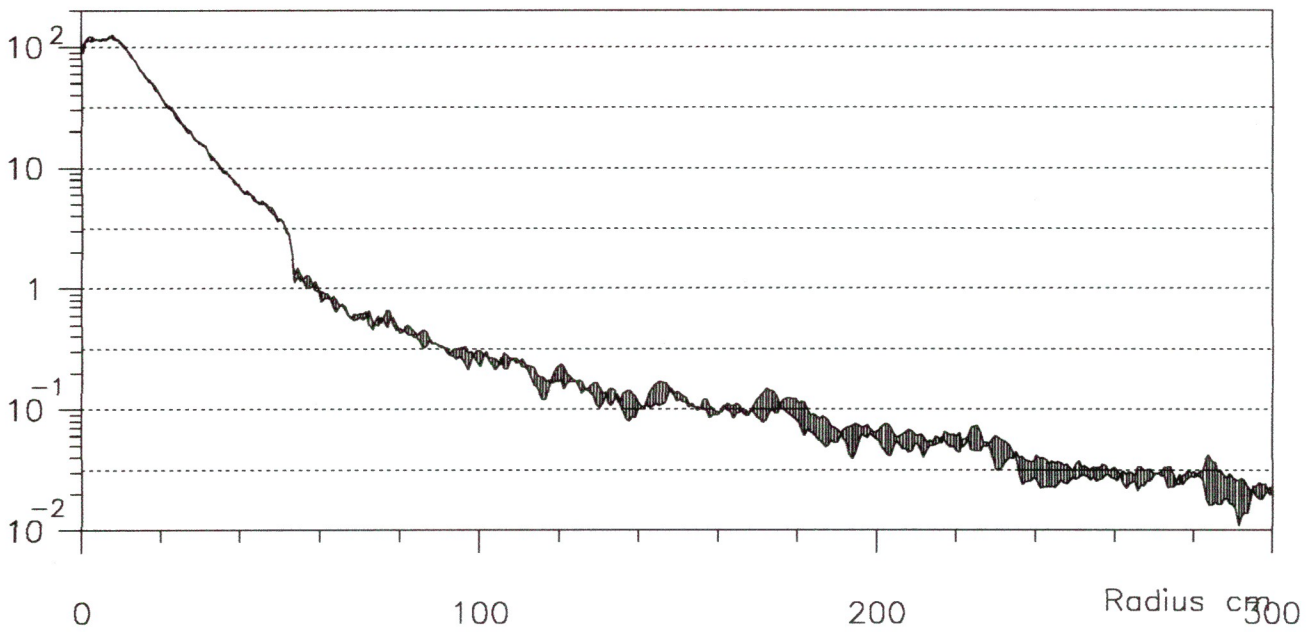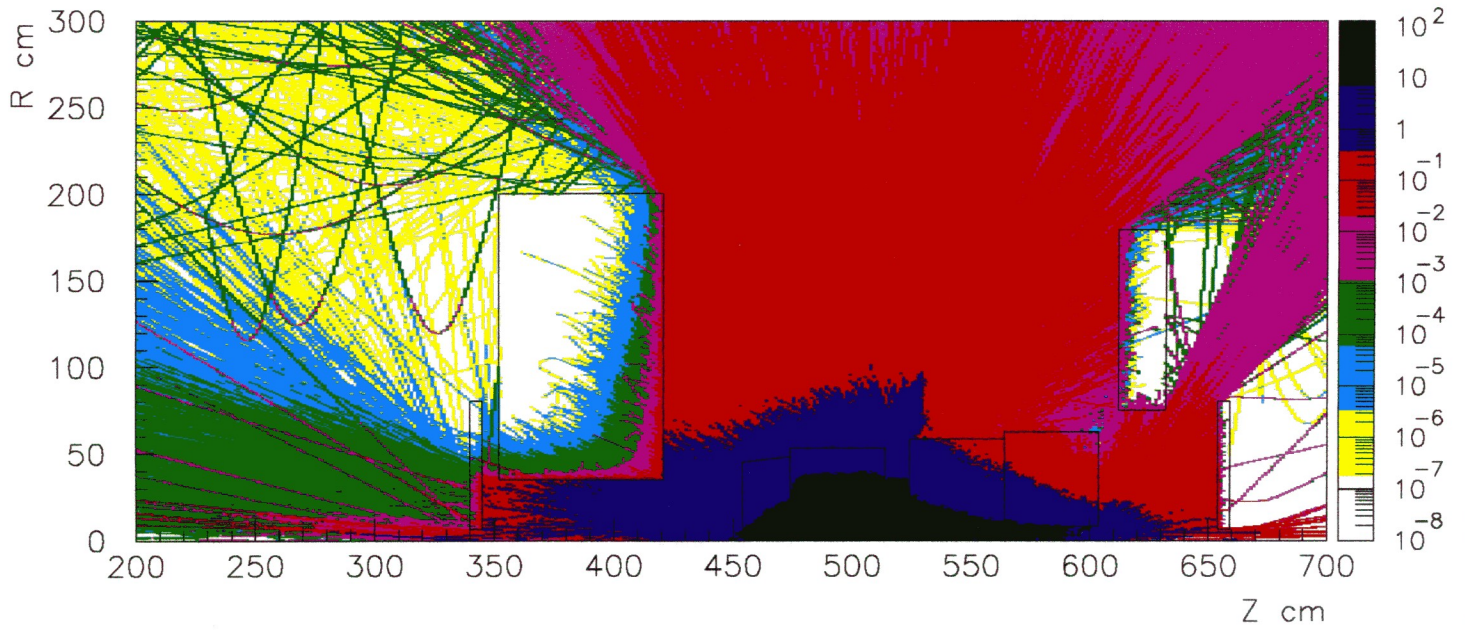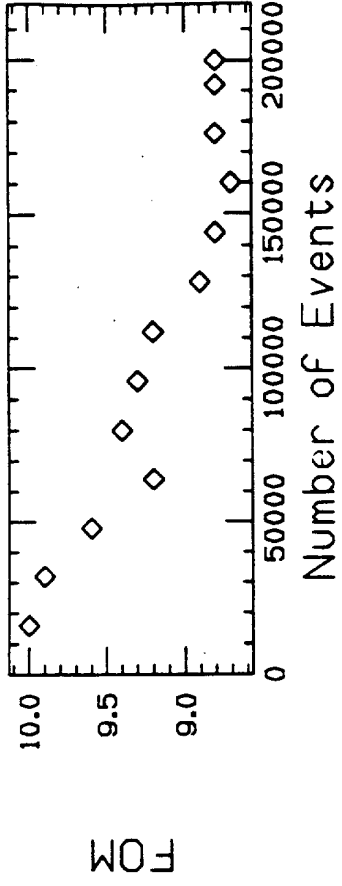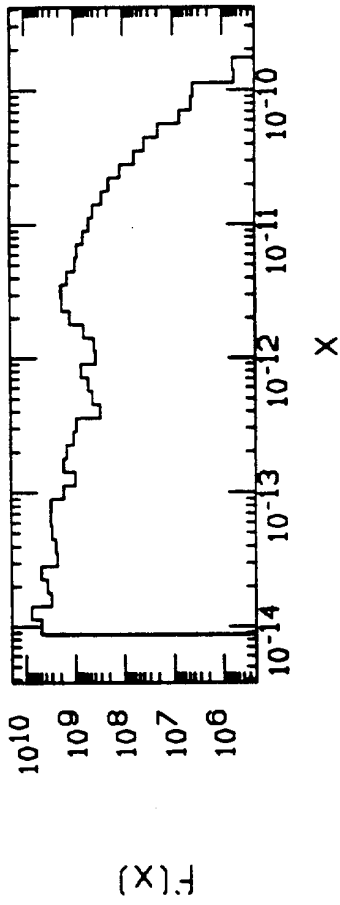
Figure 19 Dose point 19, Full Shielding   mSv/hr
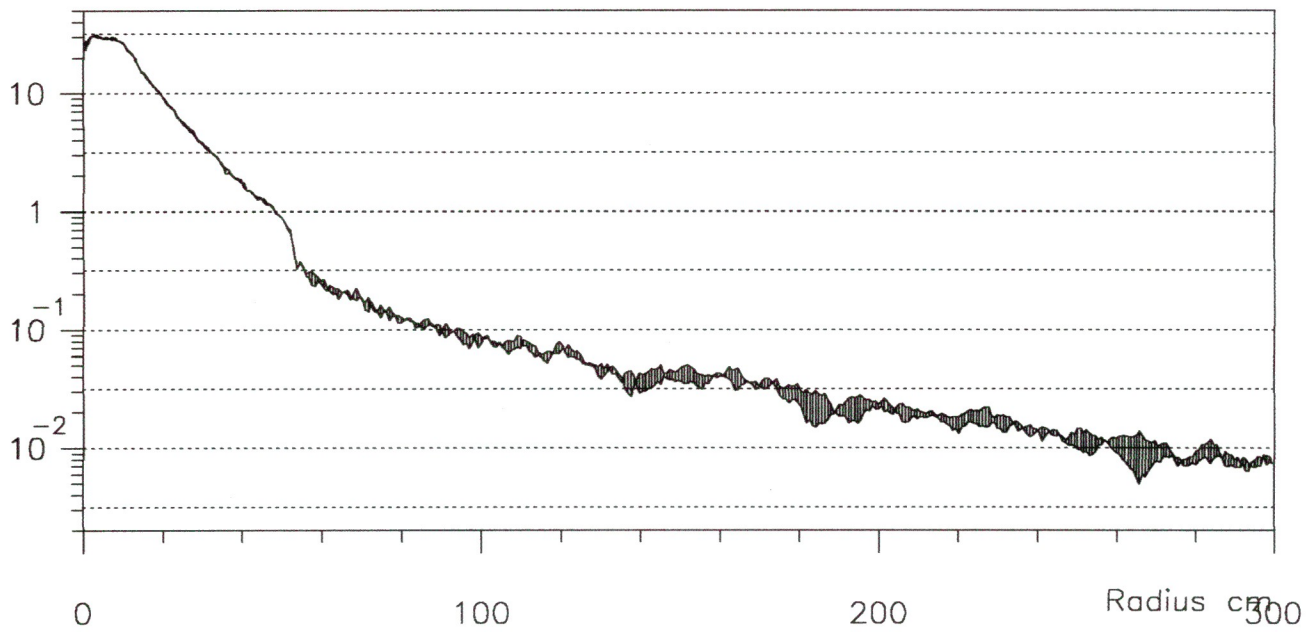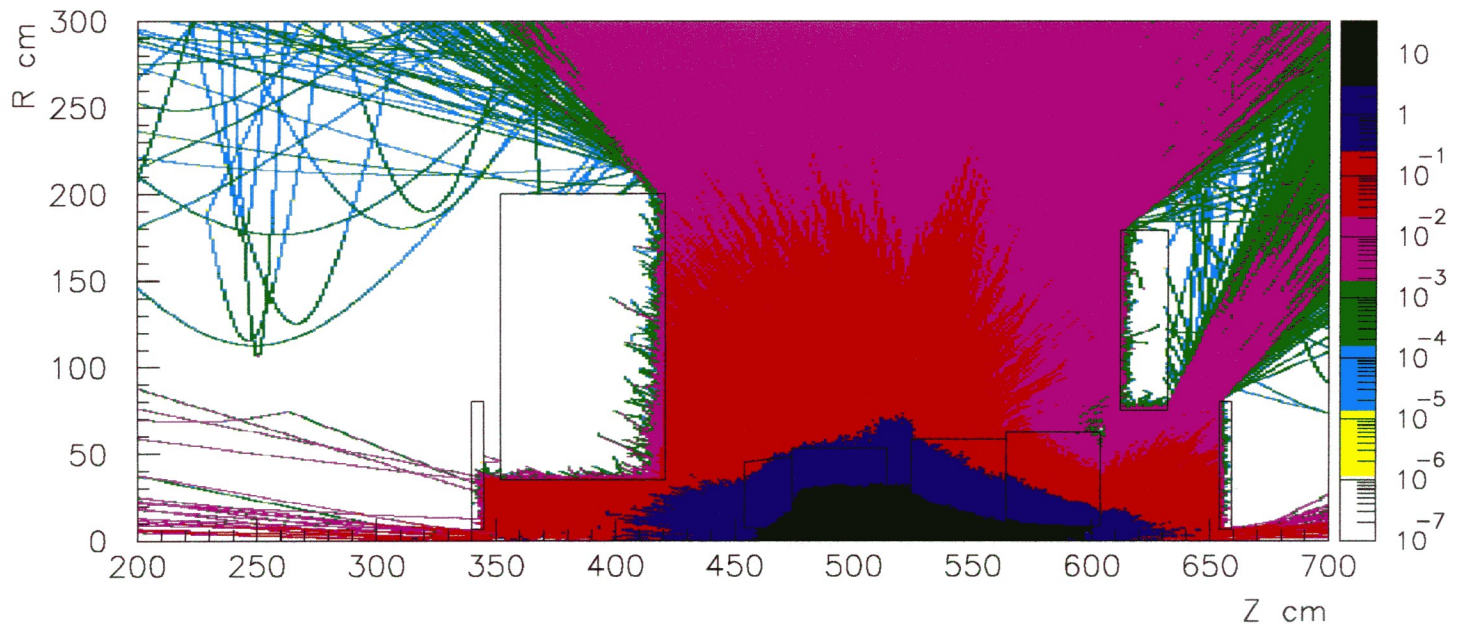
Figure 20 R=300 Z=300

Figure 21 FCAL3 R=0 Z=700